Critical Heat Fluxes Caused by An Increasing Heat Input and A Rapid Depressurization

1998

Katsuya FUKUDA

TABLE OF CONTENTS

ABSTRACT

The present thesis describes the research results mainly concerned with the critical heat fluxes resulting from exponentially increasing heat inputs (power transient) and from rapid depressurization (pressure transient).

Chapter 1 is an introduction to the transient boiling heat transfer caused by rapidly increasing heat input or decreasing pressure. The previous studies on power transient and pressure transient were reviewed with a special weight on the works by Sakurai et al.. The purposes of the study were described in this chapter.

In Chapter 2, the apparatus and methods commonly used for the steady and transient boiling experiments in Chapters 3 to 5 for exponentially increasing heat inputs were described. A cylindrical stainless steel pressure vessel which was capable of operating pressures up to 5 MPa, was used as a test vessel. The vessel was equipped with a pressure transducer and a K-type thermocouple for the measurements of system pressure and bulk liquid temperature respectively. The vessel was connected with a pipe through a valve and an air-driven booster pump to a liquid feed tank for the purpose of pre-pressurization. The apparatus and methods for pressure transient experiments were described in Chapter 6 separately.

In Chapter 3, the steady-state pool boiling critical heat fluxes (CHFs) on

the test heaters with different diameters and with different shapes in water for the ranges of subcoolings from zero to 180 K and of pressures from atmospheric to 2 MPa measured were described. The CHFs for the subcoolings lower than around 40 K for each pressure were clearly dependent on the pressures. On the other hand, those for the subcoolings larger than about 60 K were almost independent of the pressures except those for the pressures lower than around 200 kPa. The CHFs for the subcoolings higher than 20 K at each pressure disagreed with the corresponding values obtained from the existing CHF correlations given by Kutateladze, Ivey and Morris, and Zuber based on the hydrodynamic instability (HI). The CHFs derived from the modified Kutateladze correlation which was taken into account the nonlinear effect of subcooling, agree with the measured CHFs for the subcoolings lower than around 40 K at the pressures up to 200 kPa within the difference of ±5 %. The empirical equation for the CHF values for higher subcoolings higher than around 40 K at higher pressures higher than around 400 kPa was presented. Effects of the heater shapes on the constants in CHF correlations were examined for almost same experimental conditions. The trend of CHF for high subcoolings suggests that there exist another mechanism of heat transfer crisis at CHF different from that due to the HI, which is only applicable for the lower subcoolings. The existence of the mechanism for high subcoolings at high pressures based on the heterogeneous spontaneous nucleation in originally

flooded cavities on the heater surface in fully developed nucleate boiling regime was confirmed for the test heater with various shapes and cylinder diameters.

In Chapter 4, the transient boiling heat transfer processes including boiling incipience and the transition to film boiling due to exponential heat input, $Q_0 \exp(t/\tau)$, were measured for a 1.2 mm-diameter platinum horizontal cylinder with commercial surface in a pool of water at the pressures ranging from 101.3 kPa to 2063 kPa, for the periods, τ, from 2 ms to 20 s and for the subcoolings from 0 to 180 K measured are described. The processes for the case with pre-pressurization before each experimental run measured are described. The typical trend of critical heat fluxes the exponential periods is as follows: the critical heat flux (CHF) first increases from the steady-state value, then decreases and again increases with a decrease in period not only for the pre-pressurized case but also non-pre-pressurized one, though the trend was not observed completely for the short period range tested here at high pressures for the non-pre-pressurized case. However, the CHFs for the periods are generally separated into first, second and third groups for long, short and intermediate periods respectively.

The CHF for very short periods which increase with a decrease in period from the minimum CHF become almost in agreement with each other even for the cases without and with the pre-pressure. The mechanism of the transition at the CHF from single phase non-boiling regime to film boiling regime is considered to be a consequence of the heterogeneous spontaneous nucleation,

HSN, in originally flooded cavities on the cylinder surface not only for the pre-pressurized case but also for the non-pre-pressurized case, though the HSN for the latter case occurs with the several nucleation from active cavities. The effects of high subcooling and high pressure on the transition to film boiling due to the heat inputs with a wide range of increasing rate for the non-pre-pressure and pre-pressure cases are described.

In Chapter 5, the critical heat fluxes (CHFs) on 1.2mm horizontal cylinders with mirror finished and Emery-3 finished rough surfaces (MS and RS) in a pool of water due to exponentially increasing heat inputs, $Q_0 \exp(t/\tau)$, with the periods, τ, ranged from 20 s down to 2 ms at the pressures ranging from atmospheric up to 2 MPa for the subcoolings ranging from zero up to 80 K measured for the cases without and with the pre-pressure are described. The obtained data compared with the corresponding data for the cylinder with commercial surface (CS) mentioned in Chapter 4. The existence of three groups of the CHFs for the periods tested here as with that for the commercial test cylinder were clearly observed for the cylinders with MS and RS though the CHFs for the shorter periods belonging to the second group were not observed for the cylinder with commercial surface (CS) except those for the saturation condition at around atmospheric pressure, and those for high subcoolings at higher pressures. At the CHFs belonging to the second group the direct or semi-direct transition clearly occurs from transient conduction regime to film boiling

without or with the vapor bubbles for a while with instantaneous increasing of heat flux for both cylinders of MS and RS. At the CHFs, the transitions occur due to the explosive-like heterogeneous spontaneous nucleation in originally flooded cavities as described in Chapter 4 for the cylinder with CS. It should be noted that (as a typical example) the minimum CHFs for the periods of 10 ms on the MS and RS cylinders at the pressure of 1MPa for the subcooling of 40 K were about 40 % of the corresponding steady-state CHF. It was observed that the trend of CHFs for the periods belonging to the second and third groups are significantly affected by the cylinder surface conditions.

In Chapter 6, transient boiling on single horizontal cylinders in water caused by rapid depressurization from initial natural convection or partial nucleate boiling were investigated. For an initial heat flux and a pressure-reduction period respectively larger and shorter than certain threshold values, a transition to film boiling was observed. In a rapid transient due to depressurization from initial natural convection, the transient boiling heat transfer process followed a hypothetical nucleate boiling curve that lied at the higher superheat side of the successive steady-state fully developed nucleate boiling curves corresponding to each transient pressure. The critical heat flux value was far lower than the steady-state critical heat flux at the corresponding pressure. The effects of the following parameters: initial heat flux, pressure-reduction rate, initial pressure and cylinder diameter, on the transient heat

transfer processes (nucleate boiling heat transfer, critical heat flux, transition to film boiling or not, film boiling heat transfer), were examined. A mechanism, based on heterogeneous spontaneous nucleation from the originally flooded cavities on the solid surface, was suggested for the transition from non-boiling to film boiling under rapid depressurization.

In Chapter 7, the summarized conclusions of Chapters 3 through 6 are described.

NOMENCLATURE

A, B, C	= constants in Eq.(3-4)
c_p	= specific heat at constant pressure, $J/(kgK)$
d	= cylinder diameter, m
g	= acceleration of gravity, m/s^2
Gr^*	= $g\beta q d^4/k\nu^2$, modified Grashof number
h_c	= conduction heat transfer coefficient, $W/(m^2K)$
h_{com}	= non-boiling combination heat transfer coefficient, $W/(m^2K)$
h_n	= natural convection heat transfer coefficient, $W/(m^2K)$
h_{lg}	= latent heat of vaporization, J/kg
K_1	= constant in Eq.(3-2)
K_2	= constant in Eq.(3-1)
K_3	= constant in Eq.(3-3)
k	= thermal conductivity, $W/(m\,K)$
L'	= non-dimensional length in Eq.(3-5)
P	= pressure absolute, Pa
P^*	= pressure in gauge, Pa
P_{in}	= initial pressure absolute, Pa
P_{in}^*	= initial pressure gauge, Pa

Pr = Prandtl number

Q = heat generation rate, W/m^3

Q_0 = initial exponential heat input, W/m^3

q = heat flux, W/m^2

q_{cr} = critical heat flux, W/m^2

$q_{cr,C}$ = critical heat flux for commercial surface condition, W/m^2

$q_{cr,D}$ = critical heat flux at direct transition point, W/m^2

$q_{cr,M}$ = critical heat flux for mirror surface condition, W/m^2

$q_{cr,R}$ = critical heat flux for rough surface condition, W/m^2

$q_{cr,sat}$ = q_{cr} for saturated condition, W/m^2

$q^*_{cr,sat}$ = q_{cr} due to HSN for saturated condition, W/m^2

$q_{cr,sub}$ = q_{cr} for subcooled condition, W/m^2

q_i = heat flux at the initiation of boiling, W/m^2

q_{in} = initial heat flux, W/m^2

q_{over} = heat flux at overshoot point, W/m^2

q_{st} = steady-state critical heat flux, W/m^2

$q_{st,sat}$ = q_{st} for saturated condition, W/m^2

$q_{st,sub}$ = q_{st} for subcooled condition, W/m^2

R_f = $Gr^* Pr^2/(4 + 9 Pr^{1/2} + 10 Pr)$

T_w = heater surface temperature, K

T_{sat} = saturation temperature, K

t = time, s

ΔT_c = surface superheat at critical heat flux, K

ΔT_i = surface superheat at boiling initiation, K

ΔT_{iLH} = lower limit of HSN surface superheat, K

ΔT_{over} = surface superheat at overshoot point, K

ΔT_{sat} = $(T_w - T_{sat})$, surface superheat, K

ΔT_{sub} = $(T_{sat} - T_B)$, liquid subcooling, K

α = boiling heat transfer coefficient $(= q/\Delta T_{sat})$, W/m^2K

β = expansion coefficient, $1/K$

μ = $[\rho_l c_{pl}/(k_l \tau)]^{1/2}$, m^{-1}

ν = kinematic viscosity, m^2/s

ρ = density, kg/m^3

σ = surface tension, N/m

τ = exponential period, s

τ_p = pressure reduction period, s

Subscripts

B	= bulk
g	= vapor
l	= liquid
s	= solid

CHAPTER 1

INTRODUCTION

1.1 TRANSIENT BOILING HEAT TRANSFER

The correct understanding and prediction of the transient boiling heat transfer caused by rapidly increasing heat input (power transient) or decreasing pressure (pressure transient) are important as the database for the safety assessment of nuclear reactor accidents caused by a power burst and a pipe rupture, and also interesting as a fundamental problem of time varying boiling heat transfer.

1.1.1 Previous Studies on Power Transients

The power transient in water was first studied by Rosenthal (1957). He showed that the temperature rise of the heater before the incipient boiling could be computed by the transient conduction equation. Johnson et al. (1966) performed an extensive experimental study of transient boiling heat transfer in water caused by exponential heat inputs under pressures ranging from 0.1 to 13.78 MPa. They showed that the incipient boiling superheat was higher for

shorter exponential period and for lower system pressure. They also showed that the critical heat flux for exponential heat input exceeded the steady-state critical heat flux by a factor as large as 4.

Sakurai and Shiotsu (1977a, 1977b) investigated the transient boiling heat transfer for exponential heat inputs, $Q_0 \exp(t/\tau)$, to a platinum wire in saturated water at pressures from atmospheric to 2 MPa. They observed for the first time the anomalous trend of CHFs. Namely, the CHF first gradually increased from the steady-state CHF up to a maximum CHF, and then it decreased down to a minimum CHF and again increased with a decrease in the exponential period, τ, from 20 s down to 5 ms. The CHFs were generally classified into mainly three groups with respect to the periods. Namely, the first, second and third ones were for longer, shorter and intermediate periods respectively. For example, the first group was for the periods longer than around 0.1 s, the second one was for the periods shorter than around 0.005 s, and the third one was for the periods between around 0.005 s to 0.1 s for the case of saturated water at atmospheric pressure.

1.1.2 Models for Incipient Boiling Superheat and CHF in Power Transients

Sakurai and Shiotsu (1977b) observed that the CHFs belonging to the first group existed on the points around the extension of the steady-state nucleate

boiling curve on the graph of heat flux, q, versus surface superheat, ΔT_{sat}. Based on this fact, they explained that the mechanism of CHF belonging to the first group would be the time lag of heat transfer crisis due to the hydrodynamic instability near solid surface, which occurs at the steady-state CHF. The steady-state CHF model due to the hydrodynamic instability was suggested by Kutateladze (1959) and Zuber (1959). After that, the transient CHF theoretical model due to the liquid-layer evaporation model was first suggested by Serizawa (1983).

On the other hand, the anomalous trend of CHFs belonging to the second and third groups for the period means that there exists another mechanism for the CHFs belonging to the second and third groups. However, the mechanism of CHFs for intermediate and short periods has never been resolved for a long time.

After that, Sakurai et al. (1992) carried out the experiments of the CHFs in liquid nitrogen caused by exponentially increasing heat inputs to a platinum horizontal cylinder at various pressures just as with the experiments for water mentioned above. The exponential periods were ranged from 20 s to 5 ms (from quasi-steady to rapid ones). They observed, for all the exponential periods tested, the direct transition from a non-boiling regime such as natural convection or transient conduction regime to film boiling without nucleate boiling at around atmospheric pressure. On the other hand, at the pressures higher than around atmospheric up to 2 MPa, the CHFs for periods first gradually increased from

the steady-state CHF to a maximum CHF, then it decreased and again increased with a decrease in period. This trend of CHFs for periods at higher pressures was just as with that clearly obtained by the water experiment at atmospheric pressure: direct transition to film boiling occurred in transient conduction regime for short periods. They assumed that the direct transition to film boiling occurred due to the explosive-like heterogeneous spontaneous nucleation (HSN) in originally flooded cavities at the HSN surface superheat lower than that of homogeneous spontaneous nucleation. All the cavities on the surface that could serve as nucleation sites would initially be flooded, since the liquid surface tension is so low that vapor is not entrained in surface cavities and there is no dissolved gas in liquid nitrogen except for possible trace amount of helium, hydrogen and neon. It was made clear that there exist the mechanisms of incipient boiling in liquid nitrogen due to the HSN in originally flooded cavities on the solid surface different from that due to the nucleation from active cavities of originally entrained vapor on the solid surface in water.

Then, Sakurai et al. (1993) intended to realize the initial boiling on a horizontal cylinder due to the HSN even in water by pre-pressurizing the water in the boiling vessel with an appropriate high pressure before each run, by which the boiling initiation from the active cavities previously entraining vapor would be eliminated. They performed the water experiments at pressures up to 1 MPa and liquid subcoolings up to 30 K for the cases without and with the pre-

pressurization by a 5 MPa before each experimental run. The anomalous trends of CHFs for the periods were observed for the case with pre-pressurization just as with that observed in the liquid nitrogen experiments mentioned above. The direct transition to film boiling was observed for a wide range of exponential period at atmospheric pressure. It was recognized that the direct transition at the initial boiling occurs due to the explosive-like HSN in originally flooded cavities.

A theoretical initial boiling temperature model for the lower limit of HSN temperature in saturated liquids due to a quasi-steadily increasing heat input (namely, a steady-state HSN temperature) was given by Sakurai et al. (1993, 1994). The model was shown to describe well the experimental data of steady-state HSN temperature in the liquids such as liquid nitrogen, liquid helium, ethanol and water pre-pressurized by appropriately high pressure.

1.1.3 Pressure Transients

Sakurai et al. (1980) carried out the experimental study on transient boiling heat transfer on a horizontal cylinder in a pool of water caused by rapid depressurization. They clearly observed that the initial non-boiling state on the test heater was switched over to a film boiling state after the rapid depressurization, and that the critical heat fluxes for these processes were

considerably lower than the steady-state critical heat fluxes at the corresponding pressures. The mechanism of this decrease in CHF during the pressure reduction has never been resolved for a long time.

1.2 THE PURPOSES OF THIS STUDY

The purposes of this study are, (1) to obtain systematically the database for the critical heat fluxes resulting from exponentially increasing heat inputs with various exponential periods on the test cylinders with commercial, mirror and rough surfaces in water for wide ranges of subcooling and pressure, (2) to obtain the database for the critical heat fluxes under rapid pressure reduction for wide ranges of initial pressure, initial heat flux, pressure reduction rate and cylinder diameter, and (3) to discuss whether these experimental results can be explained based on the CHF model suggested by Sakurai et al. mentioned above.

CHAPTER 2

EXPERIMENTAL APPARATUS AND METHOD FOR CHAPTERS 3 TO 5

2.1 APPARATUS AND METHOD

The apparatus used to measure the steady and transient boiling phenomena in Chapter 3 to 5 is shown schematically in Fig.2-1. It mainly consists of a boiling vessel (1), a pressurizer (5), and a liquid feed tank (8) with a booster pump (9). The boiling vessel is a cylindrical stainless steel pressure vessel of 20-cm inner diameter and 60-cm height capable of operating up to 5 MPa. The vessel has two sight ports and is equipped with a pressure transducer and a sheathed 1-mm diameter K-type thermocouple that is used to measure the bulk liquid temperature. A test heater (2) is supported in the vessel. The vessel is connected with a pipe through a valve and a booster pump to the liquid feed tank. The air-driven booster pump is used for the pre-pressurization before each experimental run.

The block diagram of the heating device for the test heater, and the measuring and data processing system are shown in Fig.2-2. A power amplifier controlled by a high-speed analog computer supplies direct current to the test

heater. The analog computer computes the instantaneous power generation rate in the heater and compares it with the reference value, $Q_0 \exp(t/\tau)$. Thus, the computer controls the output of the power amplifier so that the two values (heat generation rate and the reference value) are equal. In this way, steadily and exponentially increasing heat input is supplied to the heater. The analog computer also computes the instantaneous mean temperature of the heater and cuts off the power supply to the heater when the calculated mean temperature reaches a preset value. This procedure prevents the heater from actual burnout. The power amplifier consists of 800 power transistors in parallel and can supply 2000 A at 40 V. The heat generation rate in the heater is calculated from the measured voltage difference between the potential taps of the heater and the current measured using a Manganin standard resistance. The instantaneous mean temperature (volume averaged) of the heater, T_m, is calculated from the unbalanced voltage of a double bridge circuit including the heater. The instantaneous surface heat flux, q, is then obtained from the following heat balance equation for a given heat generation rate, Q:

$$q = \frac{1}{4} Q d - \frac{1}{4} c_{ps} \rho_s d \frac{dT_m}{dt} \tag{2-1}$$

The instantaneous surface temperature of the heater, T_w, is obtained solving the

following conduction equation using a digital computer for a given heat generation rate with given surface heat flux as a boundary condition:

$$k_s \frac{1}{r} \frac{\partial}{\partial \tau} \left(r \frac{\partial T}{\partial t} \right) + Q = c_{ps} \rho_s \frac{\partial T}{\partial t} \tag{2-2}$$

In data processing, a digital computer was used. The unbalanced voltage of the double bridge circuit including the heater, and the voltage differences between the potential taps of the heater and across the standard resistance were fed to the digital computer through an analog-to-digital converter (ADC). The fastest sampling speed of the ADC was 5 μs/channel. The experimental error is estimated to be about ±1 K in the heater surface temperature and ±2 % in the heat flux.

2.2 TEST HEATERS

The platinum horizontal cylinders of 1.2 mm in diam. and 90 mm in length were used as test heaters to measure steady and transient boiling phenomena. Two fine 30-μm diameter platinum wires were spot-welded as potential taps at around 20 mm from each end of the cylinder heater. The effective length of the heater between the potential taps was about 50 mm. These

test heaters were annealed and their electrical resistance-temperature relations were measured in water and glycerin baths. The measuring accuracy was estimated to be within ±0.5 K.

The 2-mm of platinum and 5-mm diam. stainless steel horizontal cylinders were also used to measure steady-state critical heat fluxes respectively.

2.3 EXPERIMENTAL PROCEDURE

Distilled and demineralized water is degassed by keeping it boiling for 30 minutes at least in the boiling vessel and in the water feed tank. The water was fully filled in the boiling vessel with the free surface only in the pressurizer and liquid feed tank. Water temperatures in the boiling vessel and in the pressurizer were separately controlled to realize the desired saturated and subcooled conditions. Pre-pressurization before each experimental run for a time of about 3 minutes was performed by the booster pump up to 5 MPa. The pre-pressurization at a high system pressure can be performed without increasing the amount of dissolved gases in water.

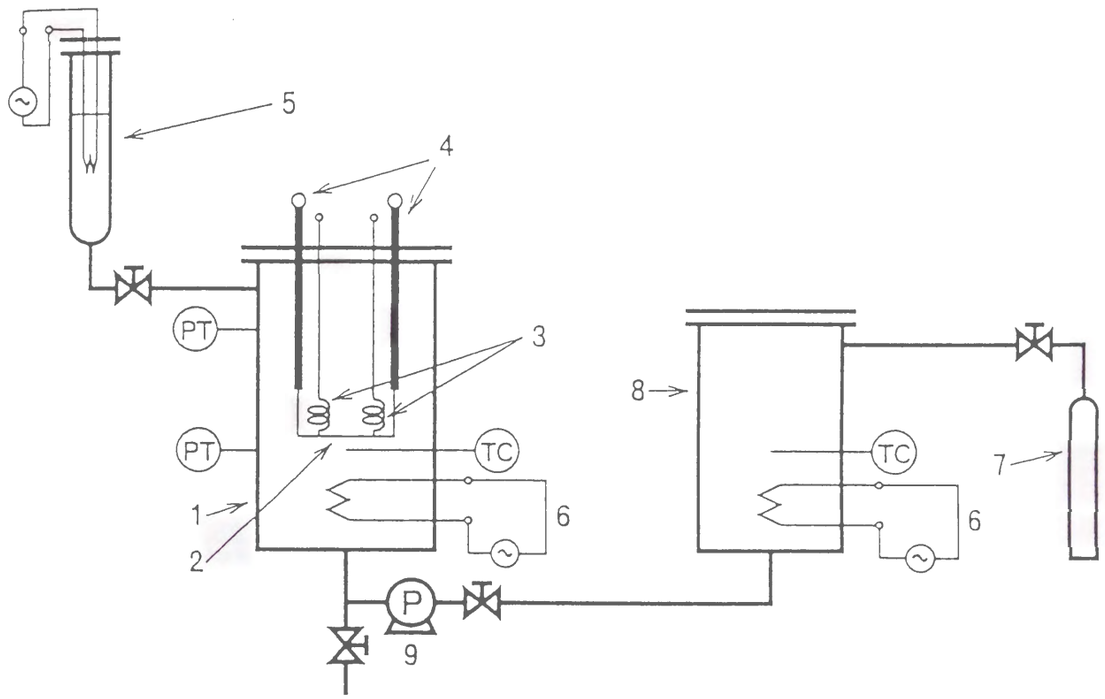

1 Boiling Vessel
2 Test Heater
3 Potential Taps
4 Electrodes
5 Pressurizer
6 Sheathed Heater
7 He Gas
8 Liquid Feed Tank
9 Booster Pump
(PT) Pressure Transducer
(TC) Thermocouple

Fig. 2-1 Schematic of experimental apparatus.

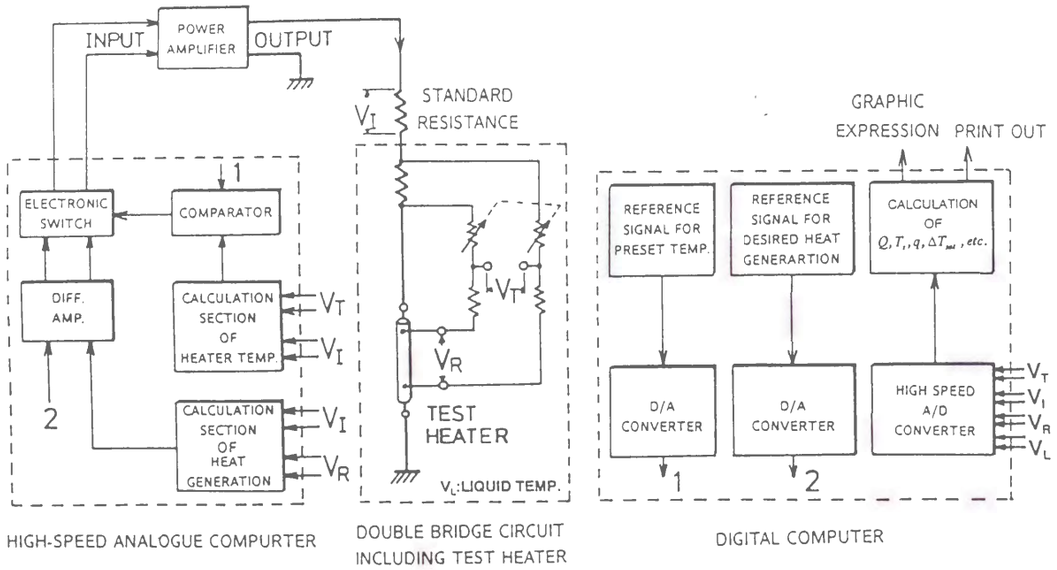

Fig. 2-2 Block diagram of the heating device for the test heater, and the measuring and the data processing system.

CHAPTER 3

STEADY-STATE POOL BOILING CRITICAL HEAT FLUX ON A HORIZONTAL CYLINDER IN WATER AND ITS MECHANISM

3.1 INTRODUCTION

The correct understanding of the cooling limits of high heat fluxes encountered in many important engineering and scientific systems especially in plasma-facing components in fusion reactors becomes necessary. Many experimental investigations for highly subcooled flow boiling of water were carried out recently. On the other hand, though the critical heat fluxes in a pool of water up to high subcoolings and pressures are important as the fundamental database to understand those at zero velocity of water, no systematic studies on the critical heat fluxes in pool boiling of water for wide ranges of subcooling and pressure exist till quite recently. Sakurai et al. (1993, 1995) carried out the pool boiling experimental studies for high subcoolings at high pressures in water due to quasi-steadily increasing heat inputs as a part of their transient boiling experiments. They suggested based on their data for water that there exist two different mechanisms for heat transfer crisis at critical heat flux for low and high subcooled regions. The former would be due to hydrodynamic instability and the

latter would be due to heterogeneous spontaneous nucleation in originally flooded cavities on the solid surface in fully developed nucleate boiling regime.

The purpose of this chapter is to confirm the existence of the latter CHF mechanism for the test heaters with different diameters and shapes in water at pressures.

3.2 EXPERIMENTAL RESULTS AND DISCUSSION

3.2.1 Experimental Conditions

Pool boiling critical heat fluxes were measured on a 1.2-mm diameter horizontal cylinder test heaters in water for the pressures ranging from 101.3 kPa to 2063 kPa, and for the liquid subcoolings from 0 to 180 K. Heat input to the test heater was increased quasi-steadily as an exponential time function with the period of 20 s. The experiments for the case with pre-pressurization before each experimental run were also carried out for the experimental conditions same as those for the case without pre-pressurization. The pre-pressurization was made at a high pressure of around 5 MPa for a time of about 3 minutes. The critical heat fluxes were also measured on test heaters of various shapes such as a vertical ribbon (thickness of 0.2 mm, width of 5.4 mm, and the effective length of 34.2 mm), a vertically oriented horizontal ribbon (thickness of 0.2 mm, width of 5.4 mm, effective length of 24.6 mm) and a lower-side insulated horizontal

flat ribbon (horizontal plate, thickness of 0.49 mm, width of 6 mm, effective length of 34.2 mm) for wide ranges of experimental conditions without pre-pressurization.

3.2.2 Critical Heat Flux for a 1.2 mm Horizontal Cylinder

The CHF values, q_{cr}, on a 1.2 mm horizontal cylinder in water were measured for the ranges of pressure from 101.3 to 2063 kPa and subcooling from zero to 180 K. The obtained q_{cr} values are shown versus subcooling in Fig.3-1 with pressure as a parameter, and shown versus pressure in Fig. 3-2 with subcooling as a parameter. The CHF values for the subcoolings lower than near 40 K were clearly dependent on pressure. The q_{cr} value at each pressure almost agrees with each other for the subcooling of 40 K. The CHF values for the subcoolings higher than 40 K at pressures lower than about 200 kPa are also dependent on pressures and rapidly increase with an increase in subcooling. On the other hand, the CHF values for the subcoolings higher than 40 K at pressures higher than about 700 kPa are almost independent of pressures and gradually increase with an increase in subcooling. The CHF values do not agree with the values obtained from well known existing correlations by Kutateladze (1959), Zuber (1959), and Ivey and Morris (1962) as shown in Fig. 3-1 except those for a very narrow range of subcoolings from zero to about 20 K. The CHF values

for saturated conditions, $\Delta T_{sub} = 0$, at pressures up to 2063 kPa agreed with the values derived from the Kutateladze's correlation with the constant of 0.17 within about ±3 % error as clearly seen in Fig.3-2.

The following new correlation was derived by modifying the Kutateladze's CHF correlation for subcooled condition taking into account the non-linear effect of subcooling observed in the experimental data of this work on horizontal cylinders for wide ranges of subcooling and pressure.

$$q_{cr,sub} = q_{cr,sat}\left[1 + K_2\left(\rho_l/\rho_v\right)^{0.69}\left(c_{pl}\Delta T_{sub}/h_{lg}\right)^{1.5}\right] \tag{3-1}$$

where

$$q_{cr,sat} = K_1 h_{lg}\rho_g\left[\sigma g\left(\rho_l - \rho_g\right)/\rho_g^2\right]^{1/4} \tag{3-2}$$

where $K_1 = 0.17$. The predicted values of CHF by the correlation are shown in comparison with the experimental data in Figs. 3-1 and 3-2. The predicted values agree with the corresponding experimental data for the subcoolings from 0 to 40 K at all the pressures tested. At pressures lower than about 200 kPa, the predicted values also agree with the corresponding data for the subcoolings up to 80 K within about ±5 % difference each other. The values of CHF for the subcoolings higher than about 60 K at higher pressures do not agree with the predicted values, because the CHF becomes almost independent of the pressures

higher than around 500 kPa.

Following empirical equation of CHF that is independent of pressures for the subcoolings higher than about 60 K at pressures higher than about 500 kPa was derived.

$$q_{cr,sub} = K_3\Delta T_{sub}^{0.73} \tag{3-3}$$

where $K_3 = 3.81\times 10^5$. The curve given by Eq.(3-3) is also shown in Fig. 3-1 for comparison. The measured $q_{cr,sub}$ values lie almost within ±5 % of the corresponding values derived from Eq.(3-3).

The power value of 1.5 in Eq.(3-1) was determined so that the modified correlation can better express the experimental data for low subcoolings depending on pressures. Kutateladze supposed in his analysis that the liquid temperature in the two-phase boundary layer was saturated. However, there exists the thermal boundary layer in the liquid in the vicinity of the heating surface. The existence of thermal boundary layer was observed by Marcus and Dropkin (1965). According to their observation, the temperature at any fixed point in the thermal boundary layer was widely and rapidly fluctuating variable and the average temperature within the layer appeared to be essentially linear very near the heating surface. As the thermal boundary layer exists in the two-

phase boundary layer, average temperature of the liquid in the two-phase boundary layer is higher than the saturation temperature. The removal of the superheated liquid from the two-phase boundary layer would exist even in subcooled critical heat flux. It can be explained according to the Kutateladze's model that the power value higher than unity in Eq.(3-1) may correspond the contribution of extra sensible heat transport due to the release of superheated liquid from the two-phase boundary layer accompanied with rising vapor bubbles from the surface, instead of the release of saturated liquid predicted by the model. On the other hand, the CHF values for high subcoolings at high pressures cannot be expressed by the correlation, Eq.(3-1). This means that there exists another mechanism of heat transfer crisis at the CHF different from that based on the hydrodynamic instability.

3.2.3 Mechanism of Heat Transfer Crisis at CHF for High Subcooling at High Pressure

Sakurai et al. (1993, 1994) measured the initial boiling surface superheats, ΔT_i, in water and in liquid nitrogen at atmospheric pressure after raising the system pressure to a certain value, keeping the value for about 3 minutes and then decreased it down to atmospheric pressure. The pre-pressurization in case of water was made by hydrostatic pressure to prevent the

dissolution of gases. Their value of ΔT_i for water are shown in Fig. 3-3 versus pre-pressure. The ΔT_i values estimated from the existing cavity theory (Griffith et al., 1960) (Fabic, 1964) (Holtz, 1966) (Chen, 1968) (Dwyer, 1969) become higher for the higher value of pre-pressure. However, the measured ΔT_i values were expressed by two straight lines (a, b). The line (a) for lower pre-pressures shows the effect of pre-pressure on initial boiling surface superheat due to active cavities on the test cylinder surface. The constant line (b) for the higher pre-pressures shows that the boiling initiation mechanism was replaced from that by active cavities entraining vapor to another mechanism by which the boiling initiation occurs at a constant surface superheat independent of the pre-pressures.

On the other hand, the whole measured ΔT_i values for liquid nitrogen with pre-pressurization by helium gas were approximately expressed by the constant line (b') independently of the pre-pressure. The boiling initiation in liquid nitrogen was assumed to occur due to the heterogeneous spontaneous nucleation (HSN) in flooded cavities without the contribution of active cavities in general. Namely, there exist no active cavities on the test cylinder surface in liquid nitrogen because there is no known dissolved gas content and liquid surface tension is so low that vapor bubbles are not entrained in the surface cavities. The initial boiling in water corresponding to the constant ΔT_i line (b) was assumed to occur by the HSN in originally flooded cavities on the cylinder

surface. The potential active cavities entraining vapor for initial boiling requiring the surface superheat lower than the surface superheat corresponding to the constant ΔT_i line were eliminated by the pre-pressure higher than about 2 MPa.

All the data for the case with pre-pressurization are obtained by the pre-pressure of about 5 MPa in this work. For the pre-pressure of 5 MPa, the potentially active cavities requiring the initial boiling surface superheat lower than around 60 K (the value on the extrapolation of the curve (a) at 5 MPa) are eliminated. The HSN surface superheat is affected by the rates of increasing heat inputs (namely, by the increasing rate of surface superheat) as will be mentioned in Chapter 4. Sakurai et al. (1993, 1995) measured the lower limit of HSN surface superheat, ΔT_{iLH}, in saturated water, liquid helium I, liquid nitrogen and ethanol at various pressures. They proposed a theoretical model of HSN surface superheats for saturated liquids that can describe well their data of ΔT_{iLH}.

It is assumed that the heat transfer crisis at CHF for high subcoolings at high pressures would occur due to the explosive-like HSN in originally flooded cavities on the cylinder surface at the lower limit of HSN surface superheat in fully developed nucleate boiling (FDNB) regime. This assumption is based on the following facts. Figures 3-4 and 3-5 show the typical heat transfer processes up to CHF point through initial boiling point in water due to exponential heat inputs, $Q_0 \exp(t/\tau)$, with the period τ of 20 s (namely, quasi-steady heat

inputs) on the $\log q$ versus $\log \Delta T_{sat}$ graph. Pre-pressurization with 5 MPa for a while was made before each run. The processes in Fig. 3-4 are for the subcooling of 60 K at pressures ranging from 101.3 to 2063 kPa, and those in Fig. 3-5 are for the subcoolings ranging from 0 to 60 K at the pressure of 101.3 kPa. Solid circles show the initial boiling points and solid triangles show the CHF points in FDNB regime. Although it is not shown in these figures to avoid too much complexity, the processes up to CHF points in FDNB regime for the cases with and without pre-pressurization agreed well with each other. Let the surface superheat at CHF be ΔT_c and the initial boiling surface superheat which corresponds to lower limit of HSN surface superheat be ΔT_{iLH}. As shown in Fig. 3-4, the ΔT_c on each heat transfer process for the pressure higher than around 500 kPa almost agrees with the lower limit value ΔT_{iLH} ($\Delta T_{iLH} \approx \Delta T_c$). On the contrary, the lower limit values of HSN surface superheat, ΔT_{iLH}, for the subcoolings ranging from 0 to 60 K at atmospheric pressure are all higher than the ΔT_c, ($\Delta T_{iLH} > \Delta T_c$), as shown in Fig.3-5. Namely, the critical heat fluxes for the heat transfer processes shown in Fig. 3-5 are reached before the occurrence of explosive-like HSN. Therefore, the CHF values are well predicted by Eq. (3-1), being free from the effect of HSN. The ΔT_i, and ΔT_c for the subcooling of 60 K at pressures from 0 to about 2 MPa for the case without pre-pressurization, and initial boiling surface superheat for the case with pre-pressurization, ΔT_{iLH},

are shown versus system pressure, P, in Fig.3-6. The values of ΔT_i and ΔT_c for the pressures higher than around 700 kPa almost agree with the corresponding values of ΔT_{iLH}. This fact leads to that the $q_{cr,sub}$ values for higher subcoolings at pressures higher than around 700 kPa become lower than those calculated from Eq.(3-1) as clearly shown in Fig.3-2.

3.2.4 The CHF Correlation for High Subcooling in Water

Though Sakurai et al. (1993) have already presented a model for the lower limit of HSN temperature that was shown to be applicable for similar solid surfaces in various liquids under saturated condition, a general prediction of CHF values for high subcoolings at high pressures is difficult at present. This is because there are no general expressions for the HSN surface superheat and the heat transfer in fully developed nucleate boiling regime for a certain solid surface. More extension of the research works for the problems are needed. It is possible to derive an empirical correlation for solid surfaces with similar surface conditions such as the cavity size distribution, wettability and so on for the solid surface concerned. It can be seen with sharp eyes that the experimental CHF values for high subcoolings at high pressures slightly depend on pressures. It is supposed that appreciable pressure dependence may appear at the pressures up to critical pressure greatly higher than those tested here. In fact, as is mentioned

later, the CHF values due to HSN significantly dependent on pressure exist for whole subcoolings including saturation conditions at pressures with higher critical pressure ratio, P/P_{cr} for other liquids. Following non-dimensional empirical correlation for $q_{cr,sub}$ dependent on pressures was obtained.

$$q_{cr,sub} = q^*_{cr,sat}\left[1+\left(\rho_l/\rho_g\right)^{0.5}\left\{A\left(c_{pl}\Delta T_{sub}/h_{lg}\right)+B\left(c_{pl}\Delta T_{sub}/h_{lg}\right)^2+C\left(c_{pl}\Delta T_{sub}/h_{lg}\right)^3\right\}\right] \quad (3\text{-}4)$$

where $q^*_{cr,sat}$ is the potential CHF for saturated condition due to the heterogeneous spontaneous nucleation, although the actual CHF occurs due to the hydrodynamic instability below the value under the condition. The $q^*_{cr,sat}$ was estimated as the heat flux on the extended developed nucleate boiling curve at the lower limit of HSN superheat ΔT_{iLH} obtained here by the method mentioned above. The $q^*_{cr,sat}$ values are 4×10^6, 4.3×10^6 and 4.5×10^6 W/m^2 for the pressures of 1082, 1475 and 2063 kPa, and the coefficients A, B and C are 0.31, 2.6 and -4.0, respectively.

Figure 3-7 shows the comparison of the typical CHF data for high subcoolings at pressures of 1082 and 2063 kPa with the corresponding CHF curves obtained from Eq.(3-4). The experimental data slightly depending on the pressures agree well with the corresponding predicted values. The $q_{cr,sub}$ values

supposed in FDNB at values of ΔT_{iLH} for subcoolings at 2063 kPa are also shown in the figure. They agree with corresponding experimental data. Effects of the test heater shapes and kinds of liquids on the correlation are shown later.

3.2.5 The CHFs for Various Shaped Heaters in Water and Their Correlations

Critical heat fluxes were measured on the cylinder test heaters with various diameters and on the heaters with different shapes for wide ranges of subcoolings and pressures. The trend of CHF versus liquid subcoolings obtained for each test heater was just similar to that obtained for the 1.2 mm-diameter horizontal cylinder mentioned before. The CHF values for the subcoolings lower than 60 K were expressed by Eqs.(3-1) and (3-2) with the coefficients K_1 and K_2, and those for the subcoolings higher than 60 K were by Eq.(3-3) with the coefficients A, B and C.

The measured CHFs on the horizontal cylinders with the diameters of 1.2, 2 and 5 mm in water were for liquid subcoolings up to 180 K and pressures up to 2 MPa. It was deduced from the results that two CHF mechanisms exist: one is due to the hydrodynamic instability (HI) and the other is due to the heterogeneous spontaneous nucleation (HSN). The CHF correlation for lower subcooling based on the hydrodynamic instability is expressed by Eqs. (3-1) and

(3-2). Equation (3-1) was obtained by modifying the Kutateladze's subcooled CHF correlation [3] taking into account the nonlinear effect of subcooling based on the experimental data. Kutateladze's correlation did not provide a good prediction of the experimental data. The values of K_1 and K_2 for the horizontal cylinder diameters of 1.2 mm, 2 mm, 5 mm were determined based on the author's data and those for the diameter of 5.8 mm were on the data by Ponter & Haigh (1969).

The constants K_1 and K_2 obtained for water are shown in Fig. 3-8 versus non-dimensional length L' expressed by Eq. (3-6). The K_1 values are close to 0.17 and are independent of the cylinder diameters tested. The K_2 values are independent of the pressures, and are only dependent on the cylinder diameters. They are on a straight line expressed by the following equation.

$$K_2 = 0.38\left(1 - \log_e L'\right) \tag{3-5}$$

where

$$L' = \frac{d/2}{\sqrt{\sigma / g\left(\rho_l - \rho_g\right)}} \tag{3-6}$$

The non-dimensional length L' means the ratio of the cylinder radius $d/2$ to the Laplace length that is proportional to the dangerous wavelength of hydrodynamic Taylor instability. The L' was used by Lienhard and Dhir (1973)

to express the effect of cylinder diameter on saturated CHF in various liquids. The values of K_1 for large and small cylinders predicted by the correlation of Lienhard and Dhir (1973) are also shown in the figure as broken lines for comparison.

The $q_{cr,sub}$ versus ΔT_{sub} relations for 2-mm and 5-mm diameter horizontal cylinders are shown with pressure as a parameter in Figs.3-9 and 3-10 respectively. The CHF data for subcoolings of up to 60 K at atmospheric pressure on 5.84 mm horizontal cylinder in water obtained by Ponter and Haigh (1969) are also shown in Fig.3-10 for comparison. The CHF data for the 5-mm diameter horizontal cylinder at the pressure of 101.3 kPa agreed well with the data by them. As shown in these figures, the trends of CHF versus liquid subcooling at pressures for all of these test heaters are similar to that for the 1.2 mm-diameter horizontal cylinder. The corresponding curves of $q_{cr,sub}$ versus ΔT_{sub} for the pressures obtained from Eqs.(3-1), (3-2) and (3-4) with the corresponding constants shown in Table 3-1 are also shown in the figures. The K_1 values for the horizontal cylinders are just the same each other, 0.17. Namely, the $q_{cr,sat}$ for such diameters are the same each other independently of the diameters. On the other hand, K_2, A, B and C for the horizontal cylinders are significantly different each other. The values of A, B and C for 5-mm diameter horizontal cylinder, the vertical ribbon and the horizontal vertically

oriented ribbon are the same as each other. The values of K_2 for the first and second ones are almost same, 0.356 and 0.375, respectively. The horizontal vertically oriented ribbon and the vertical ribbon are just the same heater except its orientation. The values of K_1 and K_2 for the horizontal vertically oriented ribbon and the vertical ribbon are significantly different though the values of A, B and C are the same each other. The value of K_2 for the horizontal flat ribbon (horizontal plate) is 0.87 which is the highest for the ribbons shown in Table 3-1. It seems that the K_2 value is higher for lower specific height. It is supposed that the K_2 value for the vertical ribbon with larger height will become about 0.375.

3.3 COMPARISON OF CHF MODEL WITH AVAILABLE DATA

3.3.1 The Subcooled CHFs in Ethanol

The CHFs in ethanol were measured by Kutateladze and Schneiderman (1953) for subcoolings ranging from about 0 to 120 K at pressures from 101.3 to 1013 kPa to determine the constants in their correlation for $q_{cr,sub}$. The CHF values were estimated from their reported values of $q_{cr,sub}/q_{cr,sat}$ by using the $q_{cr,sat}$ values given by Eq.(3-2) with K_1 of 0.13. Their data of $q_{cr,sub}$ thus estimated and the curves for 101.3 and 1013 kPa obtained by their correlation are shown in Figs. 3-11 and 3-12. The curves derived from Eqs. (3-1), (3-2) and

(3-4) with the constants shown in Table 3-2 are also shown in the figure. It seems from Fig. 3-11 that, though their data for the subcoolings lower than about 10 K at pressure of 101.3 K agree with the values derived from Eqs. (3-1) and (3-2) based on the hydrodynamic instability model, other data approximately agree with the values derived from Eq. (3-4) with the constants shown in Table 3-2. It can be assumed from these facts that most of the CHF values except those for the narrow range of subcoolings from zero to about 10 K at the pressure of 101.3 kPa are due to the HSN. As shown in Fig. 3-12, most of the data do not agree with the values derived from Eqs. (3-1) and (3-2).

3.3.2 The CHFs in Methanol

Elkassabgi and Lienhard (1988) have measured the pool boiling CHF on horizontal cylinder heaters in acetone, Freon 113, methanol and iso-propanol over ranges of subcoolings from zero to 130 K. It was suggested that there are three distinct mechanisms of heat transfer crisis at different levels of subcooling and three correlations were presented for the regions of lower, intermediate and high subcooling based on their data for horizontal cylinders. Their data for methanol are shown in Fig. 3-13 as a typical one with the curves derived from their correlations. The values derived from Eqs. (3-1), (3-2) and (3-4) with the constants shown in Table 3-2 are also shown in the figure. The CHF data for the

subcoolings lower than about 15 K agree with the values derived from Eqs. (3-1) and (3-2). Those for the subcoolings higher than about 15 K agree with the values derived from Eq. (3-4) with the constants shown in Table 3-2. Namely, it is supposed that the heat transfer crisis at the CHF occurs due to the HSN in fully developed nucleate boiling (FDNB). It should be noted that the K_2 of 0.87 is just the same as that for water for the 1.2 mm-diameter horizontal cylinder, and K_1 of 0.18 is approximately the same as 0.17 for water.

3.4 THE COMPARISON OF THE CHF CORRELATIONS FOR SUBCOOLINGS WITH EXISTING ONES

The curves representing the experimental results of $q_{cr,sub}$ for a 1.2 mm-diam. horizontal heater in water at the pressures of 101.3, 1082 and 2063 kPa derived from Eqs. (3-1) and (3-2), and at the pressures of 1082 and 2063 kPa derived from Eq. (3-4) are shown in Fig. 3-14 versus ΔT_{sub}. The corresponding curves derived from the correlations for low and intermediate subcoolings given by Elkassabgi and Lienhard (1988) and those derived from the correlation for subcoolings given by Zuber (1959) are also shown in the figure for comparison. It is recognized that the existing correlations did not explain the $q_{cr,sub}$ obtained here that are expressed well by the curves obtained from Eqs. (3-1), (3-2) and

(3-4).

3.5 CONCLUSIONS

The CHF values for wide ranges of subcoolings and pressures were measured on various shaped test heaters such as horizontal cylinders with various diameters, a vertical ribbon, a vertically oriented horizontal ribbon and a lower-side insulated horizontal flat ribbon in water. Experimental data lead to the following conclusions:

(1) The $q_{cr,sub}$ data on 1.2 mm diameter horizontal cylinder in water for subcoolings from zero to 40 K at all the pressures, and those for the subcoolings from zero to 80 K at the pressures of atmospheric and 199 kPa are dependent on the pressure. On the contrary, the $q_{cr,sub}$ data for the subcoolings from 60 K to 180 K at pressures from around 0.4 MPa to 2 MPa are almost independent of the pressure and gradually increase with an increase in subcooling.

(2) The $q_{cr,sub}$ data in the former region of lower subcooling are in good agreement with the corresponding values predicted by the modified Kutateladze's correlation presented, Eqs. (3-1) and (3-2). The correlation over-

predicts the data for other conditions. The $q_{cr,sub}$ data in the latter region are well expressed by the empirical equation given for the range of subcooling and pressure, Eq. (3-3); most of the data exist within ±5 % of the corresponding predicted values.

(3) It can be assumed from the experimental results above mentioned that there exist two different mechanisms of heat transfer crisis at $q_{cr,sub}$ for lower and higher subcoolings. Namely, the former mechanism of heat transfer crisis would be due to the hydrodynamic instability and the latter one would be due to the heterogeneous spontaneous nucleation in originally flooded cavities on the test heater surface in the fully developed nucleate boiling.

(4) Similar trend of CHF for wide ranges of subcoolings and pressures for the test heaters of various shapes was obtained. Existing correlations such as Kutateladze, Ivey and Morris, and Zuber ones cannot explain the CHF values for the subcoolings up to 180 K except those for the narrow range of subcoolings up to 20 K at the pressures.

(5) The CHF values for lower subcoolings dependent on pressure on the test heaters of various shapes in water were expressed with good accuracy by the author's modified Kutateladze correlation based on the hydrodynamic instability

model. It was clarified that the CHFs due to the conventional hydrodynamic instability exist at low pressures near atmospheric pressure for the narrow range of subcooling in ethanol and methanol.

(6) The non-dimensional empirical correlation, Eq. (3-4), for CHF values for high subcoolings at high pressures in water which slightly depend on pressures was given.

(7) It was clarified that the CHF values for subcoolings at which the heat transfer crises occur due to the HSN existed even for saturated conditions in ethanol at comparatively high pressures near critical one.

(8) The constants of correlations based on the hydrodynamic instability and the HSN for low and high subcoolings were determined by the corresponding experimental data for the test heaters with various shapes.

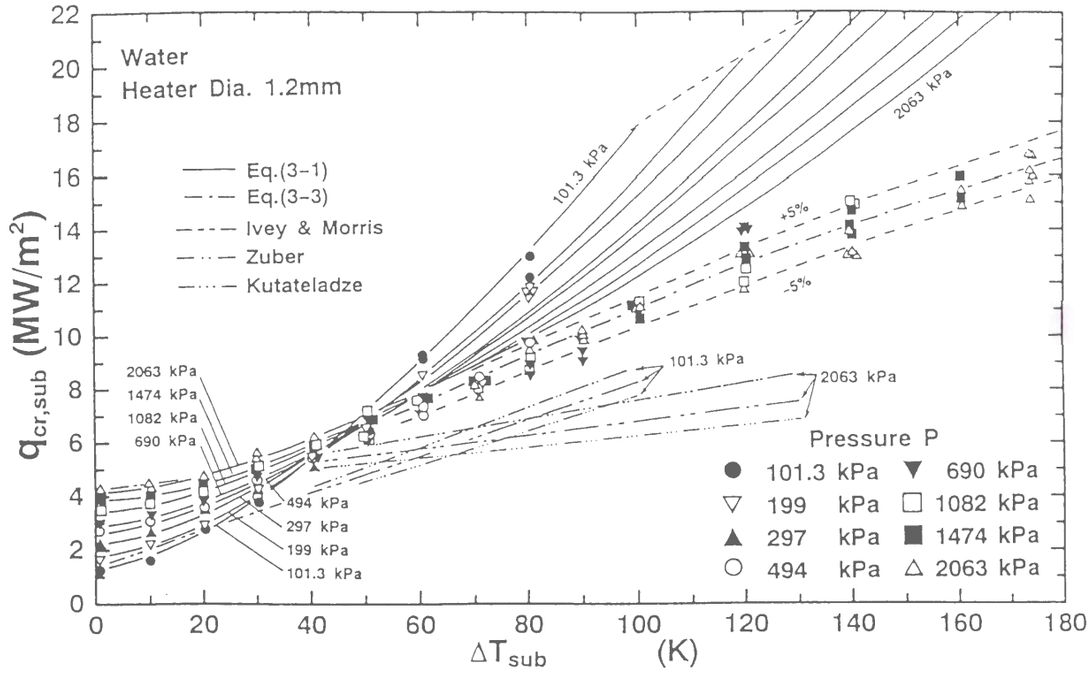

Fig. 3-1 Critical heat flux versus liquid subcooling with pressure as a parameter.

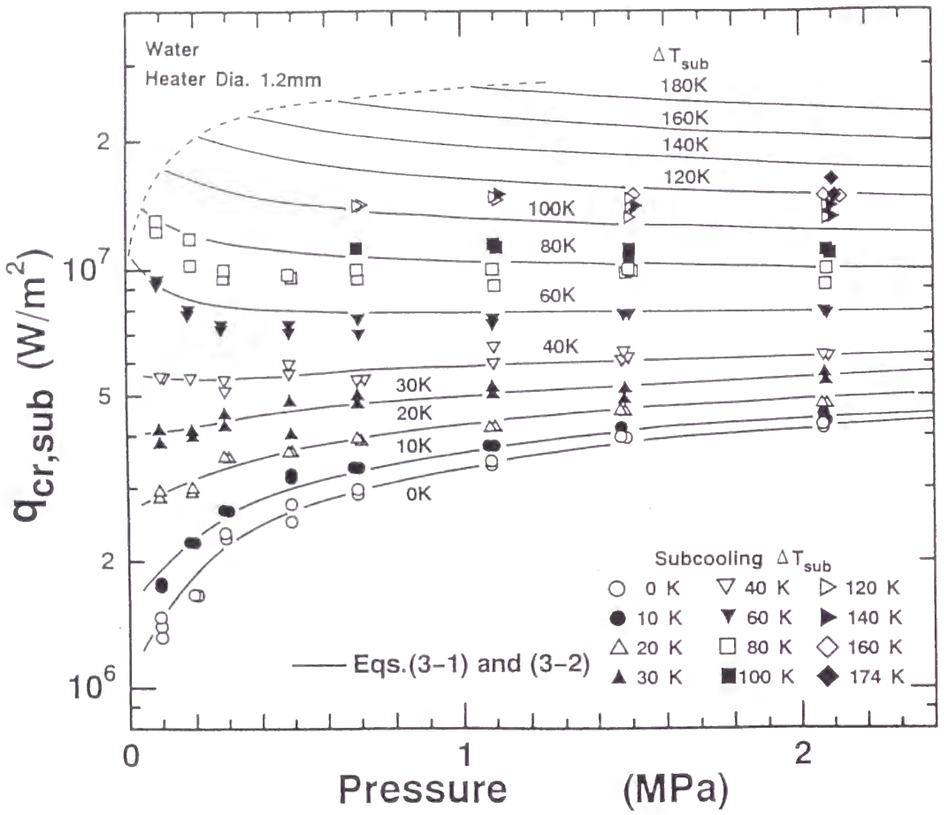

Fig. 3-2 Critical heat flux versus pressure with liquid subcooling as a parameter.

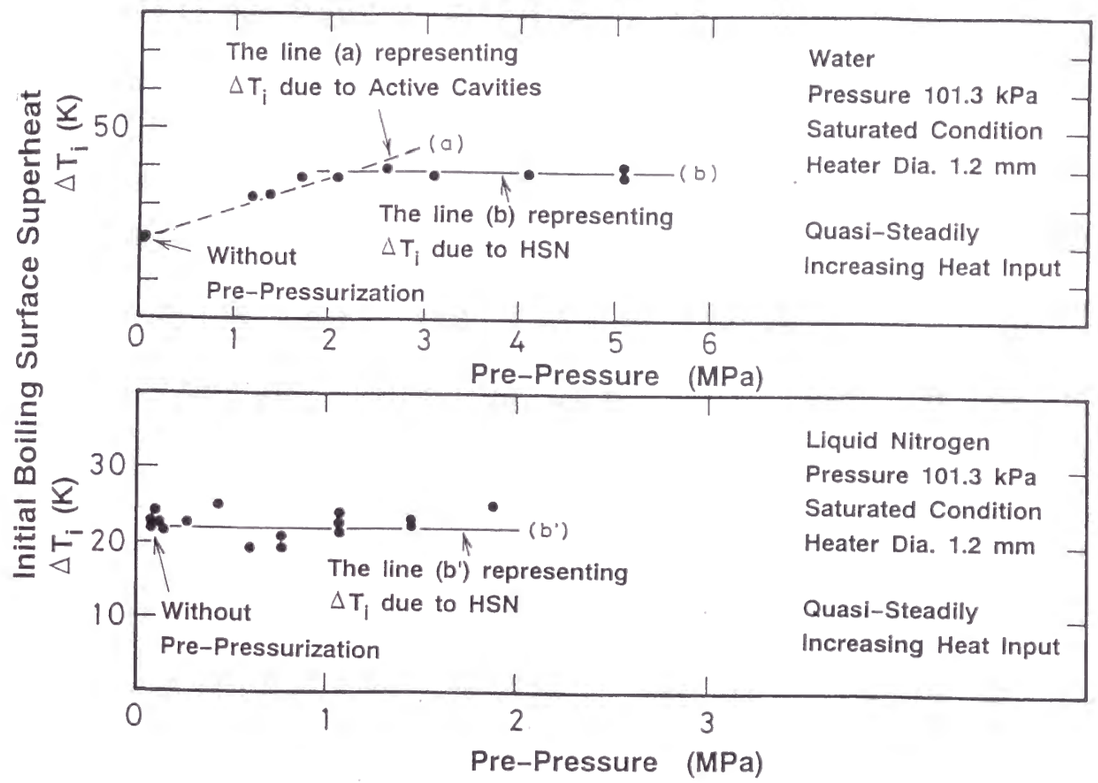

Fig. 3-3 Incipient boiling superheat versus pre-pressure of water and liquid nitrogen (Sakurai et al., 1993, 1994).

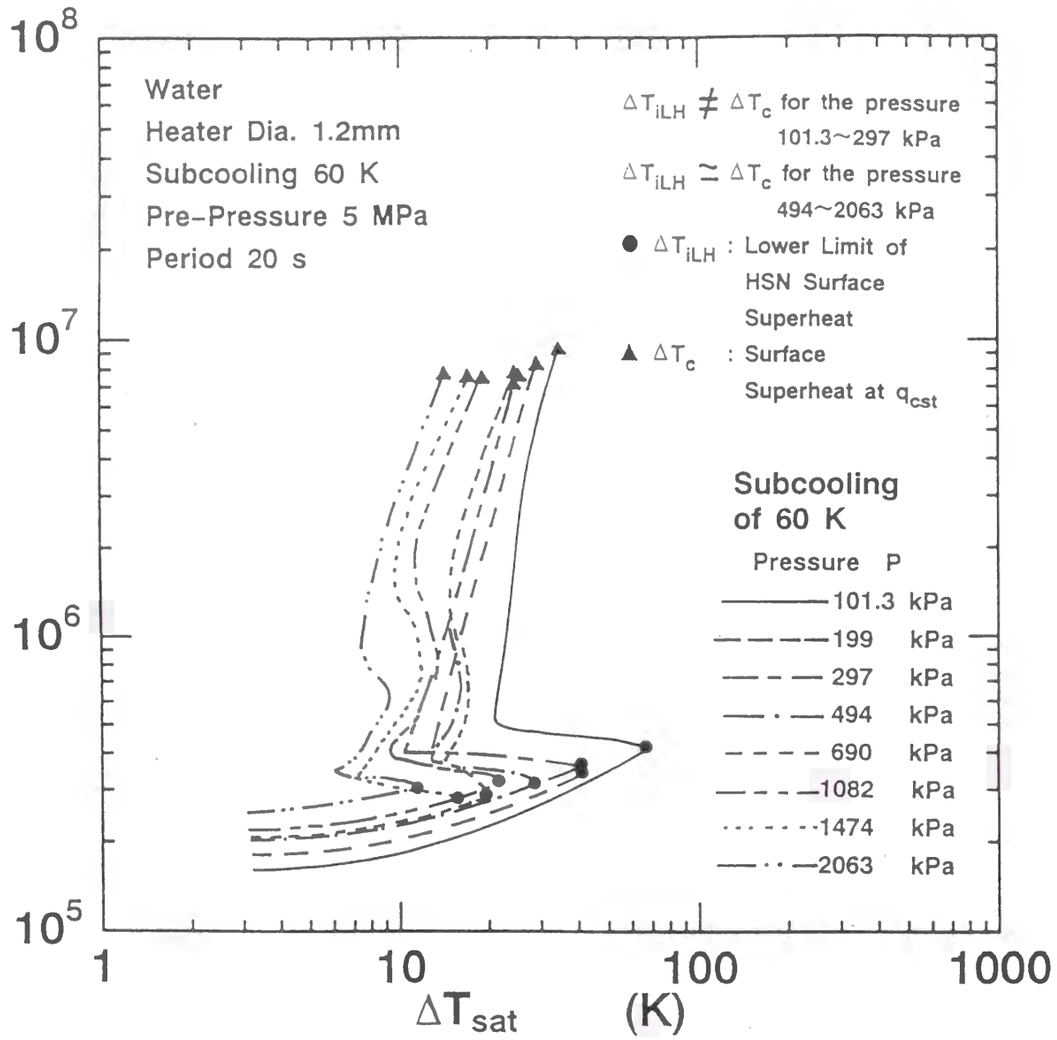

Fig. 3-4 Comparison between initial boiling surface superheat, ΔT_i, and surface superheat at critical heat flux, ΔT_c, for subcooling of 60 K at various pressures.

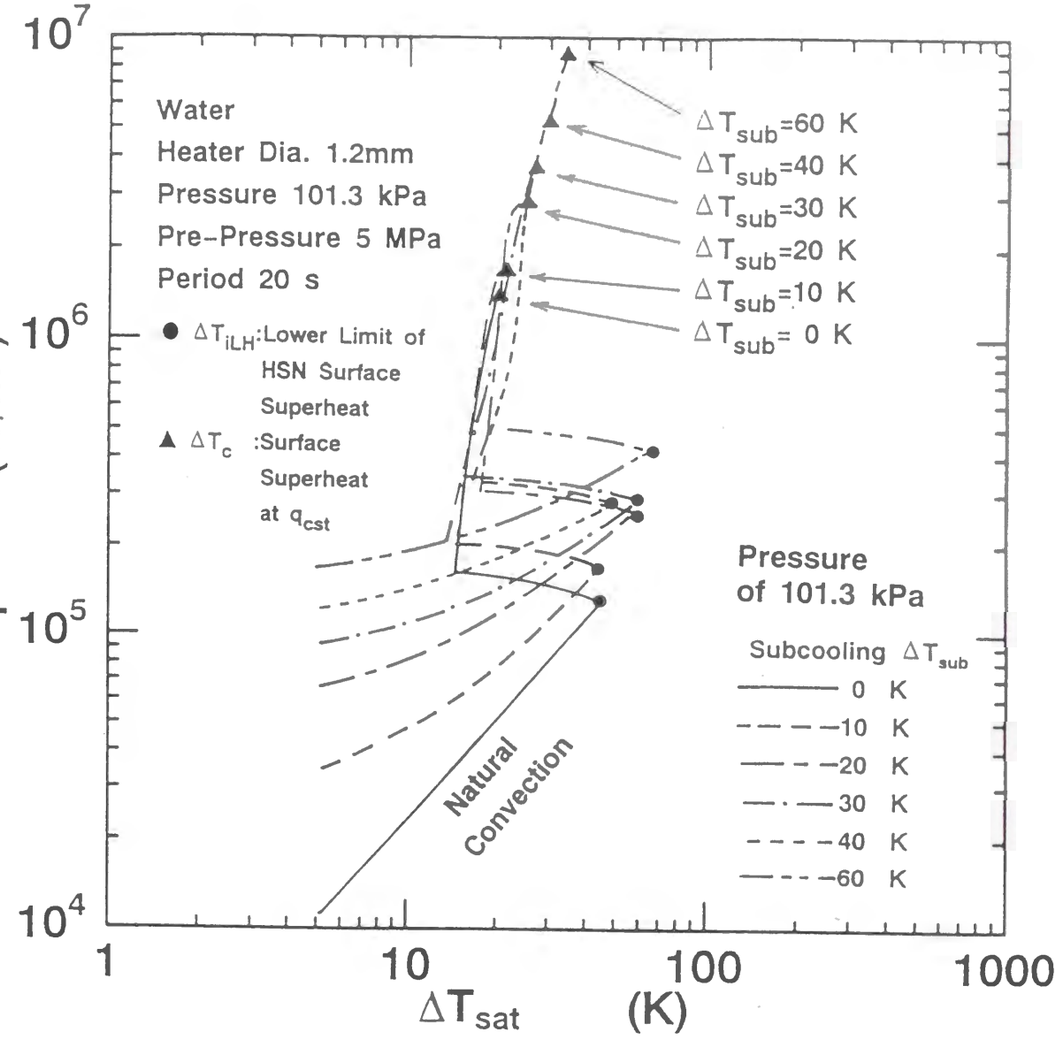

Fig. 3-5 Comparison between initial boiling surface superheat, ΔT_i, and surface superheat at critical heat flux, ΔT_c, for various subcoolings at atmospheric pressure.

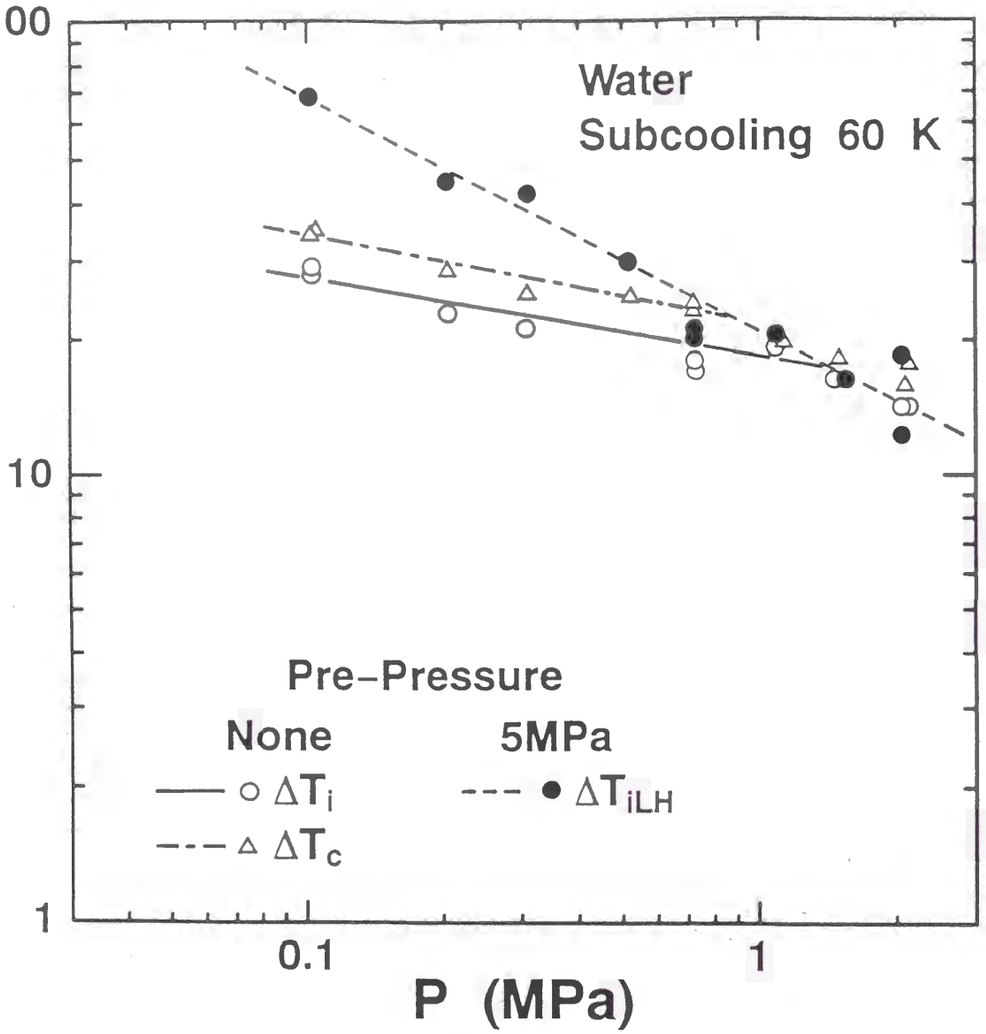

Fig. 3-6 Surface superheats ΔT_{iLH}, ΔT_i, and ΔT_c, versus pressure for subcooling of 60 K.

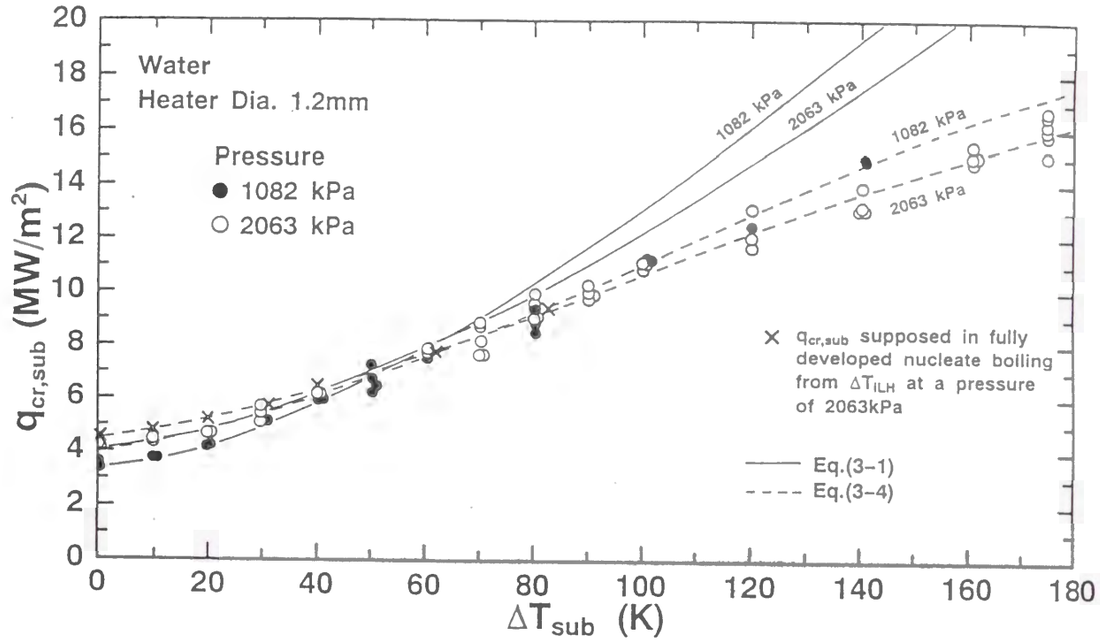

Fig. 3-7 Comparison of the typical CHF data for high subcoolings at pressures of 1082 and 2063 kPa with the corresponding CHF curves obtained from Eqs. (3-1) and (3-4).

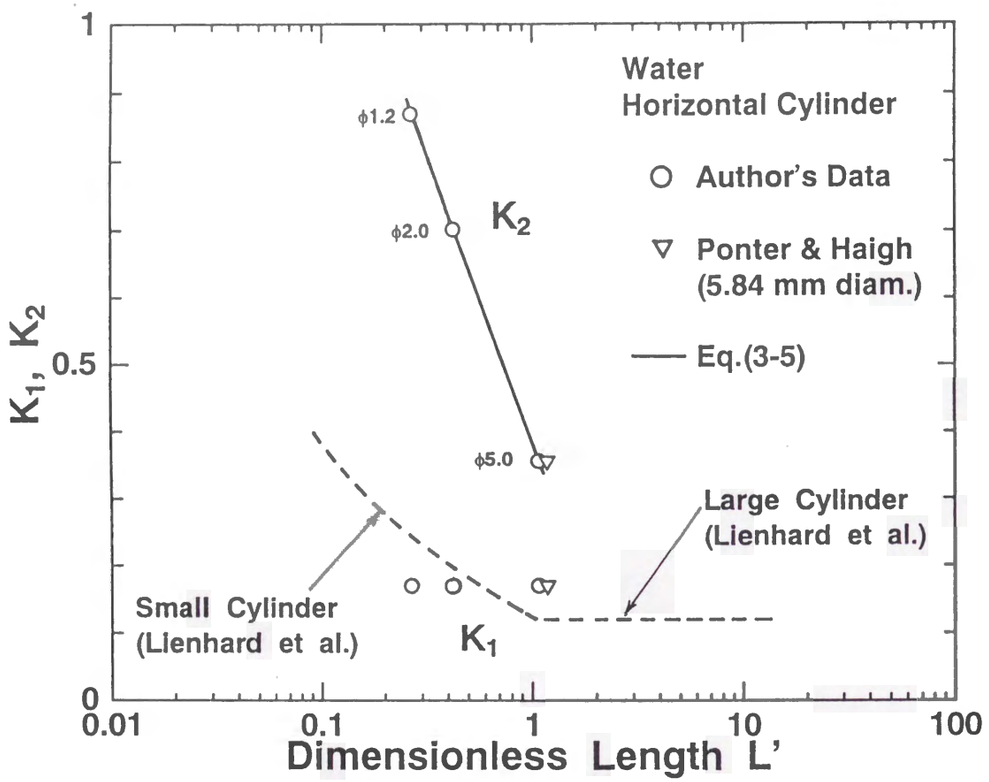

Fig. 3-8 K_1 and K_2 values obtained for water versus dimensionless length.

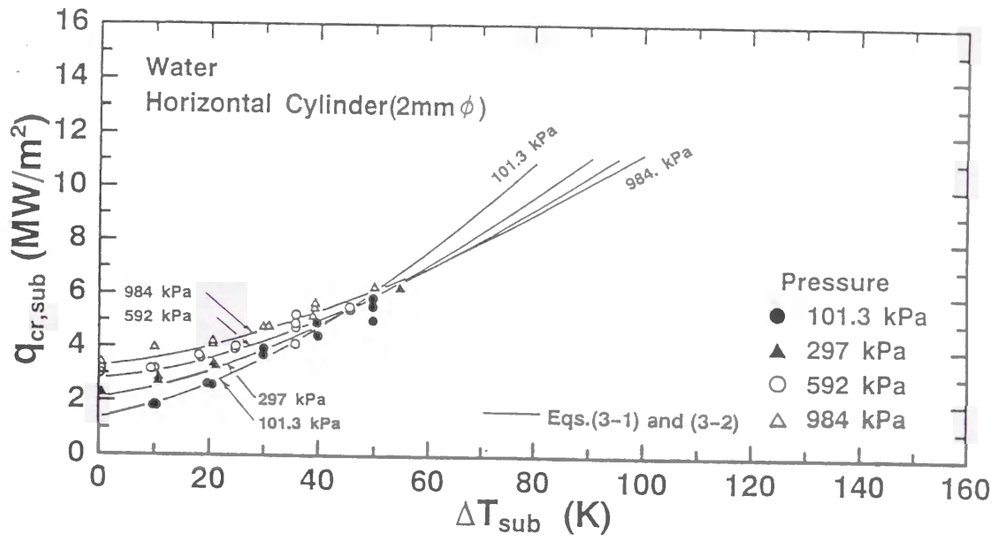

Fig. 3-9 Comparison of the typical CHF data on a 2 mm diameter cylinder with the corresponding CHF curves obtained from Eqs. (3-1) and (3-2).

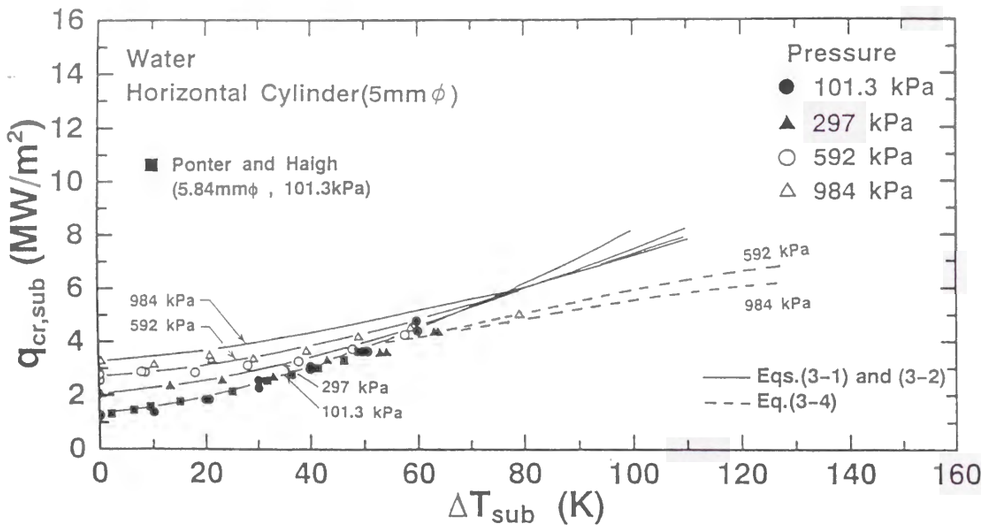

Fig. 3-10 Comparison of the typical CHF data on a 5 mm diameter cylinder with the corresponding CHF curves obtained from Eqs. (3-1) and (3-2), and those from Eq.(3-4).

Table 3-1 Constants in Eqs.(3-1), (3-2) and (3-4) for water.

Water

Heaters	K_1	K_2	A	B	C
Horizontal Plate (6mm ×50mm)	0.14	0.87	-0.204	3.35	-6.55
Horizontal Cylinder (1.2mm Diam.)	0.17	0.87	0.31	2.60	-4.10
Horizontal Cylinder (2mm Diam.)	0.17	0.702	---	---	---
Horizontal Cylinder (5mm Diam.)	0.17	0.356	-0.204	3.35	-6.55
Vertical Ribbon (5.4mm Width)	0.15	0.375	↑	↑	↑
Horizontal Vertically Oriented Ribbon (5.4mm Width)	0.12	0.679	↑	↑	↑

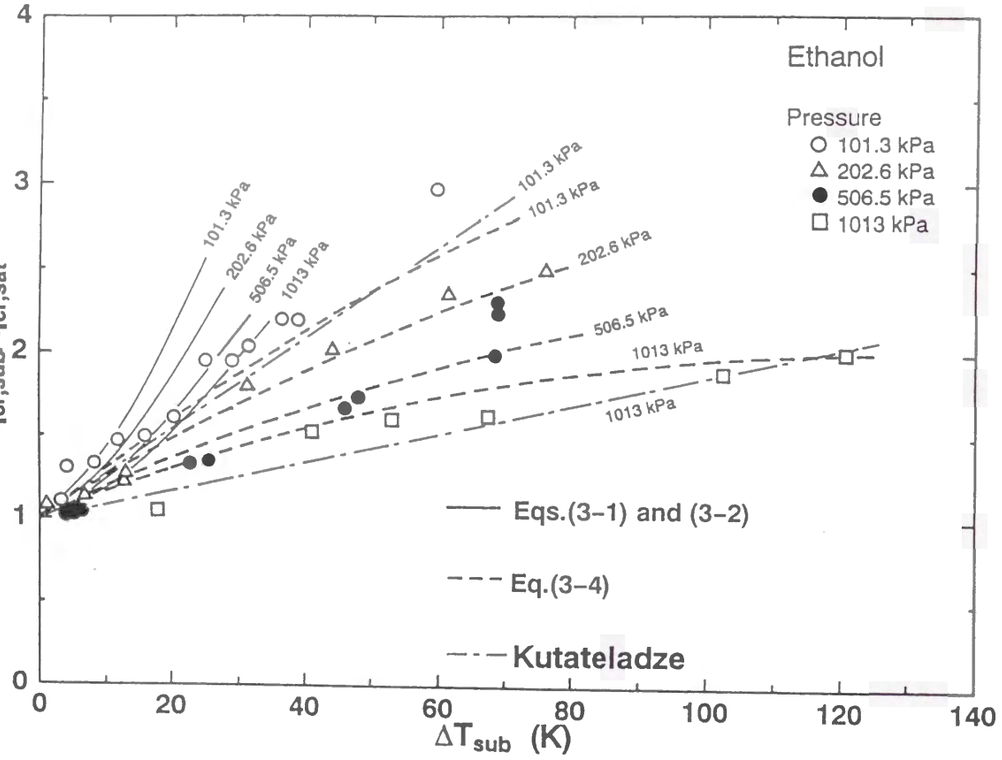

Fig. 3-11 Comparison of the CHF data for ethanol by Kutateladze with the corresponding CHF curves obtained from Eqs. (3-1) and (3-2), and those from Eq.(3-4).

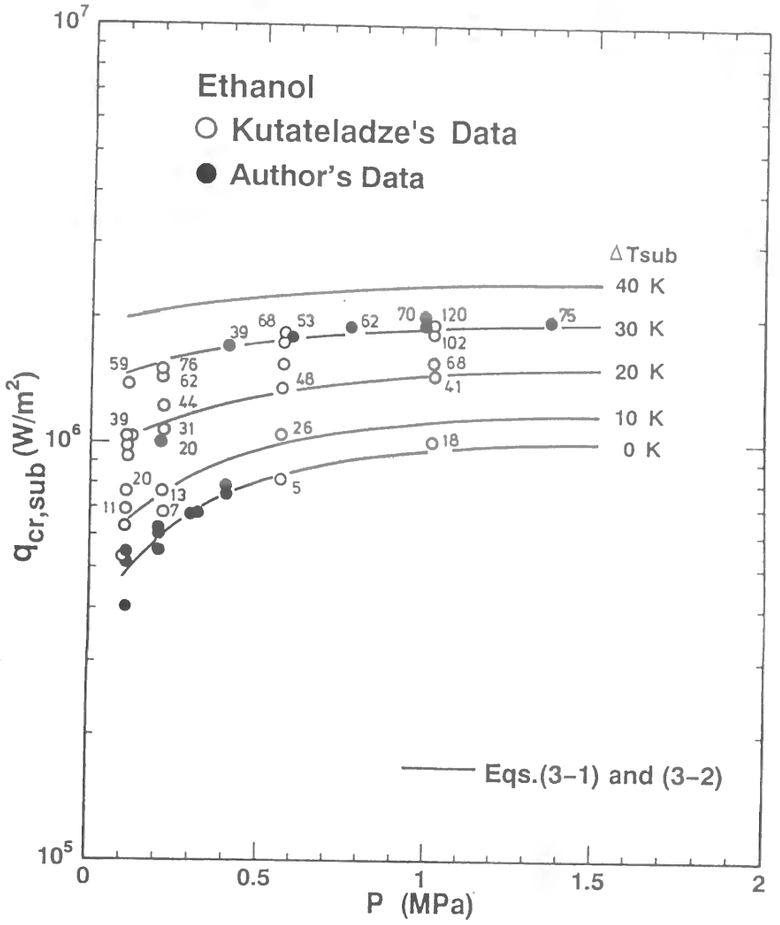

Fig. 3-12 Comparison of the CHF data for ethanol with the corresponding CHF curves obtained from Eqs. (3-1) and (3-2).

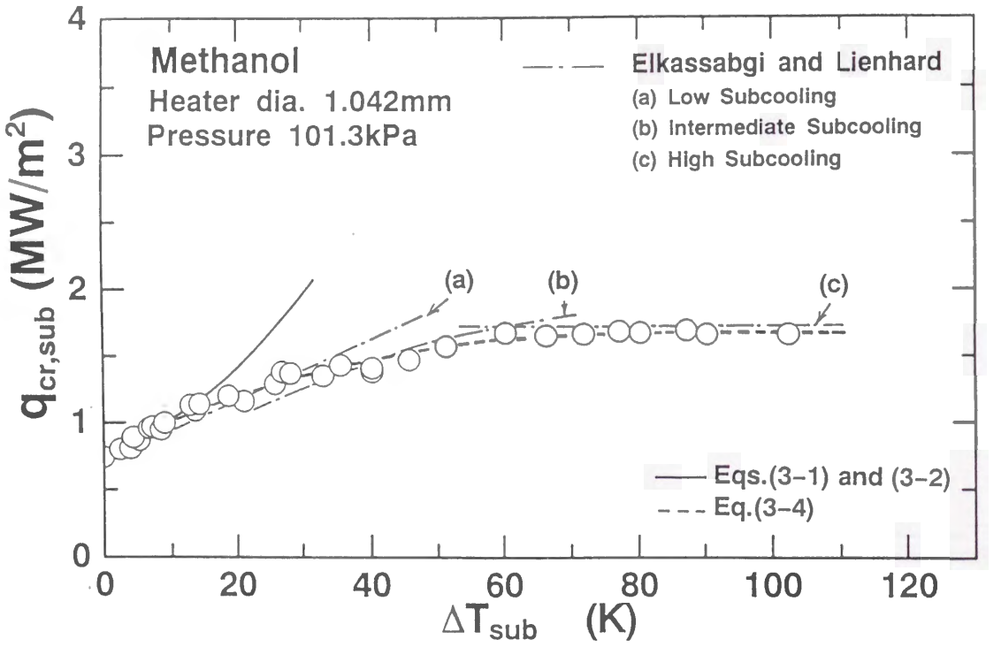

Fig. 3-13 Comparison of the typical CHF data by Elkassabgi and Lienhard in Methanol with the corresponding CHF curves obtained from their and the author's correlations.

Table 3-2 Constants in Eqs.(3-1), (3-2) and (3-4) for ethanol and methanol including K_2 values obtained by Eq. (3-5).

Ethanol

Heater	Pressure	K_1	K_2	A	B	C
Horizontal Cylinder	101.3 kPa	0.17	0.742	0.421	- 0.83	0.111
	202.6 kPa	↑	0.728	↑	↑	↑
	506.5 kPa	↑	0.702	↑	↑	↑
	1013 kPa	↑	0.672	↑	↑	↑

K_2 values: obtained by Eq.(3-5)

Methanol

Heater	Constant				
	K_1	K_2	A	B	C
Horizontal Cylinder (1.04mm Diam.)	0.18	0.880	0.378	-0.104	0.0111

K_2 values: obtained by Eq.(3-5)

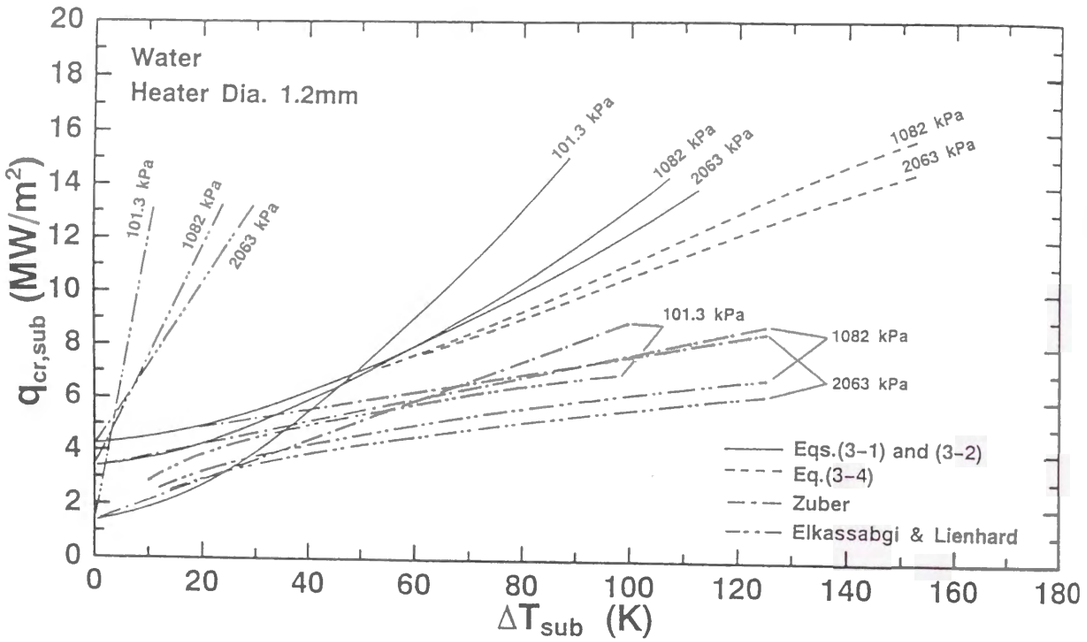

Fig. 3-14 Comparison of the CHF correlations for subcoolings with existing ones.

CHAPTER 4

TRANSIENT POOL BOILING PHENOMENA DUE TO INCREASING HEAT INPUTS

4.1 INTRODUCTION

General understanding of transient boiling phenomenon caused by an increasing heat input is important as the database for the design and safety evaluation of several engineering systems. The transient phenomena including boiling incipience and transition from non-boiling regime to film boiling in water and liquid sodium are to be clarified for the safety assessment of nuclear reactor accidents caused by power burst. Those in liquid helium and liquid nitrogen are for the stability of superconducting magnets cooled by cryogenic liquids due to the local thermal disturbance in the magnets, and the cooling stability for microelectronic assemblies. Nevertheless, the generalized mechanism for the phenomenon has never been resolved.

The anomalous trend of transient critical heat fluxes with respect to the periods, τ, of exponentially increasing heat inputs, $Q_0 \exp(t/\tau)$, that the q_{cr} first gradually increases from the steady-state one, then decreases and again increases with a decrease in the period over the range from 10 s down to 5 ms

(the decrease of period means an increase in the rate of heat input) has been clearly observed on a 1.2 mm platinum horizontal cylinder in water at atmospheric pressure by Sakurai and Shiotsu (1974, 1977a, 1977b) for the first time, though some papers on transient pool boiling due to exponential heat inputs had been reported previously (Rosenthal et al., 1957) (Johnson et al., 1962) (Hall et al., 1966).

The trend of the q_{cr} with respect to τ showed that there exist two main mechanisms of the transition to film boiling for long periods and for short periods, respectively. The q_{cr} for a long period existed on a point around the extension of steady-state nucleate boiling curve on the heat flux, q, versus surface superheat, ΔT_{sat}, graph. The mechanism of the q_{cr} would be roughly explained as the time lag of the heat transfer crisis which occurs at the steady-state critical heat flux. There exist some models for steady-state heat transfer crisis based on hydrodynamic instability by Kutateladze (1959), Zuber (1959), Lienhard and Dhir (1973), Haramura and Katto (1983), and so on. The steady-state q_{cr} model is not the scope of this study. On the other hand, the q_{cr} for a short period existed on the heat transfer process with rapidly increasing heat flux and slightly increasing surface superheat from the incipient boiling point. The incipient boiling point was on the conduction heat transfer process corresponding to the period tested on the q versus ΔT_{sat} graph. Though it was

supposed that the transition mechanism for the short period was different from that for the long period, the mechanism has never been resolved for a long time.

Recently, the direct transitions from a non-boiling regime to film boiling have been observed by Sakurai et al. (1992) on a horizontal cylinder in liquid nitrogen in the transients caused by exponential heat inputs with the periods ranging from 100 s down to 5 ms, (namely for quasi-steady heat inputs and for very rapid ones) at around atmospheric pressure. At pressures higher than atmospheric, the direct transitions have been observed only for shorter periods. The longest limit of the exponential period for the existence of the direct transition depends on pressure; it is shorter for the higher pressure. At pressures higher than around atmospheric, the q_{cr} first gradually increased from steady state one, then decreased and again increased with a decrease in the period. This trend of q_{cr} versus τ at pressures is similar to that obtained by the water experiment at atmospheric pressure. On the other hand, the direct transitions to film boiling under high pressures occurred from the conduction heat transfer without or with increasing heat flux for a short period of time. It would be assumed that the transitions occurred due to the explosive-like heterogeneous spontaneous nucleation (HSN) in originally flooded cavities without the contribution of active cavities entraining vapor for boiling incipience. Namely, there is no dissolved gas in liquid nitrogen except for possible trace amount of helium, hydrogen and neon. The HSN means the spontaneous nucleation

influenced by a solid surface. The occurrence of HSN at temperatures considerably lower than the homogeneous nucleation temperature could not be explained by considering the HSN on a perfectly flat solid surface, but could be explained by the HSN in initially flooded cavities on the solid surface (Sakurai et al., 1992, 1993).

After that they (Sakurai et al., 1993) carried out water experiments similar to the liquid nitrogen experiments for the pressures up to about 2 MPa and liquid subcoolings up to 30 K. The water experiments were for the cases without and with the pre-pressurization by high pressure (around 5 MPa) for a while in the test vessel before each experimental run (Case 1 and Case 2, respectively). For the Case 2, the anomalous trend of q_{cr} was observed with respect to period at various pressures, which was just similar to that obtained by the liquid nitrogen experiments mentioned above. The direct transition to film boiling was observed for a certain range of period, which depends on pressure. It would be considered that the boiling inception and direct transition occurred due to the HSN in originally flooded cavities. Namely, by the pre-pressurization, the possibility of initial boiling due to the potentially active cavities entraining vapor which requires the surface superheat not only smaller but also sufficiently higher than the HSN surface superheat is eliminated. On the other hand, the q_{cr} for a short period for the case without pre-pressurization (Case 1) obviously agreed with that with pre-pressurization (Case 2), though the surface superheat

at the q_{cr} for the former case was considerably lower than that for the latter case. However, the surface superheat at the critical heat flux for the former case almost agreed with the HSN surface superheat (incipient boiling surface superheat) for the slow increasing rate of surface superheat for the latter case. They considered that the q_{cr} for the case without pre-pressurization occurred due to the HSN in initially flooded cavities and the vapor bubbles from active cavities lead to the occurrence of HSN at lower surface superheat because of the decrease of surface superheat increasing rate.

The purpose of this chapter is firstly to obtain an extended data of the q_{cr} values due to exponential heat inputs in water for the exponential periods and subcoolings over the ranges of 2 ms to 20 s and zero to 80 K at pressures ranging from 101.3 to 2063 kPa in cases with and without pre-pressurization, secondly to investigate the effect of high subcoolings at high pressures on the main two mechanisms of q_{cr} depending on the exponential periods, and thirdly to observe in detail the direct transition to film boiling for the case with pre-pressurization and to clarify the incipient boiling and the transition to film boiling for a wider range of subcoolings for the cases with and without pre-pressurization.

4.2 EXPERIMENTAL RESULTS AND DISCUSSION

4.2.1 Experimental Conditions

The dynamic heat transfer processes including boiling incipience and transition to film boiling due to exponential heat inputs were measured for a 1.2 mm diameter horizontal cylinder in water for the wide ranges of exponential period, system pressure and liquid subcooling. The ranges are of pressure from 101.3 kPa to 2063 kPa, of exponential period from 2 ms to 20 s and of liquid subcooling from 0 to 80 K.

The experiments for the case with pre-pressurization at a high pressure of around 5 MPa for a time period of about 3 minutes before each experimental run were also carried out for the same experimental conditions as for the case without pre-pressurization.

4.2.2 Transient Boiling Process

Figure 4-1 shows typical changes in the heater surface temperature, T_w, and the heat flux, q, with time for the exponential heat input, Q. The heater surface temperature at first increases with an increase in the heat input. Boiling starts at T_i beyond saturation temperature T_{sat}. The temperature differences of $\Delta T_i = T_i - T_{sat}$ is called the incipient boiling surface superheat. The heater surface temperature increases up to maximum temperature overshoot, then

decreases and again increases with lower rate. When the heat flux reaches a certain value, q_{cr}, which is named the transient critical heat flux, the heater temperature rapidly increases.

4.2.3 Transient Critical Heat Flux under Saturated Condition

Transient critical heat fluxes due to exponential heat inputs to the horizontal test cylinder in a pool of water were obtained for wide ranges of exponential periods, pressures and subcoolings. The transient critical heat fluxes with the pre-pressurization were also obtained. The former and the latter ones without and with the pre-pressurization are called as those for the Case 1 and Case 2, respectively

Figure 4-2 shows typical results of transient critical heat flux q_{cr} versus exponential periods τ at pressures of 101.3, 690, 1082 and 2063 kPa under saturated conditions. The relation between the critical heat flux and the exponential period at each pressure can be classified into three groups as clearly seen in the data for the Case 1 at atmospheric pressure and those for the Case 2 at pressures of 101.3, 690 and 1082 kPa. The three groups of q_{cr} for periods at atmospheric pressure for the Case 1 are shown in Fig. 4-2 as a typical.

The first group of q_{cr} at 101.3 kPa for the Cases 1 is for the periods

longer than around 100 ms, and that for the Case 2 is for the periods longer than around 3 s. At pressures higher than atmospheric, the first groups of q_{cr} for the Cases 1 and 2 are for the periods longer than around 200 ms. The q_{cr} values in the first group at each pressure for both cases agree with each other. The q_{cr} points in the first group at each pressure exist on the extrapolation of steady-state developed nucleate boiling curve on the graph of $\log q$ vs. $\log \Delta T_{sat}$ as shown later in Fig. 4-9. Therefore, it can be assumed that the heat transfer crisis at the q_{cr} which is larger than the steady-state critical heat flux q_{st} is due to the time lag of the hydrodynamic instability which starts at q_{st}.

The curves representing the q_{cr} values of the first group for periods at the pressures are expressed by the following empirical equation:

$$q_{cr,sub} = q_{st,sub}\left(1 + 0.21\tau^{-0.5}\right) \tag{4-1}$$

where $q_{st,sub}$ is given by Eq. (3-1) in Chapter 3. The curves for the pressures obtained from Eq. (4-1) are shown in Fig. 4-2 in comparison with the corresponding experimental data.

The critical heat fluxes of the second group for the Case 1 at atmospheric pressure are for the periods shorter than 9 ms. Those for the Case 2 at pressures of 101.3, 690 and 1082 kPa are for the periods shorter than around 2 s, 40 ms,

and 7 ms, respectively. The q_{cr} versus period at each pressure has a linear asymptotic line on a log-log graph. The q_{cr} of second groups at pressures higher than 690 kPa for the Case 1 and at the pressure of 2063 kPa for the Case 2 were not observed for the periods tested here. However, it is supposed that the q_{cr} values for the second group will be observed for the periods sufficiently shorter than the shortest one tested here and the q_{cr} values for the Cases 1 and 2 will agree with each other for the same period.

The q_{cr} in the second group for the Case 2 are expressed by the following equation:

$$q_{cr,sub} = h_{com}\left[\Delta T_i(\tau) + \Delta T_{sub}\right] \tag{4-2}$$

where h_{com} is the transient non-boiling heat transfer coefficient and $\Delta T_i(\tau)$ is the HSN surface superheat as a function of τ. The values of $\Delta T_i(\tau)$ were measured for periods at pressures. The non-boiling heat transfer coefficient h_{com} is approximately expressed as follows (Sakurai et al., 1977a).

$$h_{com} = \left[h_c^4 + h_n^4\right]^{1/4} \tag{4-3}$$

If the period is sufficiently short and therefore the increasing rate of the surface

temperature is too rapid for natural convection to contribute appreciably to the heat transfer before the initiation of boiling, liquid would act as an infinite solid with regard to heat transfer. The heat transfer coefficient in this case can be obtained as a function of time by solving the transient heat conduction equation. The coefficient for exponential heat input thus obtained is infinite at $t = 0$ but it decreases rapidly and approaches a certain asymptotic value of h_c with the increase in t/τ (Sakurai et al., 1977a). For $t/\tau \geq 3$, it is well expressed by,

$$h_c = \left(k_l \rho_l c_{pl}/\tau\right)^{1/2} K_1(\mu D/2) \Big/ K_0(\mu D/2) \cong \left(k_l \rho_l c_{pl}/\tau\right)^{1/2} \tag{4-4}$$

where $\mu = \left[\rho_l c_{pl}/k_l \tau\right]^{1/2}$, and K_0 and K_1 are the modified Bessel functions of the second kind of zero and first orders. The initial value Q_0 of the heat input is so low that the increase in heater temperature before $t/\tau = 3$ is insignificant. The non-boiling heat transfer coefficients for $\tau \leq 0.1$ s can be well expressed by Eq. (4-4) (Sakurai et al., 1977a). On the other hand, when the increasing rate of the heat input is sufficiently low, heat would be transferred by natural convection. Natural convection heat transfer coefficient h_n is expressed by the following equation (Takeuchi et al., 1995)

$$h_n = \left(k_l / D\right) \times 10^z, \text{ or } Nu = 10^z \tag{4-5}$$

where

$$z = 0.194 + 0.141 \log R_f + 0.6 \times 10^{-2} \left(\log R_f\right)^2 - 0.1 \times 10^{-3} \left(\log R_f\right)^3 - 0.9 \times 10^{-5} \left(\log R_f\right)^4$$

and

$$R_f = Gr^* \, Pr^2 / \left(4 + 9\, Pr^{1/2} + 10\, Pr\right).$$

It was already confirmed that the h_n correlation based on the rigorous numerical solutions for various liquid with the Prandtl numbers smaller than 10 more correctly evaluate the natural convection heat transfer coefficients as compared with existing correlations such as Churchill and Chu's one (1975) and Raithby and Holland's one (1985). The non-boiling heat transfer coefficients for $\tau \geq 5$ s can be well expressed by Eq. (4-5) (Sakurai et al., 1977a). The intermediate period region (0.1 s $< \tau <$ 5 s) is the transition region from natural convection heat transfer to conduction heat transfer. The non-boiling heat transfer coefficients including the transition region are expressed by the Eq. (4-3).

The longer limit of the period for the second group becomes shorter with an increase in pressure. In the Case 2 transients for the second group, the direct

or semi-direct transitions from non-boiling regime to film boiling occur at the q_{cr} without or with the heat flux increase for a short period of time. It should be noted that the minimum q_{cr} values for the longest period for the second group at each pressure are extremely lower than the corresponding q_{st}.

These transient heat transfer processes including direct and semi-direct transitions for the Case 2 in water correspond to those for the liquid nitrogen experiments (Sakurai et al., 1992) under the same conditions at pressures higher than atmospheric. Therefore, it can be assumed that there exists no contribution of active cavities on the solid surface in both liquids. The initial boiling would occur due to HSN in originally flooded cavities.

On the other hand, as clearly shown in the figure, the q_{cr} for short periods at atmospheric pressure in the Cases 1 and 2 (in other words, in the cases with and without the contribution of active cavity for initial boiling) agreed with each other, though the surface superheat at q_{cr} for the former case is lower than that for the latter case. It would be considered that the q_{cr} for short periods with the contribution of active cavities for the Case 1 probably occur due to the HSN in originally flooded cavities, though the nucleate boiling from active cavities coexists with it. A few vapor bubbles growing up from active cavities remaining on the cylinder surface before the detachment lead to the occurrence of the heterogeneous spontaneous nucleation at the surface superheat lower than that

for the same period for the Case 1. This is because the increasing rate of surface superheat on the local positions of the cylinder surface is decreased due to the increased heat flux by the bubbles; the surface superheat at initial boiling due to HSN decreases with a decrease in the increasing rate of surface superheat.

The third group of q_{cr} is for the intermediate range of period between those corresponding to the maximum and minimum q_{cr}, and those are about 100 ms and 10 ms at atmospheric pressure for the Case 1. The q_{cr} in the group decreases or gradually increases with a decrease in period and then approaches the curve representing the q_{cr} at which the direct or semi-direct transitions to film boiling occurs. The transition to film boiling at the q_{cr} in the group occurs in incompletely developed nucleate boiling due to originally unflooded cavities with entrained vapor, and vapor entrained cavities activated from flooded cavities by neighboring vapor bubbles. The q_{cr} becomes lower than that supposed due to the hydrodynamic instability.

4.2.4 Transient Critical Heat Flux under Subcooled Condition

The values of q_{cr} at 1082 kPa for the Case 1 and Case 2 are shown versus periods with liquid subcooling as a parameter in Fig. 4-3 as a typical for subcoolings at a high pressure. The q_{cr} values of the first group are for the

periods longer than around 200 ms for $\Delta T_{sub} = 0$ K, and longer than around 500 ms for $\Delta T_{sub} = 20$ K and longer than around 2 s for $\Delta T_{sub} = 40$ K for both cases. The heat transfer crisis for the subcoolings at the q_{cr} larger than q_{st} is considered to be due to the same mechanisms as that for the saturated condition mentioned before.

On the other hand, the q_{cr} values of first group for the subcoolings of 60 and 80 K are for the periods longer than around 20 ms for both cases. As mentioned in the previous section, the heat transfer crisis at q_{st} (steady-state q_{cr}) for the high subcoolings was assumed to occur due to the HSN in originally flooded cavities on fully developed nucleate boiling at the heat flux lower than that supposed by the hydrodynamic instability. The q_{cr} in the first group very gradually increases with a decrease in the period. It should be noted that the q_{cr} at the period of 20 ms is only about 140 % of the q_{st}. The curves representing the relation of q_{cr} versus period for the high subcooling at the high pressure are expressed by the following equation.

$$q_{cr,sub} = q_{st,sub}\left[1 + 2.3 \times 10^{-2} \tau^{-0.7}\right] \quad (4\text{-}6)$$

The slight increase in q_{cr} on fully developed nucleate boiling is due to the slight increase of the HSN surface superheat. It is not due to the time lag of the

hydrodynamic instability that starts at the steady-state critical heat flux. The curves obtained by Eq. (4-6) are shown in Fig. 4-3 in comparison with the corresponding experimental data.

The second group q_{cr} for the Case 1 are obtained only for the period of 2.1 ms at $\Delta T_{sub} = 20$ K and 2.9 ms at $\Delta T_{sub} = 60$ K. Therefore, the asymptotic lines of the critical heat fluxes of the second group for the Case 1 were not obtained. However, the asymptotic lines for the Case 2 were obtained for all the subcoolings. The q_{cr} in the second group for the Case 1 will be measured by using the exponential heat inputs with periods shorter than the shortest one tested here. The q_{cr} value will exist on the asymptotic line of corresponding subcooling for the Case 2. The asymptotic line for each subcooling has almost the same gradient on the graph and it moves upwards for higher liquid subcooling.

The critical heat fluxes in the third group are those for the intermediate range of period between those for the first and second groups. With a decrease of period in the range, the q_{cr} slightly increases and then obviously decreases and finally approaches the asymptotic line for each subcooling.

The q_{cr} for periods obtained for subcooling of 60 K at pressures of 494, 690, 1082 and 2063 kPa for the both cases are shown in Fig. 4-4. The q_{cr} values for periods over the range from 30 ms to 20 s are independent of pressure. The

q_{cr} values for the period of 20 s correspond to steady-state values for the pressures. The q_{cr} values for the pressures of 690 and 1082 kPa for the Case 1 decrease with a decrease in period from around 30 ms down to the values which are significantly lower than the corresponding steady-state critical heat fluxes. These q_{cr} values for periods around 3 ms for the both Cases 1 and 2 are on the asymptotic line representing the q_{cr} values for periods in the second group on the graph of the figure. The values are equal to about 60 % and 70 % of the corresponding steady-state critical heat fluxes, respectively. This means that both transitions are near direct ones to film boiling and the effect of vapor bubbles from active cavities for the Case 1 on the transition is negligibly small. The q_{cr} for subcooling of 80 K at pressures of 494, 690, 1082 and 2063 kPa for the both cases are shown versus period in Fig. 4-5. The trend of dependence on the period is almost similar to that for the subcooling of 60 K shown in Fig. 4-4. The curves obtained by Eq. (4-6) are shown in Figs. 4-4 and 4-5 for comparison.

4.2.5 Typical Transitions to Film Boiling at CHF

There exist two types of boiling incipience on the cylinder surface in a liquid due to an increasing heat input. One is that from originally unflooded active cavities entraining vapor and the other is that from another mechanism

without contribution of the active cavities. The former is observed in water and the latter is in liquid nitrogen, liquid helium, ethanol, and in water pre-pressurized by appropriately high pressures. The latter boiling mechanism would be due to the HSN from originally flooded cavities on the cylinder surface in the liquids.

Typical data of transient incipient boiling heat flux q_i and critical heat flux q_{cr} obtained for the periods, τ, ranging from 2 ms to 20 s at atmospheric pressure, in the cases without and with pre-pressurization (Cases 1 and 2, respectively) are shown versus τ in Fig.4-6. The incipient boiling surface superheat ΔT_i and surface superheat at the critical heat flux ΔT_c for the data shown in Fig. 4-6 are shown versus τ in Fig. 4-7.

As shown in Fig. 4-6, the q_{cr} values for the Cases 1 and 2 increase, then decrease and again increase with a decrease in period. The data are clearly classified into three groups for the cases. First ones for the Cases 1 and 2 are for the periods longer than 100 ms and 3.3 s respectively, second ones are for periods shorter than 5 ms and 2 s, and third ones are for the period between 5 ms and 100 ms, and between 2 s and 3.3 s, although the q_{cr} values for the periods between 2 s and 3.3 s for the Case 2 were not observed.

As shown in Fig. 4-7, the incipient boiling superheats ΔT_i for the Case 2 due to the HSN are far higher than the corresponding values for the Case 1.

The HSN surface superheat is affected by the rates of increasing heat inputs (namely, by the increasing rate of surface superheat). It has a lower limit value for the period longer than around 50 s and increases gradually with the decrease in the period from 50 s down to about 2 s. It has a constant value for the periods from 0.1 s to 2 s, and again increases with the decrease in the period. The values of ΔT_i for the periods shorter than 2 s are all in agreement with the corresponding values of ΔT_c. In the Case 1 transients, the values of ΔT_c for the q_{cr} in the first group are almost in agreement with the corresponding values of ΔT_i. The values of ΔT_c for the q_{cr} in the third group become higher than the corresponding values of ΔT_i with the decrease in the period from 100 ms to 5 ms.

Typical heat transfer processes for various periods for the both cases are shown in Fig. 4-8. The processes with the q_{cr} belonging to the first group are for the periods of 10 s and 100 ms for the Case 1 and for the periods of 10 s for the Case 2. The processes with the q_{cr} belonging to the second group are for the periods of 2.1 s, 1 s, 100 ms, and 10.9 ms for the Case 2, and the process for the third group is for the period of 10.9 ms for the Case 1.

The q_{cr} in the first group for both cases are those at which the transitions from fully developed nucleate boiling (FDNB) to film boiling occur after the preceding transitions from the non-boiling regime to FDNB as shown

in Fig. 4-8. The q_{cr} values gradually increase with a decrease in period. The increase of the q_{cr} in the first group is roughly explained as the time lag of the heat transfer crisis which occurs at the steady-state critical heat flux.

The q_{cr} for the Case 2 changes to that of the second group at the period around 2 s. The q_{cr} in the second group for the Case 2 is that at which direct transition from non-boiling regime to film boiling occurs. The non-boiling regime for period around 2 s corresponds to quasi-steadily increasing natural convection. The direct transitions from not only rapidly increasing conduction regime but also quasi-steadily increasing natural convection regime were observed in pre-pressurized water as shown in Fig. 4-8. The q_i values in the second group are equal to q_{cr}. The direct transition to film boiling at the incipient boiling point on non-boiling regime such as rapid conduction and quasi-steadily increasing natural convection was also observed in liquid nitrogen (Sakurai et al., 1992). It would be considered that the direct transition occurs due to the heterogeneous spontaneous nucleation in originally flooded cavities not only in liquid nitrogen but also in pre-pressurized water. The q_{cr} values in the second group for the Case 1 almost agree with those for the Case 2 though the surface superheats at the q_{cr} are lower than those for the Case 2 as shown in Figs. 4-6 and 4-7. Almost same processes for the periods of 10.9 ms for Cases 1 and 2 on q versus ΔT_{sat} graph can be seen in Fig. 4-8. The q_{cr} in the second

group for the Case 1 are those at which transitions to film boiling occur with the nucleate boiling for a period of time after the boiling incipience. Namely, it could be expected that the number of vapor bubbles from active cavities on the cylinder surfaces increases with an increase in heat flux and surface superheat due to a rapidly increasing heat input, and then the transition to film boiling occurs at around the lower limit of heterogeneous spontaneous nucleation temperature. This is because the vapor bubbles from active cavities cause the surface superheat increasing rate to decrease and lead the HSN to occur at the local surface superheat near the lower limit of HSN surface superheat.

The third group of q_{cr} exists for the Case 1 as shown in Fig. 4-6 and the q_{cr} decreases with a decrease in period from the maximum q_{cr} down to the minimum one. It was assumed that the heat transfer crisis at the q_{cr} in the third group would occur due to the HSN in originally flooded cavities on a solid surface in the FDNB or insufficiently developed nucleate boiling at the surface superheat of around the lower limit of HSN temperature as a result of accompanying gradual increase in the surface superheat. This transition occurs at the heat flux below the value derived from Eq.(4-1) which express the q_{cr} with respect to τ in the first group for the Case 1.

4.2.6 Transient Heat Transfer Processes

The heat transfer processes for the periods of 510 ms under saturated condition at 1082 kPa for the Cases 1 and 2 are shown on the q vs. ΔT_{sat} graph in Fig. 4-9 as the typical ones in which the transition to film boiling occurs at the q_{cr} of first group. The transition to fully developed nucleate boiling (FDNB) firstly occurs in quasi-steadily increasing natural convection regime for the period of 510 ms at points A and A' for the Cases 1 and 2. Initial boiling at point A or A' occurs due to nucleation from active cavities entrained vapor or due to heterogeneous spontaneous nucleation (HSN) in initially flooded cavities. The surface superheats for the cases are 9 K and 25 K, respectively. The lower limit of HSN surface superheat, ΔT_{iLH}, which was obtained as an initial boiling surface superheat for the period of 20 s for Case 2 under the same conditions is shown as an open circle. The surface superheat for the period of 510 ms at point A' was almost in agreement with the value of ΔT_{iLH}. At the transition points A and A', the surface superheat and the heat flux rapidly change through the processes of AB and A'B' to FDNB. The decrease of surface superheat in each process is due to the activation of flooded cavities. The activation progresses for the slow increasing heat input such as that for the period of 510 ms. After that the heat flux increases along the fully developed nucleate boiling (FDNB) curve up to the heat flux (points C, C') where the transition from FDNB to film boiling

occurs. As shown in the figure, the q_{cr} points exist on the extrapolation of the steady-state FDNB curve. The q_{cr} values agree with each other and the surface superheats at q_{cr} are lower than the value of ΔT_{iLH}. Little influence of the pre-pressurization on the FDNB heat transfer and on the transition from FDNB to film boiling can be seen, though the heat transfer processes from the boiling initiations to FDNB are considerably different each other. Therefore, it would be considered that the heat transfer crisis at the q_{cr} in the first group which is larger than the q_{st} is due to the time lag of hydrodynamic instability which starts at the q_{st}.

The heat transfer processes for the subcooling of 60 K for the same period and pressure in both cases are also shown on the graph as typical ones under subcooled condition. The transition to FDNB occurs in quasi-steadily increasing natural convection regime for the subcooling at points As and As' for the Cases 1 and 2. The surface superheats for the cases are 23 K and 26 K respectively. The former value for the Case 1 is far higher than that for the saturated condition at point A (about 9 K) though the latter value almost agrees with the value at point A'. The surface superheats are slightly higher than the lower limit of HSN surface superheat ΔT_{iLH} shown as an open circle on the solid curve. The surface superheat and heat flux change through the processes of As Bs and As' Bs' to FDNB. The process As Bs for the Case 1 almost agrees

with that for the Case 2, As' Bs', though the surface superheat for the process soon after the initial boiling point is slightly lower than that for the Case 2. The heat fluxes at Bs and Bs' are as high as that slightly lower than the steady-state critical heat flux $q_{st,sub}$. The activation of originally flooded cavities is relatively slow to progress under high subcooling for the increasing heat input with the period of 510 ms. The q_{cr} points Cs and Cs' exist on the extrapolation of the steady-state FDNB curve and the critical heat fluxes agree with each other. The surface superheats at the q_{cr} points of Cs and Cs' almost agree with the ΔT_{iLH}. As mentioned before, the heat transfer crisis at the q_{cr} occurs due to the HSN.

The heat transfer process for the period of 2.9 ms at 1082 kPa under saturated condition for the Case 2 is shown in Fig. 4-10 as a typical one with the q_{cr} of second group. The q_{cr} for the Case 1 for the same period belongs to the third group, whose heat transfer process is also shown in the next figure. The q_{cr} in the second group under saturated condition is not obtained for the Case 1 even at the shortest period tested here. As shown in the figure, boiling firstly occurs in conduction regime for the period at the surface superheat of 60 K (point A') and then the heat flux and surface superheat rapidly decreases and increases, respectively, to film boiling. The q_{cr} at point A' is the direct transition heat flux from non-boiling to film boiling.

The heat transfer processes for the subcooling of 60 K for the same

period and pressure for the Cases 1 and 2 are also shown on the graph as typical ones under subcooled condition. The heat transfer processes after the initial boiling points As and As' are near direct transitions to film boiling. The surface superheats at the initial boiling points are 50 K and 54 K, respectively. The values of q_{cr} for both cases are almost in agreement with each other and are significantly lower than $q_{st,sub}$ as shown in the figure.

Figure 4-11 shows the heat transfer processes as typical ones with the q_{cr} of third group. at 1082 kPa. The heat transfer processes plotted are that for the period of 2.9 ms under saturated condition for the Case 1, and those for the period of 53.5 ms and liquid subcooling of 60 K for the Cases 1 and 2. In the former heat transfer process under saturated condition, the heat flux rapidly increases with a slight decrease of surface superheat up to q_{cr} after the boiling initiation at point A. The surface superheat at the q_{cr} is 29 K. The heat flux reaches the maximum value at point C before reaching the FDNB regime with a decrease in surface superheat due to the activation of originally unflooded cavities. The explosive-like HSN occurs at point C, which has become possible to occur at the point due to the decrease of surface superheat increasing rate. In the latter heat transfer processes under subcooled condition, boiling initiates on conduction regime at points As and As' for the Cases 1 and 2. The surface superheats for the cases are 28 and 32 K, respectively. After the boiling

inception, surface superheat first increases, then decreases and again increases with an increase in heat flux. The transient heat transfer process for the Case 1 almost agrees with that for the Case 2, though the surface superheat for the process just after the initial boiling is slightly lower than that for the Case 2. It should be noted that the heat flux for each case increases after the initial temperature overshoot and setback on the higher superheat side of the steady FDNB curve almost parallel to it and has a maximum value. Namely the critical heat flux is reached before the originally flooded cavities are fully activated. However, it is supposed that the heat transfer crisis at the q_{cr} occurs due to the HSN in originally flooded cavities.

4.3 CONCLUSIONS

(1) The dynamic heat transfer processes including boiling incipience and transition to film boiling due to exponential heat inputs were measured on a horizontal cylinder in water for the exponential periods from 2 ms to 20 s, for the pressures from atmospheric to 2063 kPa, and for the subcoolings from 0 to 180 K for the cases without and with the pre-pressurization.

(2) Direct transitions from non-boiling regime to film boiling in the pre-pressurized water by the pressure of 5 MPa for a while were clearly confirmed

not only for rapidly increasing heat inputs but also for quasi-steadily increasing ones at around atmospheric pressure.

(3) Typical trend of critical heat fluxes with respect to the exponential periods is as follows: the critical heat flux gradually increases from the steady-state value, then decreases and again increases with a decrease in period from the longest one tested here not only for the pre-pressurized case but also non-pre-pressurized one, though the trend was not observed completely for the short period range at high pressures for the non-pre-pressurized case.

(4) The critical heat fluxes for short periods for both cases which increase with a decrease in period from the minimum critical heat flux become almost in agreement with each other. The mechanism of the transition to film boiling regime was considered to be a consequence of the heterogeneous spontaneous nucleation, HSN, in originally flooded cavities on the cylinder surface not only for the pre-pressurized case but also for the non-pre-pressurized case, though several nucleation from active cavities coexist with the HSN for the latter case.

(5) Typical trend of q_{cr} with respect to the period for the high subcoolings such as 60 K and 80 K at pressures higher than 400 kPa is independent of the pressure and almost same each other for both cases. The q_{cr} values for short periods

significantly lower than steady-state values were confirmed even for non-pre-pressurized case.

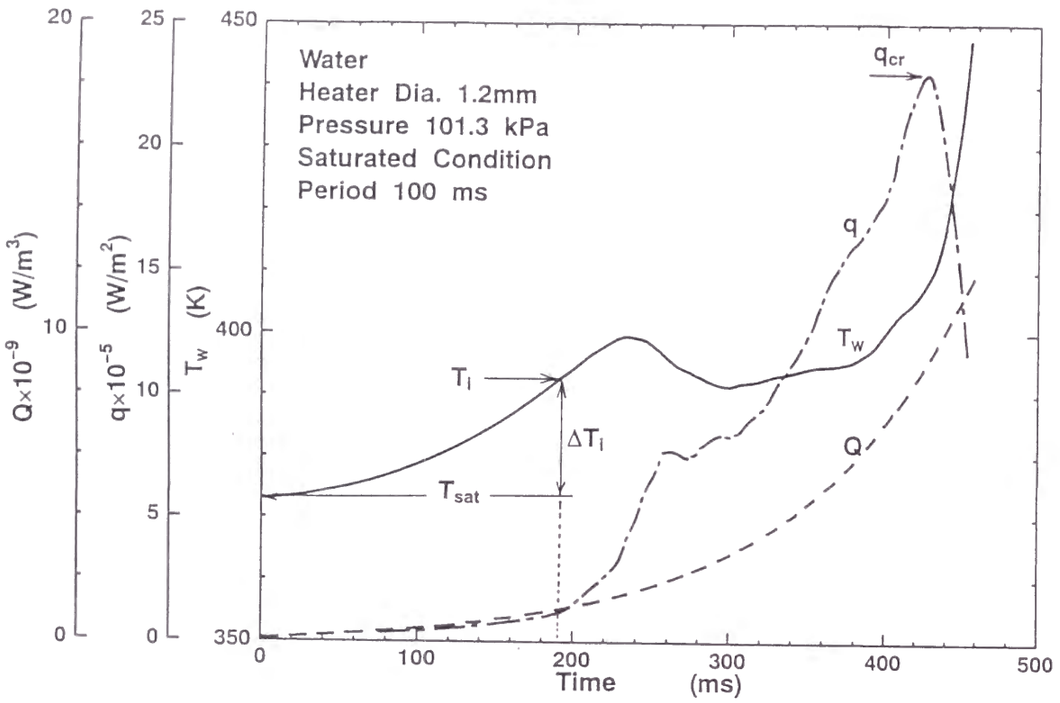

Fig. 4-1 Illustrative time traces of heat input Q, heater surface temperature T_w, and heat flux q.

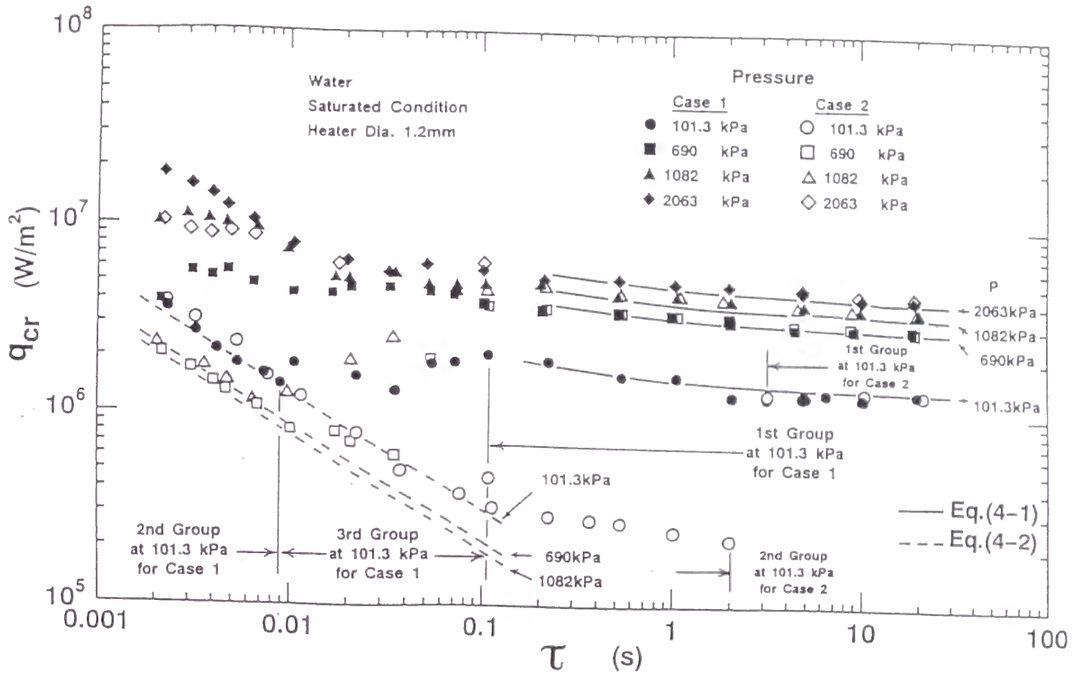

Fig. 4-2 The relation between q_{cr} and τ under saturated conduction at various pressures for the cases without and with pre-pressurization.

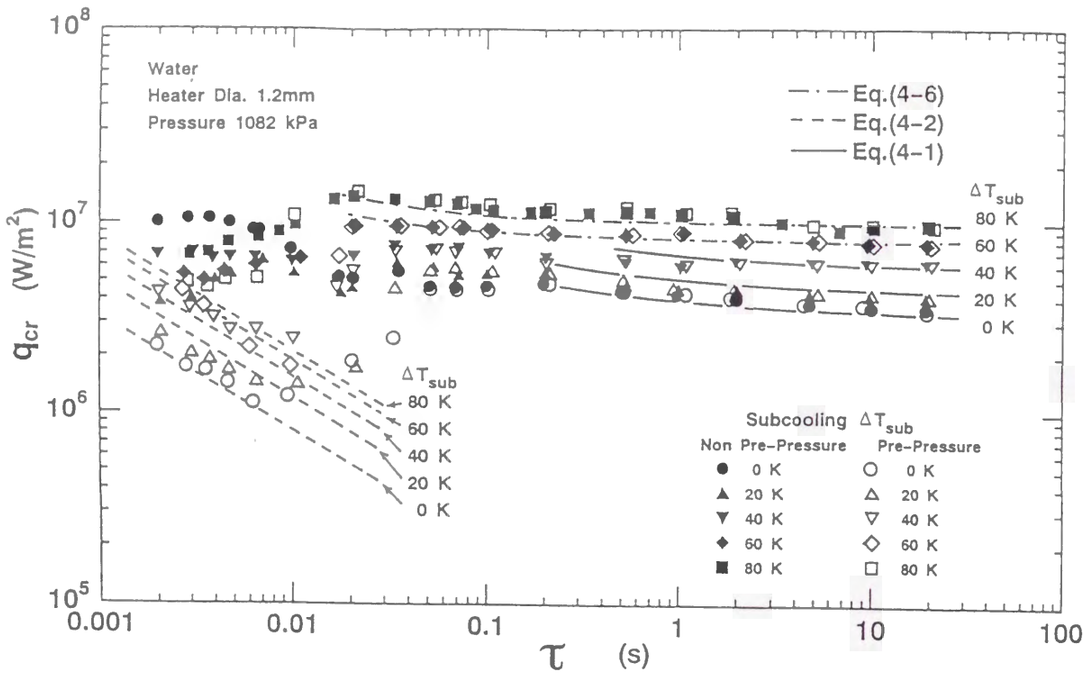

Fig. 4-3 The relation between q_{cr} and τ for various subcooling at a pressure of 1082 kPa for the cases without and with pre-pressurization.

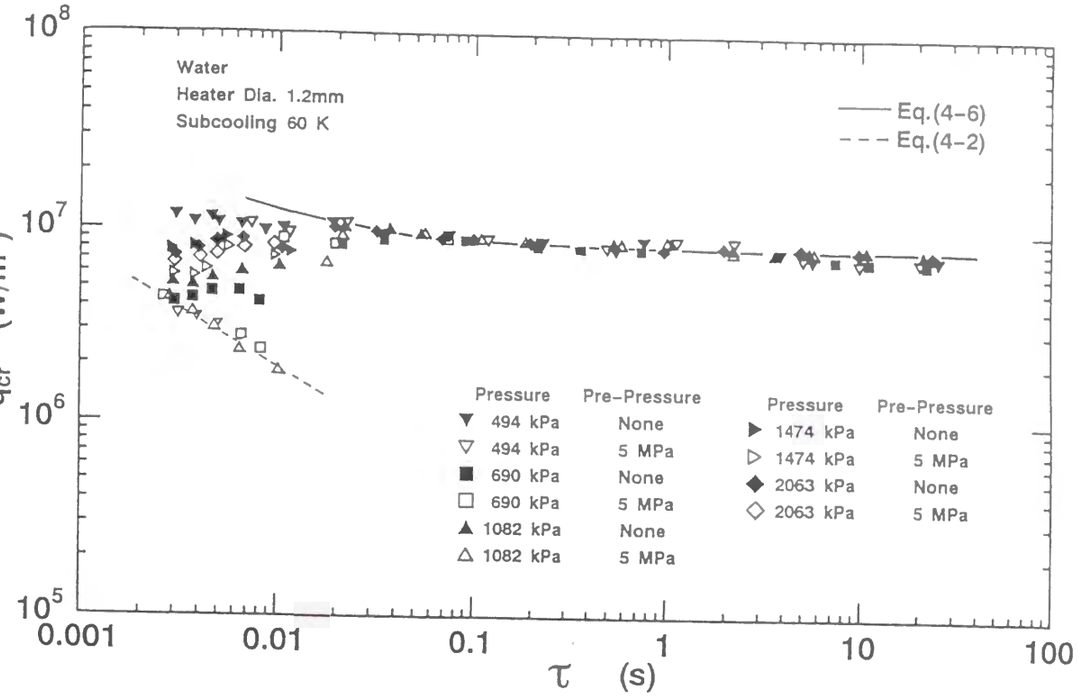

Fig. 4-4 The relation between q_{cr} and τ for subcooling of 60 K at various pressures for the cases without and with pre-pressurization.

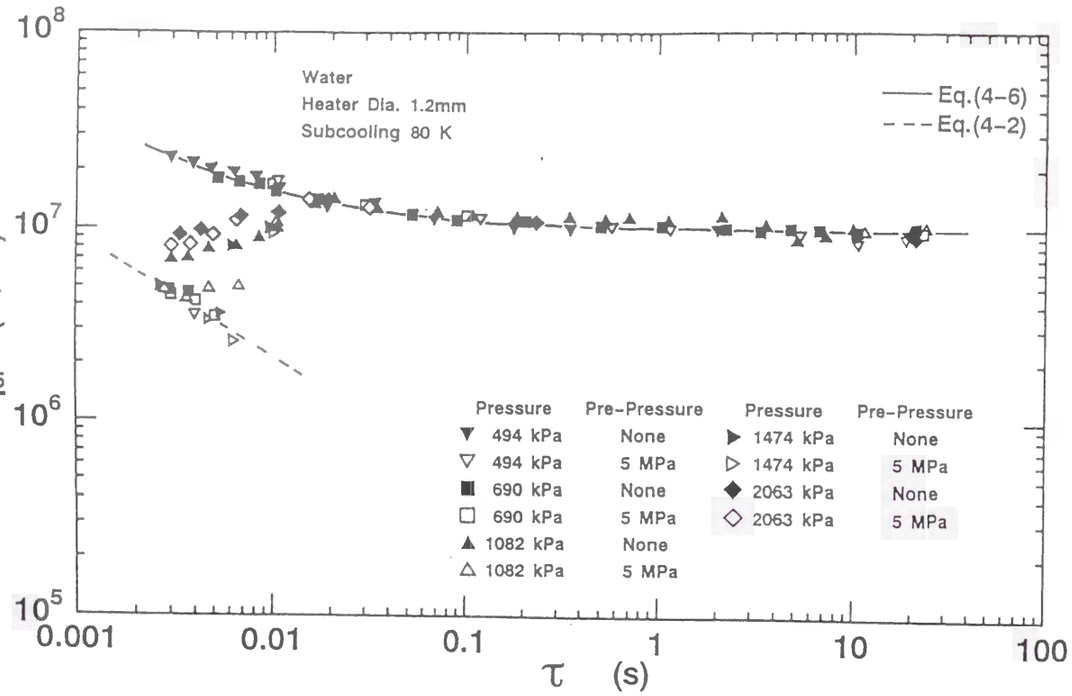

Fig. 4-5 The relation between q_{cr} and τ for subcooling of 80 K at various pressures for the cases without and with pre-pressurization.

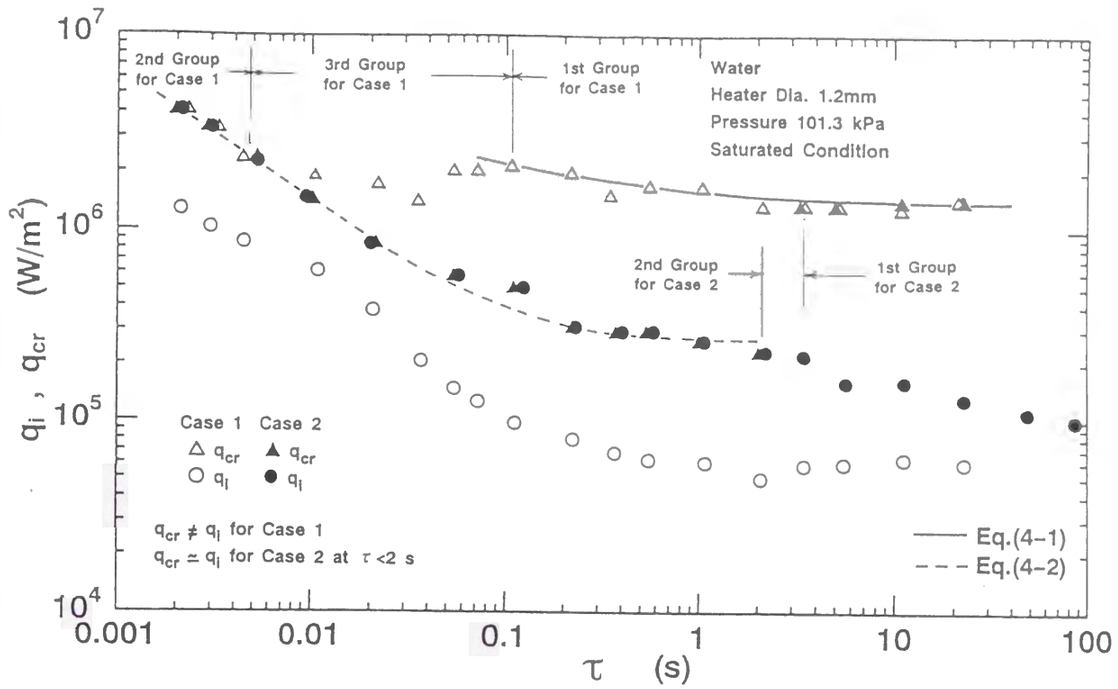

Fig. 4-6 Boiling initiation heat flux q_i, critical heat flux q_{cr} versus exponential period τ for saturated water at atmospheric pressure.

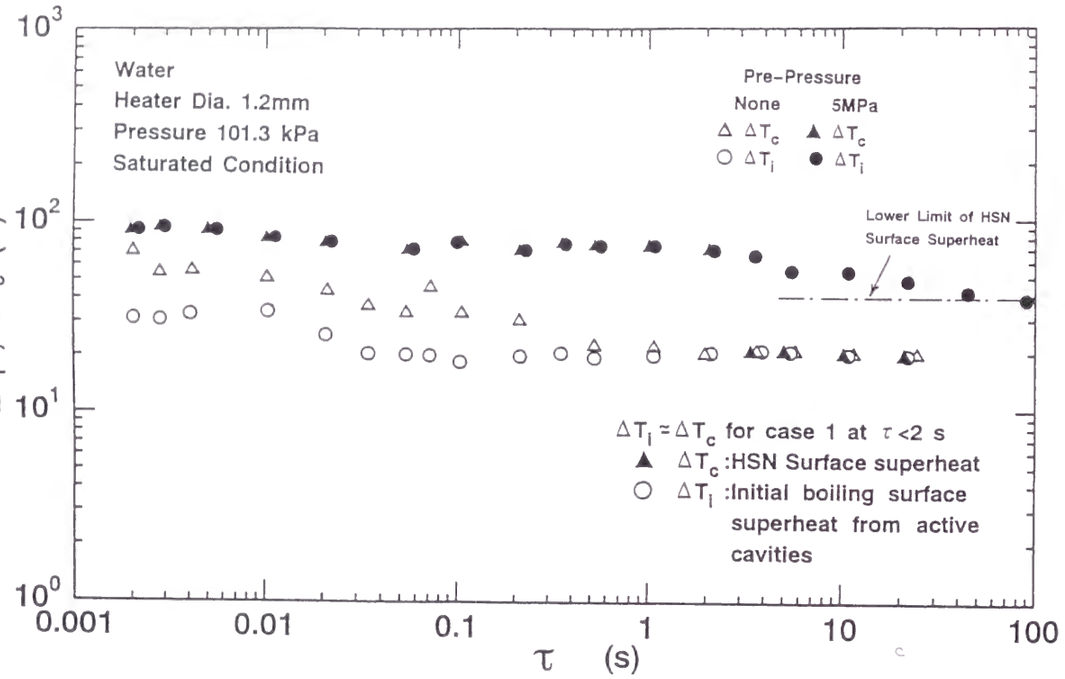

Fig. 4-7 Surface superheats at boiling initiation ΔT_i, and surface superheats at critical heat fluxes ΔT_c versus period for the same data in Fig. 4-6.

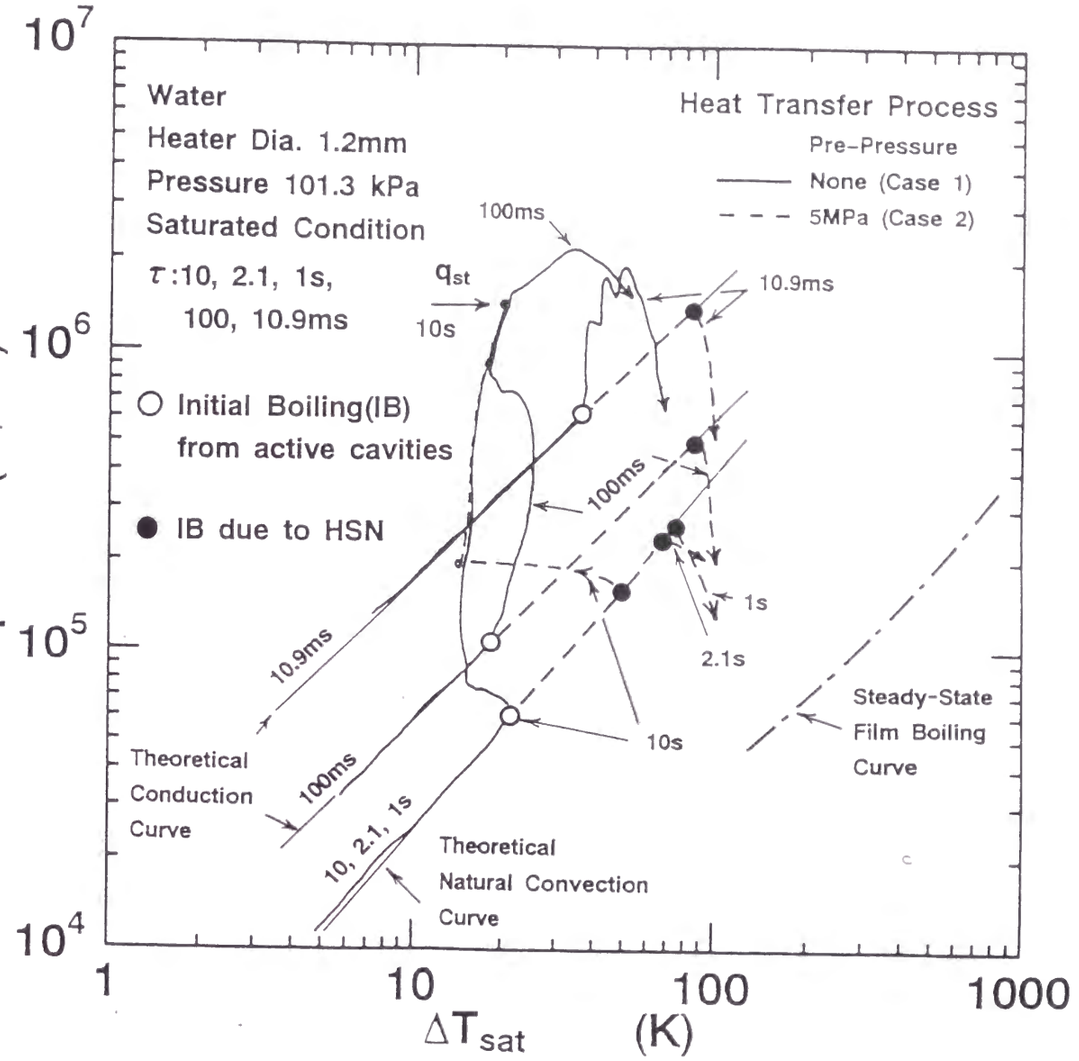

Fig. 4-8 Typical heat transfer processes for the cases without and with pre-pressurization in saturated water for periods.

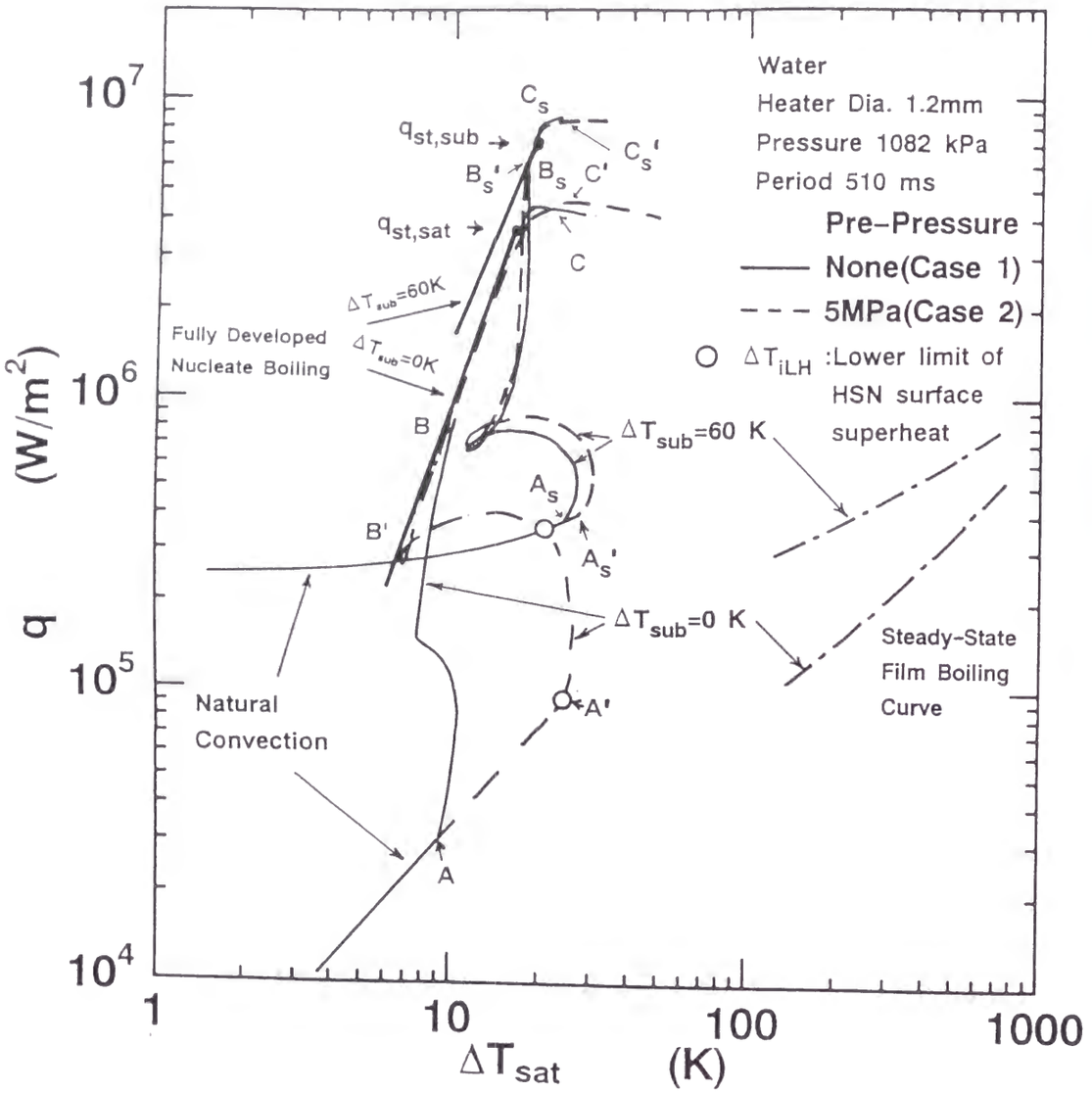

Fig. 4-9 Typical heat transfer processes with the q_{cr} of 1st group at saturated and subcooled conditions for the period of 510 ms for the Cases 1 and 2.

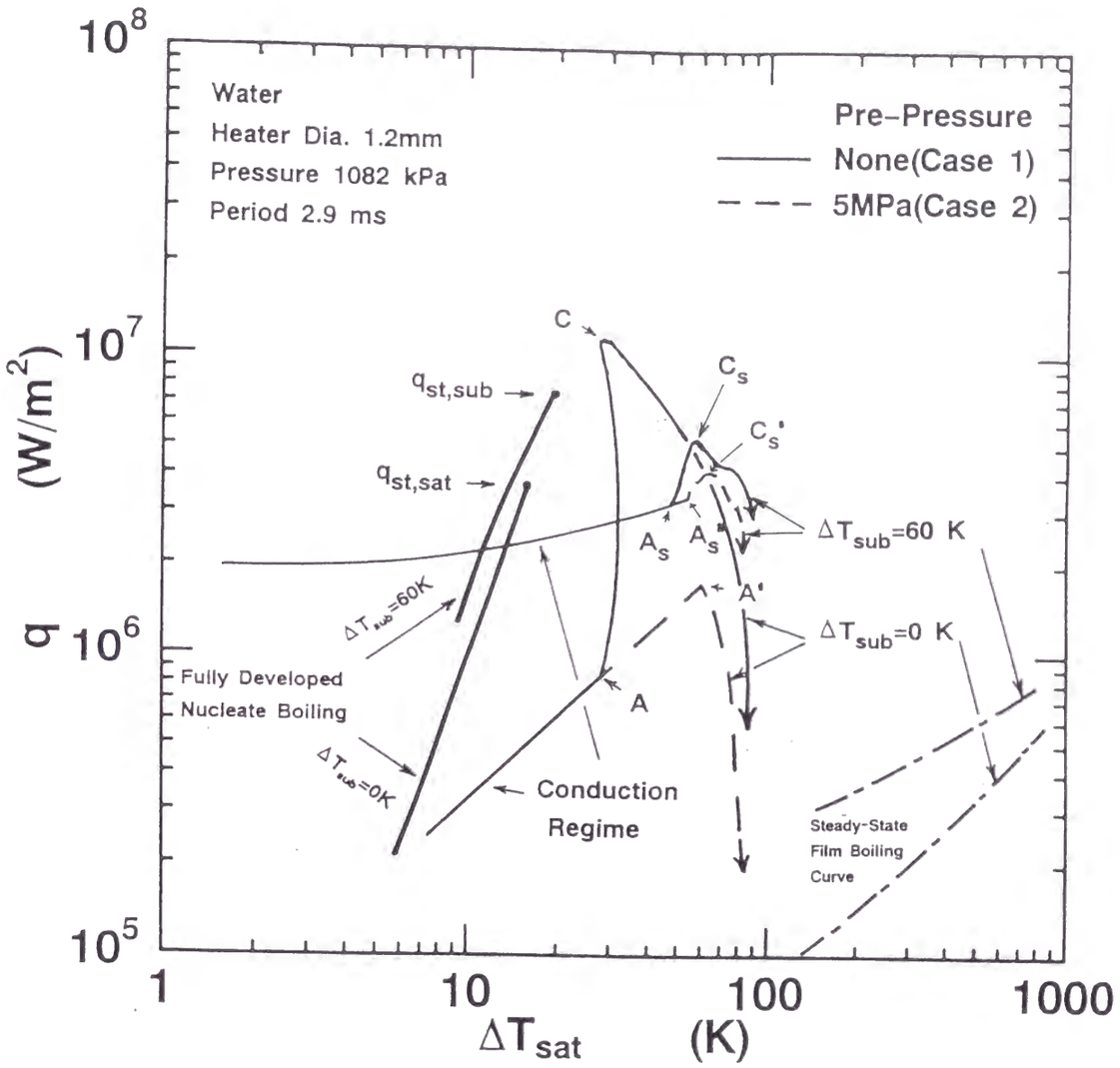

Fig. 4-10 Typical heat transfer processes with the q_{cr} of 2nd group for the period of 2.9 ms at saturated condition for the Case 2 and at subcooled condition for the Cases 1 and 2.

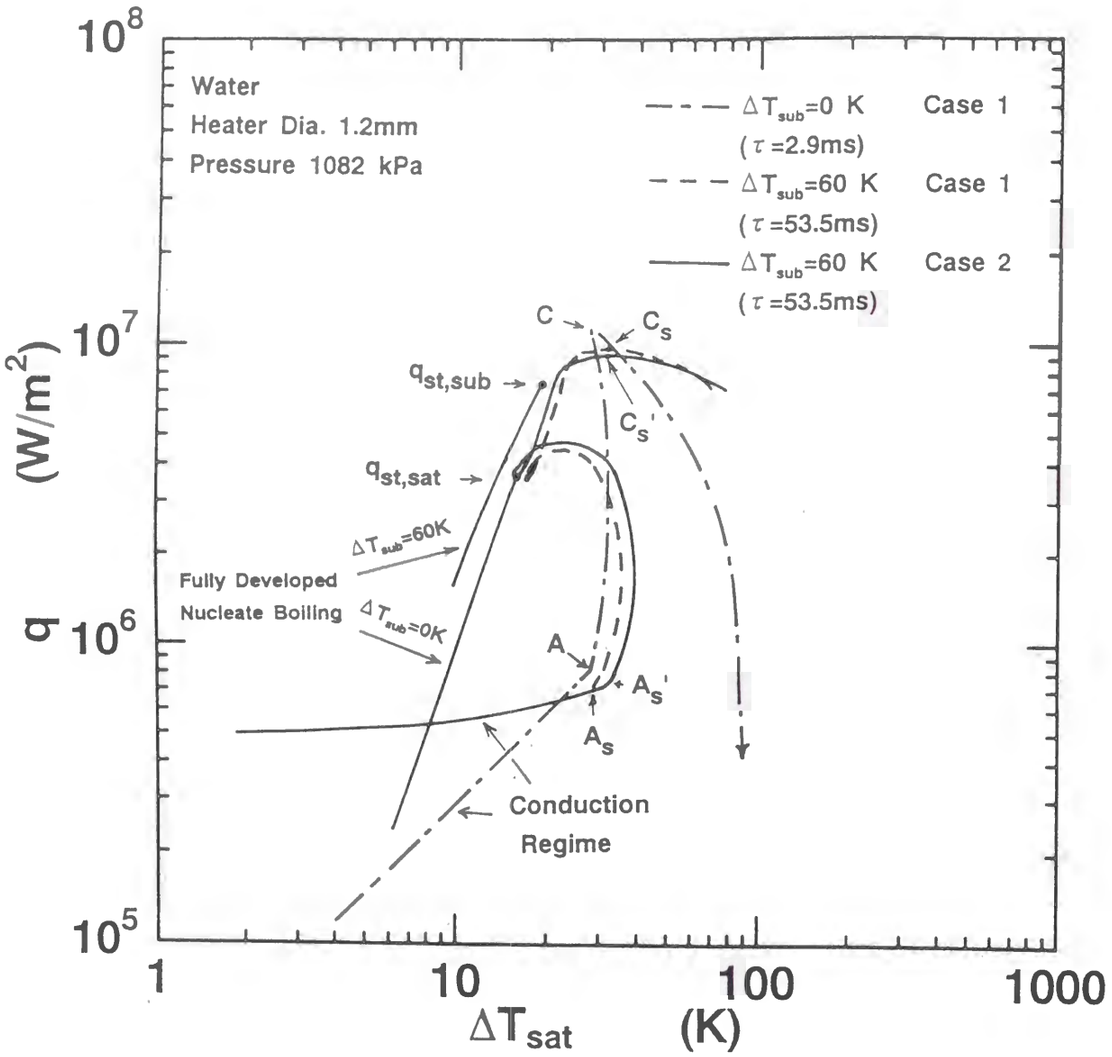

Fig. 4-11 Typical heat transfer processes with the q_{cr} of 3rd group at saturated condition for the period of 2.9 ms for the Case 1 and at subcooled condition for the period of 53.5 ms for the Cases 1 and 2.

CHAPTER 5

EFFECT OF SURFACE CONDITIONS ON TRANSIENT CRITICAL HEAT FLUX

5.1 INTRODUCTION

In the previous Chapters 3 and 4, steady-state and transient CHFs on a 1.2 mm diameter horizontal cylinder with commercial surface in water were obtained for exponential heat inputs for subcoolings from 0 to 80 K at pressures from atmospheric one up to 2063 kPa. The effects of exponential period, subcooling and pressure on the steady-state and transient critical heat fluxes were clarified.

The typical trend of CHFs versus exponential periods was such that the CHFs gradually increased from the steady-state CHF with a decrease in the period up to a maximum CHF value, decreased down to a minimum CHF value and again increased. This trend means that there exists two different mechanics of the CHF for long periods and short periods. It was considered that the former one for long periods would be due to the time lag of the hydrodynamic instability (HI) which starts at the steady-state critical heat flux in fully developed nucleate boiling (FDNB), and the latter one would be due to the

heterogeneous spontaneous nucleation (HSN) in flooded cavities which coexists with vapor bubbles growing up from active cavities in the liquids. The correlations for steady-state and transient critical heat fluxes were presented for wide ranges of pressures and subcoolings.

The purpose of this chapter is to investigate the effect of the surface conditions of the test cylinders, such as the mirror and the rough ones, on the transient critical heat fluxes caused by the exponentially increasing heat input.

5.2 EXPERIMENTS

5.2.1 Test Heaters

The platinum horizontal cylinders with commercial, rough and mirror surfaces (CS, RS and MS) of 1.2 mm in diam. and 90 mm in length were used as test heaters to measure steady and transient boiling phenomena. The rough surface was finished using Emery-3. The mirror surface was finished using alumina suspension with the average particle size of 0.3 μm finally. The three kinds of platinum cylinder surfaces with commercial, rough and mirror conditions were photographically examined using the Scanning Electron Microscope (SEM) with the JEOL Electron Probe Micro-analyzer.

The Photos.1, 2 and 3 show the surface conditions with commercial, rough and mirror surfaces obtained by a magnification of 1000 (1 mm = 1 μm in

Photos.). As shown in the Photo.1 for the CS, many grooves and scratches with about 1 μm or less in width on the surface were observed. Photograph 2 for the RS shows grooves with complicated structure of about 10 μm or less in width. Photograph 3 for the MS shows the grooves and scratches shorter than 0.5 μm in width and the micro-pits with average diameters of about 1 μm.

5.2.2 Experimental Conditions

The dynamic heat transfer processes including boiling incipience and transition to film boiling in water due to exponential heat inputs $Q_0 \exp(t/\tau)$ were measured on the test heaters with different surface finishes above mentioned Exponential period, τ, was ranged from 2 ms to 20 s. System pressure and liquid subcooling were ranged from 101.3 kPa to 2063 kPa and from 0 to 180 K.

The experiments for the case with pre-pressurization at a high pressure of around 5 MPa for a time period of about 3 minutes before each experimental run were also carried out for the same experimental conditions. By the pre-pressurization, the initial boiling caused by an increasing heat input occurs due to the heterogeneous spontaneous nucleation in originally flooded cavities taking place of that due to active cavities entraining vapor. This is because the boiling initiation from the active cavities is eliminated by the appropriate pre-

pressurization as mentioned in Chapter 3. The steady-state critical heat fluxes for wide ranges of subcoolings and pressures up to 180 K and 2063 kPa were also measured for the cylinder surfaces.

5.3 EXPERIMENTAL RESULTS AND DISCUSSION

5.3.1 Effect of Surface Conditions on CHFs at Saturated Pressures

The CHFs versus exponential periods for the test cylinders with mirror surface (MS) and rough surface (RS) under the same experimental conditions as those for the cylinder with commercial surface (CS) were obtained for the cases without and with pre-pressurization (Case 1 and Case 2). The typical results for the cylinders with CS, MS and RS in saturated water under the same experimental conditions are shown in Figures 5-1, 5-2 and 5-3. The CHFs for the subcooling of 60 K at the pressure of 690 kPa are also shown in these figures as typical subcooled results for comparison. The trends of CHF versus period for the cylinders with MS and RS under saturated and subcooled conditions are clearly classified into three groups as shown in Figures 5-2 and 5-3. The CHFs belonging to the first group at the saturated pressures of 101.3, 199 and 690 kPa on the cylinders with CS and RS were well expressed by Eq.(4-1) that represents the CHF due to the hydrodynamic instability(HI) as shown in Figures 5-1 and 5-3. It was confirmed that CHFs at pressures up to about 2 MPa were expressed by

Eq.(4-1). Though CHFs for the cylinder with MS at the pressures of 101.3 and 199 kPa were also expressed by Eq.(4-1), those at the pressures higher than 494 kPa were expressed by Eq.(4-6) and the curves for the pressures almost agreed with each other. As mentioned before, the Eq.(4-6) represents the CHFs due to the heterogeneous spontaneous nucleation (HSN). This means that the transitions to film boiling occur due to HSN on the cylinder with MS at the steady-state and transient CHFs belonging to the three groups for wide ranges of pressure and subcooling. The CHFs for the subcooling of 60 K at the pressure of 690 kPa for the cylinders shown in the figures were expressed by Eq.(4-6). Though the curves of CHFs versus periods for the cylinders with CS and RS almost agreed with each other as shown in Figures 5-1 and 5-3, the curve for the MS cylinder existed parallel to the curves for CS and RS cylinders at lower side as shown in Fig. 5-2. The mirror surface condition substantially affects steady-state and transient CHFs belonging to the first group. It was confirmed that the surface superheat at each steady-state CHF agreed with the corresponding HSN surface superheat measured with the pre-pressurization before the run.

On the other hand, the CHFs belonging to the second group were clearly observed on the cylinder with MS for the period down to 2 ms at the saturated pressures of 101.3 to 690 kPa even for the case without pre-pressurization as seen in Fig. 5-2. The CHFs belonging to the second group could not be observed on the cylinder with CS. The minimum CHFs for the period of around 10 ms for

the ΔT_{sub} of 0 and 60 K at the pressure of 690 kPa were about 70 % and 40 % of the corresponding steady-state CHFs respectively even for the Case 1.

Typical heat transfer processes on the cylinders with CS and MS are shown for the saturated condition at pressure of 690 kPa in Fig. 5-4, and those on the cylinders with CS, MS and RS for the subcooling of 60 K at pressure of 690 kPa are shown in Fig. 5-5. As seen from these figures, the heat transfer processes for the period of 5 ms on the cylinder with MS have the CHFs belonging to the second group that are far lower than the corresponding steady-state CHFs. The CHFs for the period of 5 ms at the pressure of 690 kPa under the subcoolings of 0 and 60 K on the cylinders with CS and MS are significantly different each other as can be seen from the heat transfer processes up to the each CHF shown in Figs. 5-4 and 5-5. Direct transition occurred on the cylinder with MS, and semi-direct transition occurred on the cylinder with CS.

The CHFs on the cylinder with RS at the saturated pressures of 101.3 and 199 kPa, and for the subcooling of 60 K at the pressure of 690 kPa are shown for the Cases 1 and 2 in Fig. 5-3. The trend of the CHF belonging to the first group versus period is almost similar to that for the cylinder with CS shown in Fig. 5-1. As shown in Fig. 5-5, the heat transfer processes up to the CHF for the periods of 20 s and 50 ms on the cylinders with CS and RS almost agreed with each other at around each CHF. On the other hand, the CHFs for the shorter period of 5 ms belonging to the second group were clearly observed for the RS

cylinder and were similar to those obtained by the cylinder with MS as is seen in Figs. 5-3 and 5-5. It should be noted that the trend of CHFs on the cylinder with RS belonging to the first group with respect to the period is similar to that for the cylinder with the CS, and that belonging to the second group is similar to that for the cylinder with the MS. It seems from the surface condition of RS shown in Photo. 2 that the surface finish with Emery 3 paper merely gives large grooves but may not be effective to supply active cavities with larger radii. Moreover, some of the small cavities might have been removed by the treatment.

5.3.2 Effect of Surface Conditions on CHFs for Subcoolings at a High Pressure

The CHFs on the cylinders with MS and RS were measured for the Cases 1 and 2 at the pressure of 1082 kPa for the subcoolings of 20, 40, 60 and 80 K. The CHFs were compared with those for the cylinder with CS. The results for the cylinders with CS, MS and RS are shown in Figs. 5-6, 5-7 and 5-8 respectively. The trend of CHFs with respect to periods belonging to the first group on the cylinders with CS and RS are almost same each other. Those for the subcooling of 20 K and 40 K are well expressed by the Eq.(4-1), and those for the subcoolings of 60 K and 80 K are well expressed by Eq.(4-6). On the other hand, the CHFs on the cylinder with MS for periods belonging to the first

group for the subcoolings from 20 to 60 K are expressed by Eq.(4-6) and each steady-state CHF is lower than the corresponding CHFs for the CS and RS cylinders.

On the other hand, the CHFs belonging to the second group clearly exist for the cylinders with MS and RS for both Cases 1 and 2. The CHFs for the same period for the Cases 1 and 2 for each cylinder almost agree with each other. The direct and semi-direct transitions from conduction regime without and with several vapor bubbles occur at the CHFs. On the contrary, as is seen in Fig. 5-6, the CHFs for short periods belonging to the second group are not observed for the cylinder with CS under the same experimental conditions.

It should be noted that the CHFs for the period of 10 ms under the subcooling of 80 K are about 30 % of the corresponding steady-state CHF for the cylinder with MS, and about 40 % of the corresponding steady-state CHF for the cylinder with RS even for the case without pre-pressurization. The direct transition from the transient conduction regime to film boiling occurs at the CHF on the cylinders with MS and RS for the period of around 5 ms at the pressure of 1082 kPa.

5.3.3 Effect of Surface Conditions on CHFs for a High Subcooling at Various Pressures

The CHFs for the subcoolings of 60 K for the cylinders with CS, RS and MS are shown versus the periods in Figs. 5-9, 5-10 and 5-11. The CHFs for the long periods belonging to the first group for the Cases 1 and 2 are independent of the pressure and are expressed by the Eq.(4-6). This fact was already explained for the cylinder with CS by assuming that the transition to film boiling at the steady-state CHFs occurs due to the explosive-like HSN in FDNB at the lower limit of HSN surface superheat in FDNB regime. Though the CHFs for shorter periods belonging to the second group for the cylinder with CS were observed only for the Case 2, those for the Case 1 were not observed for the periods tested here as shown in Fig. 5-9.

On the other hand, the trend of the CHFs with respect to long periods belonging to the first group for the cylinder with RS was almost the same as that for the cylinder with CS. However, the CHFs for short periods belonging to the second group were clearly observed not only for the Case 2 but also for the Case 1 as is seen in Fig. 5-10. The minimum CHFs for the period of around 10 ms become significantly lower than the corresponding steady-state CHFs even for the Case 1. The minimum values at 690 kPa are about 35 % of the corresponding steady-state CHFs. The trend of CHFs with respect to the periods belonging to the second group was well expressed by the theoretical conduction line given by Eq.(4-2) and (4-3) as $h_m = h_c$ on the log-log graph as shown in Fig. 5-10.

The curve of CHFs belonging to the first group versus periods for the cylinder with MS at various pressures exists downward and parallel to the curves for the RS and MS cylinders, though the curves for the cylinder with CS and RS almost agree with each other as is seen in Fig. 5-11. This means that the steady-state CHFs for the cylinder with MS for the subcooling of 60 K depend on the surface conditions, because the CHFs are not due to the hydrodynamic instability (HI) but due to the HSN mentioned before. It was confirmed that the surface superheat at each CHF almost agrees with the measured lower limit of the HSN surface superheat.

The CHFs for short period belonging to the second group clearly exist for the Cases 1 and 2 on MS cylinder as is seen in Fig. 5-11. The CHFs for short periods belonging to the second group for the Cases 1 and 2 almost agree with each other, and those for the periods at the pressures were approximately expressed independently of the pressures by the single curve. The minimum CHFs for period of 10 ms at the pressure of 690 kPa for the Case 1 were about 37 % of the corresponding steady-state CHF. It should be noted that the CHFs for the short periods for Case 1 and Case 2 agreed with each other. This fact leads that the initial boiling occurs due to the HSN even for the Case 1.

5.4 CONCLUSIONS

The CHFs caused by exponentially increasing heat inputs were measured on the horizontal cylinders with mirror surface (MS) and rough surface (RS) in water for the cases without and with the pre-pressure of 5MPa (Case 1 and Case 2). They were compared with those obtained for the horizontal cylinder with commercial surface (CS) under the same condition to clarify the effect of surface conditions on the CHFs. Experimental results lead to the following conclusions.

(1) The trend of the CHFs with respect to periods is generally as follows: the CHF first increases with a decrease in period from steady-state CHF up to a maximum CHF, then it decreases down to a minimum CHF and again increases with a decrease in period. Namely, the CHFs versus periods were separated into the first, second and third groups on CHF for longer, shorter and intermediate periods.

(2) The trends of CHFs with respect to periods belonging to the first group on the cylinders with RS are expressed well by Eq.(4-1) and (4-6) at lower and higher subcoolings, respectively. They agreed with those obtained for the cylinder with commercial surface (CS). On the contrary, the trend of CHFs versus the periods belonging to the first group on the cylinder with MS at saturated pressures higher than around 400 kPa are expressed by Eq.(4-6)

because the CHFs are determined by the HSN for the cylinder with MS at the pressures. The mirror surface condition gives the significant effect on CHFs under saturated and subcooled conditions.

(3) The CHFs for the intermediate periods belonging to third group considerably depend on the surface conditions such as CS, RS and MS. The period range for the third group for the cylinders with MS and RS becomes narrow in comparison with that for the cylinder with CS. As a result, the period range of second group becomes wide in the range of the periods tested here.

(4) The second group of CHFs for short periods could not be observed for the cylinder with CS except some cases for the periods from 20 s down to 2 ms tested here. They were observed only for the case with pre-pressurization (Case2). However, they were clearly observed on the cylinders with RS and MS for both cases. The curves for the surface conditions of RS and MS agree with each other on the graph of q_{cr} versus period. They are expressed well by Eq. (4-2). However, the periods for the minimum CHF in the second group are considerably affected by the surface conditions.

(5) It should be noted that the minimum CHF for the period of about 10 ms for the subcooling of 40 K at the pressure of 1082 kPa for the cylinders with RS and

MS are about 30 % and 35 % of the corresponding steady-state CHFs respectively.

More study on the effect of cylinder surface conditions on the CHFs for short periods belonging to the second group which are determined by the corresponding HSN surface superheats is especially necessary not only for the academic interests but also for the safety assessment of nuclear reactor for abnormal conditions such as power burst in the reactor.

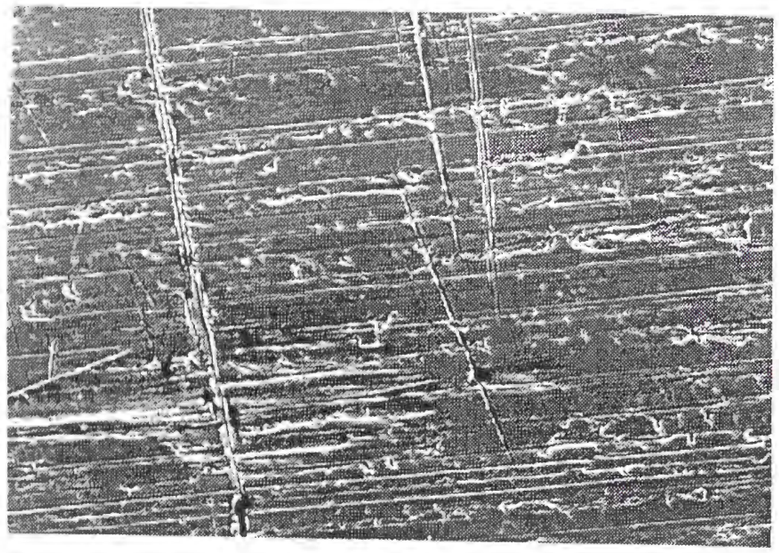

10μm

Photo. 1 Commercial surface(CS).

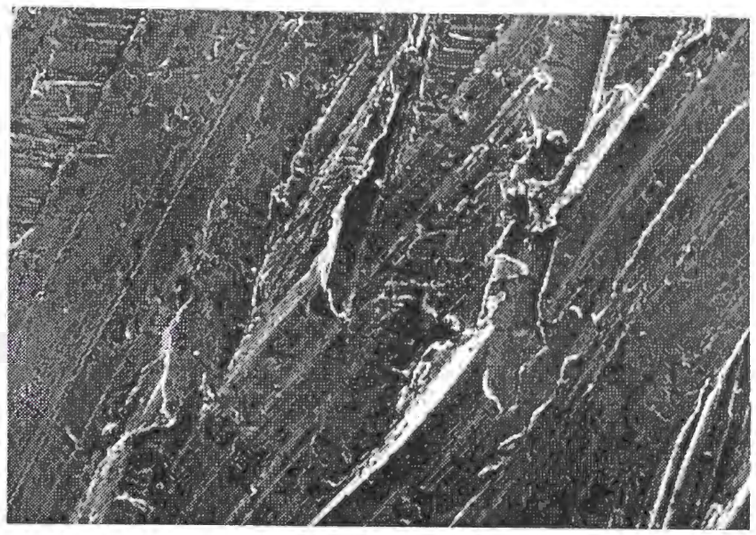

10μm

Photo. 2 Rough surface(RS).

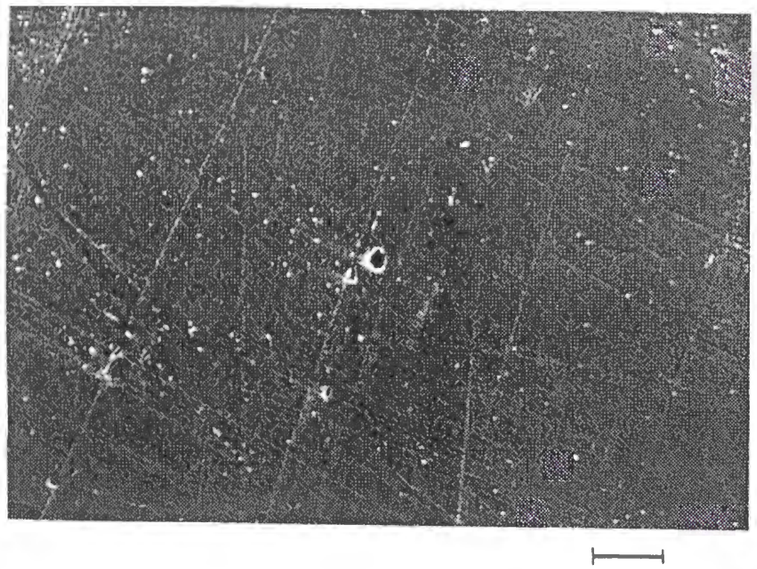

Photo. 3 Mirror surface(MS).

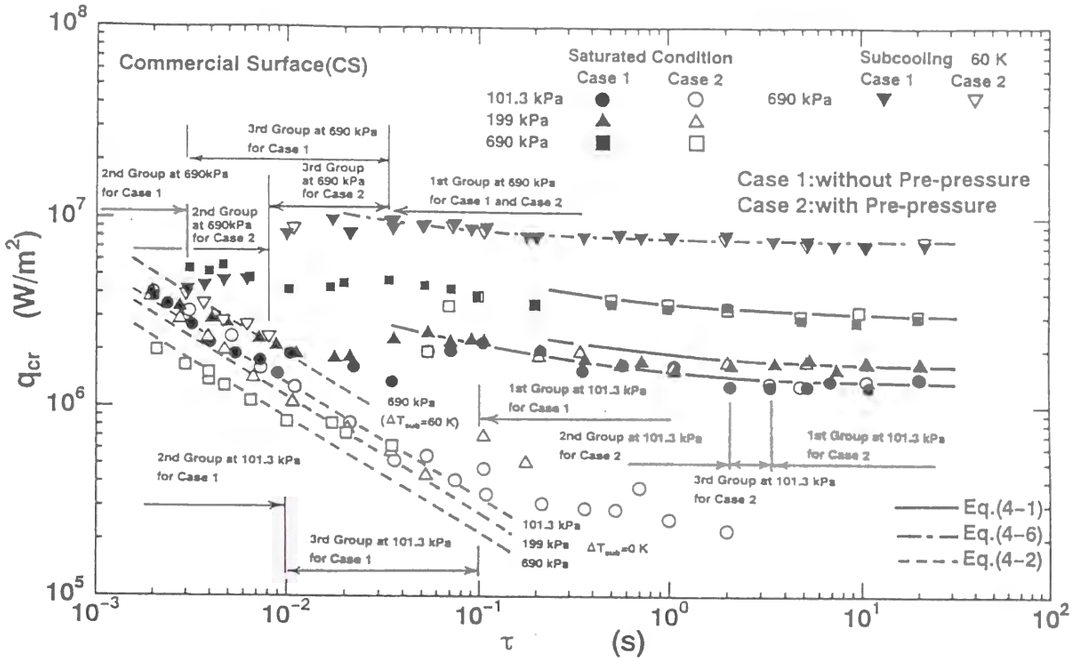

Fig. 5-1 The relation between q_{cr} and τ at pressures of 101.3, 199 and 690 kPa for the cases without and with pre-pressurization for the commercial surface.

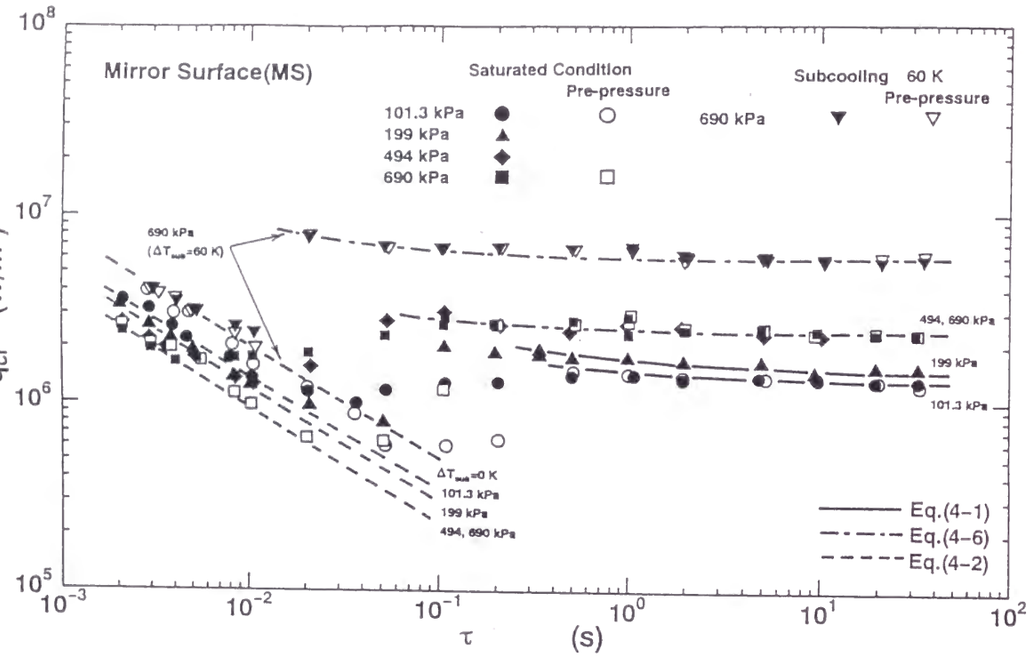

Fig. 5-2 The relation between q_{cr} and τ at pressures of 101.3, 199, 494 and 690 kPa for the cases without and with pre-pressurization for the cylinder with MS.

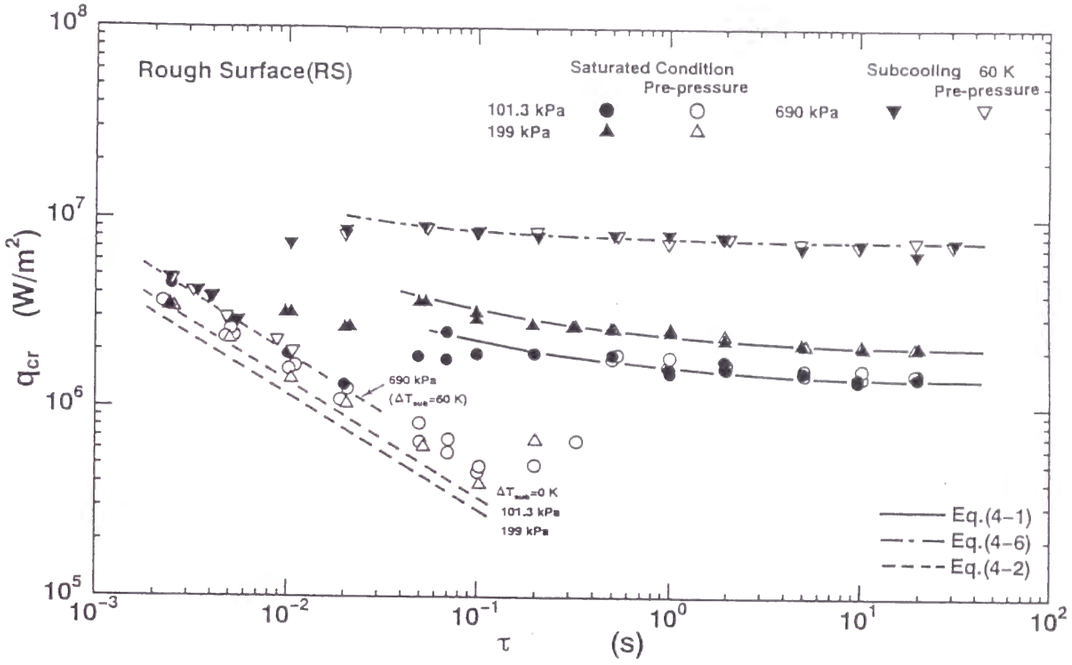

Fig. 5-3 The relation between q_{cr} and τ at pressures of 101.3, 199 and 690 kPa for the cases without and with pre-pressurization for the cylinder with RS.

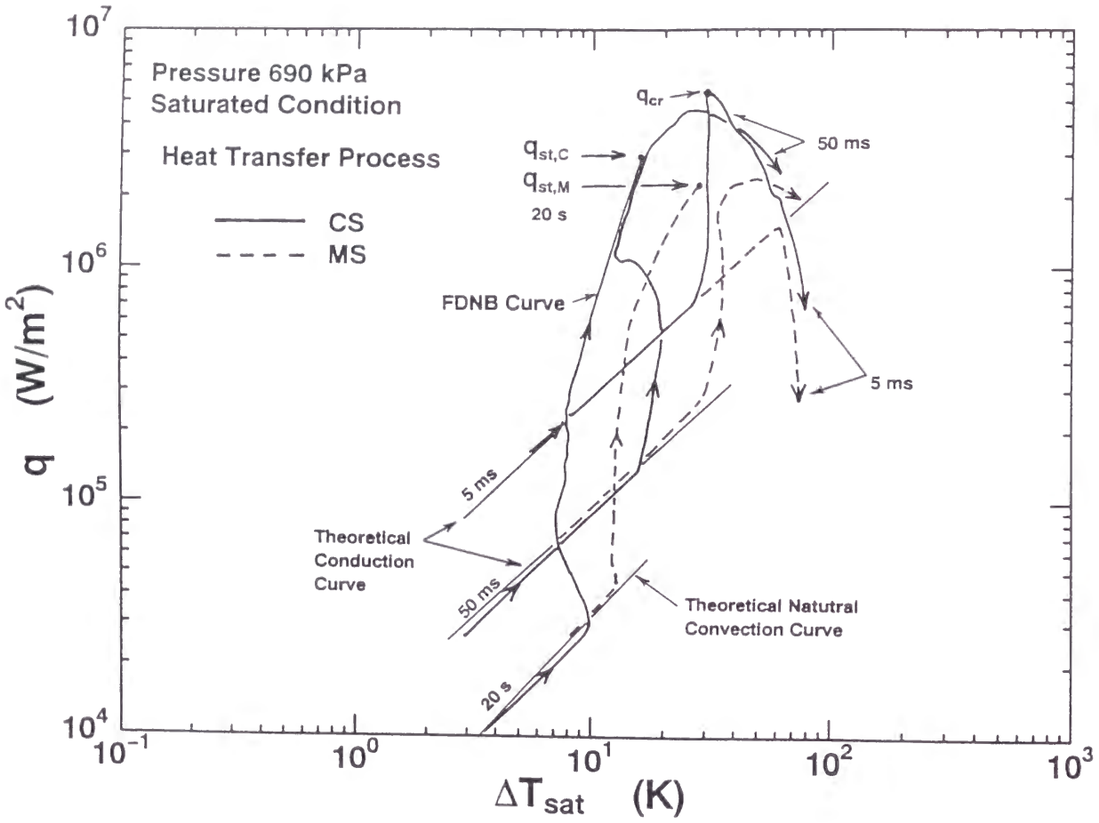

Fig. 5-4 Typical heat transfer processes for various surface conditions without pre-pressurization for exponential periods of 20 s, 50 ms and 5 ms in saturated water at a pressure of 690 kPa.

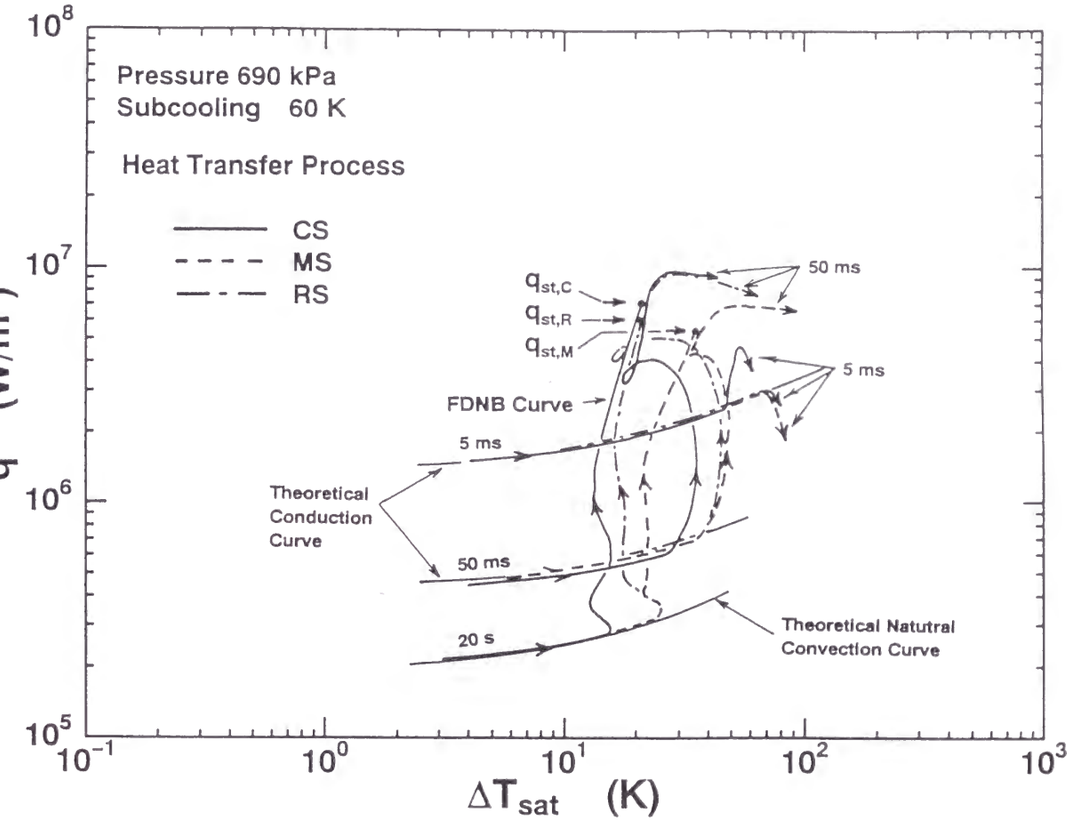

Fig. 5-5 Typical heat transfer processes for various surface conditions without pre-pressurization for exponential periods of 20 s, 50 ms and 5 ms at a pressure of 690 kPa for subcooling of 60 K.

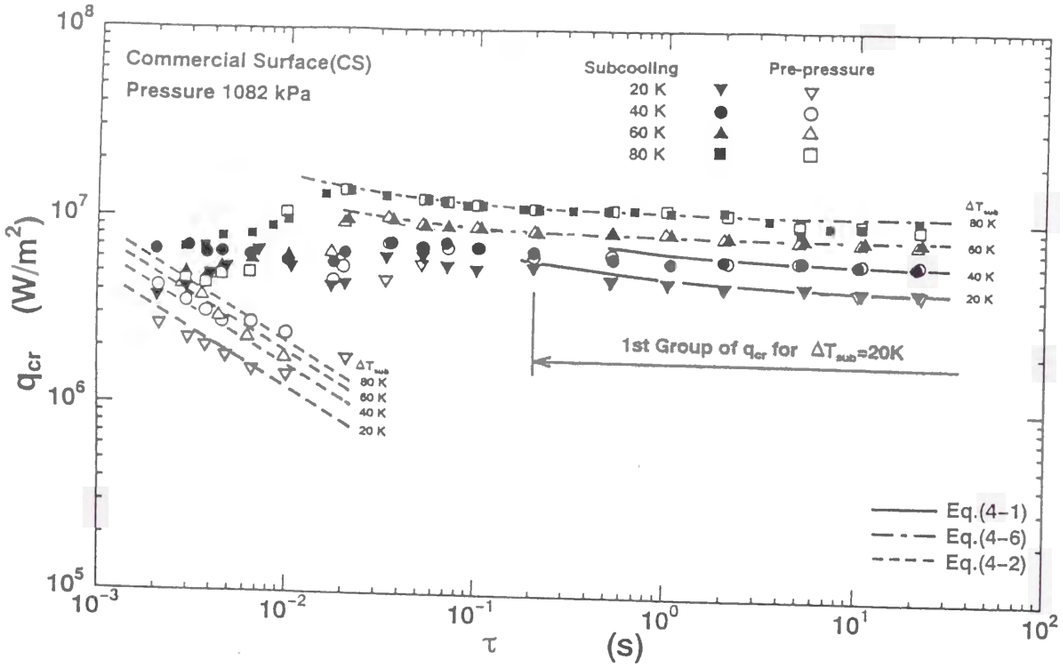

Fig. 5-6 The relation between q_{cr} and τ for various subcoolings at a pressure of 1082 kPa for the cases without and with pre-pressurization for the cylinder with CS.

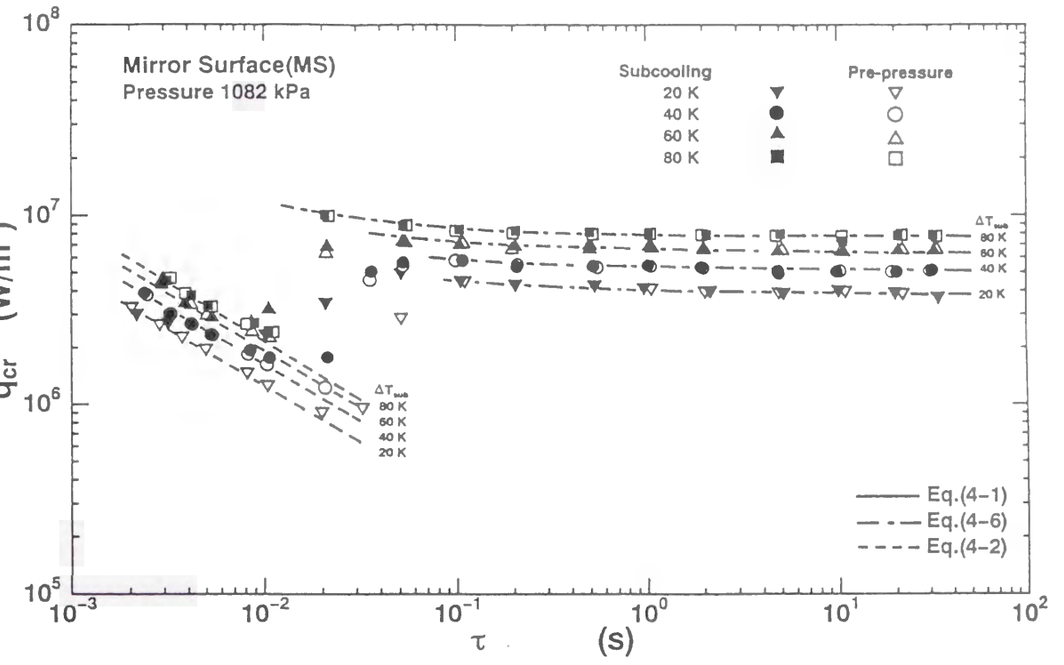

Fig. 5-7 The relation between q_{cr} and τ for various subcoolings at a pressure of 1082 kPa for the cases without and with pre-pressurization for the cylinder with MS.

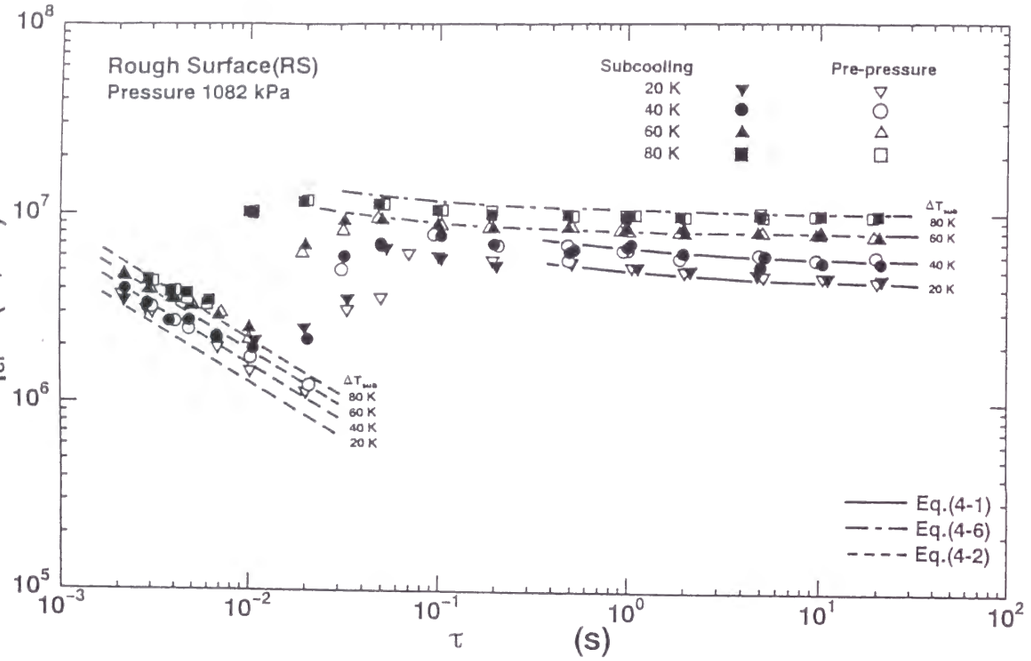

Fig. 5-8 The relation between q_{cr} and τ for various subcoolings at a pressure of 1082 kPa for the cases without and with pre-pressurization for the cylinder with RS.

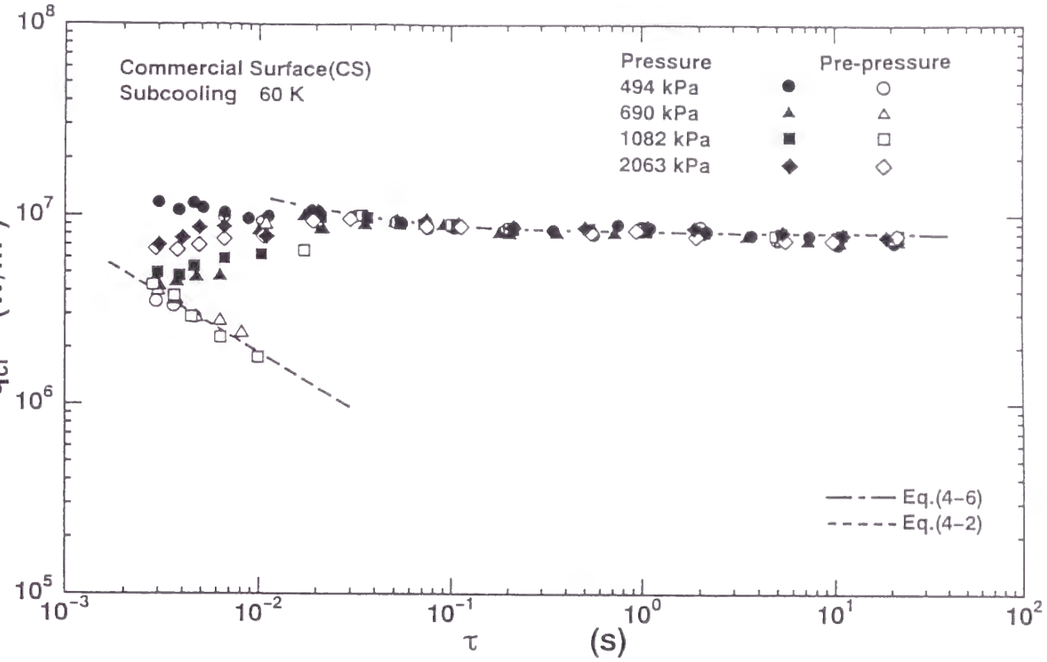

Fig. 5-9 The relation between q_{cr} and τ for subcooling of 60 K at various pressures for the cases without and with pre-pressurization for the cylinder with CS.

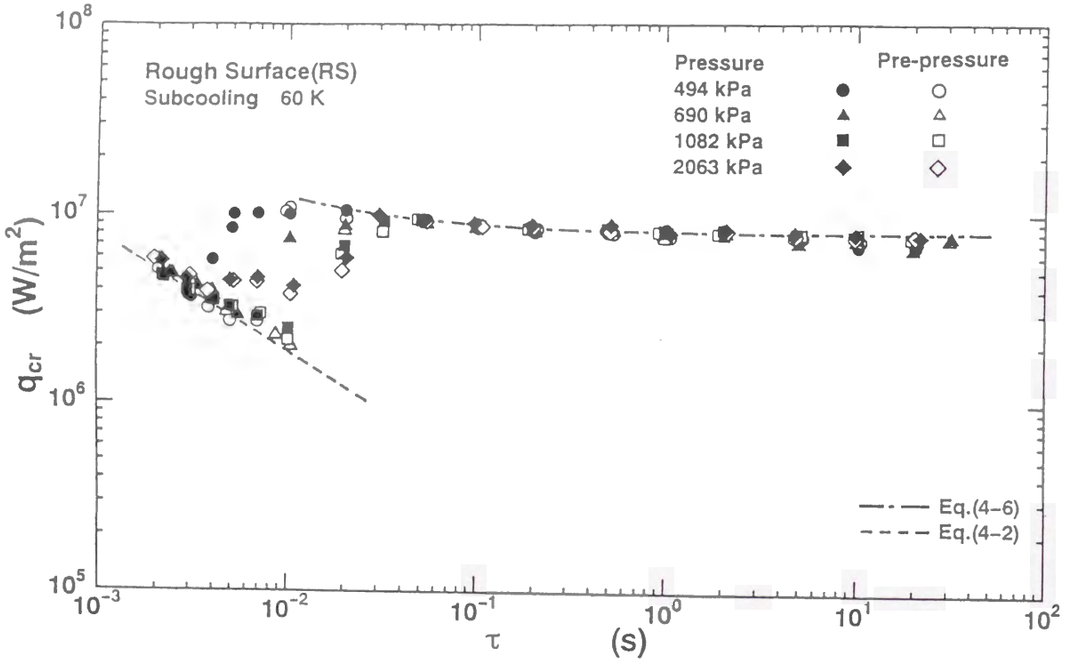

Fig. 5-10 The relation between q_{cr} and τ for subcooling of 60 K at various pressures for the cases without and with pre-pressurization for the cylinder with RS.

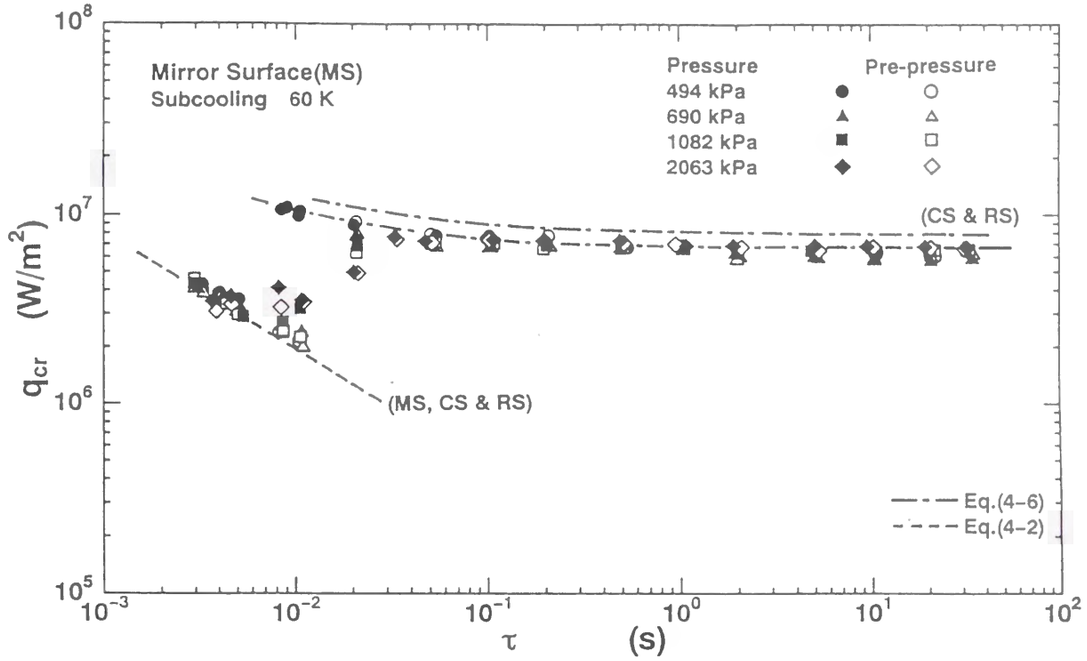

Fig. 5-11 The relation between q_{cr} and τ for subcooling of 60 K at various pressures for the cases without and with pre-pressurization for the cylinder with MS.

CHAPTER 6

TRANSIENT HEAT TRANSFER PROCESSES DURING A RAPID SYSTEM PRESSURE REDUCTION

6.1 INTRODUCTION

The semi-scale Mod-1 test demonstrated the overheating of fuel rods initially cooled by forced convection in the early stage of pressure reduction (Crapo et al., 1975). Henry and Leung (1977) presented a model to predict the regions of fuel rods which may experience limited efficient cooling during the pressure reduction. The model predicted that the regions which were cooled only by single-phase forced convection during steady-state conditions would be unable to activate the remaining preferred sites until the surface had increased in temperature to a level which satisfied the criteria for stable film boiling.

On the other hand, Sakurai et al. (1980) carried out the experimental study on transient boiling heat transfer from single horizontal cylinders in a pool of water caused by rapid depressurizations from several pressures for initial constant heat inputs: the initial heat transfer regimes corresponding to the initial constant heat inputs were natural convection and partial nucleate boiling. They clearly observed that the initial non-boiling state on the test heater was switched

over to a film boiling state corresponding to the initial heat flux after the rapid depressurization, and that the critical heat fluxes for these processes were considerably lower than the steady-state critical heat fluxes at the corresponding pressures. It is obvious that the mechanism of the transition is different from that of the usual one at the critical nucleate boiling heat flux due to the hydrodynamic instability, as pointed out by Kutateladze (1959), and Zuber (1959). However, the mechanism for the transition from initial non-boiling to film boiling was not clarified.

There are two main purposes in this chapter. First is to examine experimentally the effects of initial pressure, pressure-reduction rate, initial heat transfer regimes such as natural convection or nucleate boiling, and cylinder diameter, on the transition mechanism to film boiling. The second purpose is to discuss the mechanism for the transition from steady-state heat transfer at low initial heat fluxes to film boiling after rapid depressurization.

6.2 APPARATUS AND METHOD

The schematic diagram of the experimental apparatus is shown in Fig. 6-1. The boiling vessel is a cylindrical stainless-steel container of 20 cm in inner diameter and 60 cm height with two sight ports. The vessel has a pressure release line of 5 cm inner diameter from its upper lid to the atmosphere through

a rupture disc device. The device has a gaff with a spring for breaking the disc intentionally. A test heater is horizontally supported in the vessel.

Single cylinder test heaters of 1.2 and 3 mm-diameter platinum wires were used. The effective length of the heaters between the potential taps, on which heat transfer was measured, were 42 mm for the 1.2 mm-diameter heater and 49 mm for the 3.0 mm-diameter one. Each heater was annealed and its electrical resistance versus temperature relation was calibrated in water and glycerin baths, before using it in the experiments.

The test heater was heated by an electrical current from a power amplifier. The heating and measurement systems are the same as those explained in Chapter 2. It is possible to realize a constant heat generation rate throughout a pressure transient, in spite of the rapid variation in the electrical resistance of the heater, due to its temperature variation. The static pressure was set before each experimental run by using an electro-manometer system whose accuracy is within ± 0.7 kPa. The system pressure was measured by a quartz pressure transducer during the transient.

The vessel was filled with distilled and deionized water. The vessel was degassed before each experimental run. The system pressure in the vessel was raised to a desired initial level by introducing pressurized helium gas from a cylinder. Helium gas was used because of its low solubility in liquids. The test heater was initially either in non-boiling (natural convection heat transfer) state

or in low heat flux nucleate boiling state in subcooled water, for a heat input which was kept constant throughout each experimental run. The system pressure in the vessel was rapidly reduced by intentionally breaking the rupture disc with the gaff. The trigger signal to release the gaff was also used to start the transient heat transfer measurement.

6.3 EXPERIMENTS

6.3.1 Pressure Transient

The pressure transient experiments were performed with 1.2 and 3.0 mm-diameter horizontal cylindrical test heaters. Initial pressures were 1.08 and 1.57 MPa, for initial heat fluxes ranging from 0.2 to 0.8 MW/m^2 (from natural convection to low heat flux nucleate boiling) and a water temperature of 373 K. After the disc rupture, the system pressure decreased exponentially in time, $P^* = P_{in}^* \exp\left(-t/\tau_p\right)$, where P^* and P_{in}^* are the system pressure and the initial pressure in gauge and τ_p is the pressure-reduction period. The period was varied from 1 ms to 25 ms by varying the water level and by using various-sized orifices.

6.3.2 Steady-state

The steady-state boiling curves and critical heat fluxes were measured at several pressures corresponding to the measured instantaneous pressures during the pressure transient on the same test heaters for the liquid temperature of 373 K, for comparison. Before the steady-state run, the pressure was raised once to the initial value of the pressure transient and held at that level for one minute. Fully developed nucleate boiling (FDNB) curve at each pressure was obtained by first increasing the heat flux quasi-steadily up to that slightly lower than the critical heat flux and then decreasing it.

6.3.3 Power Transient

Transient boiling experiments for the exponentially increasing heat inputs for periods ranging from 5 ms to 10 s, were also performed at several pressures ranging between the initial one of the pressure transient and atmospheric, with pre-pressurization at the value of the initial pressure for a time period of about one minutes before each experimental run.

A curve describing the relation between the temperature overshoot, ΔT_{over}, and the heat fluxes at the overshoot points, q_{over}, for exponential periods ranging from short one to long one (this is called the hypothetical nucleate boiling curve in this work) was obtained for each fixed pressure below the initial pressure.

The high pre-pressurization and high subcooling before each run act to flood, with liquid, those cavities on the solid surface which have mouth radii greater than a certain value as mentioned in Chapter 3. It is assumed that the temperature overshoot for the increasing heat input would correspond to the surface superheat required for the start of explosive-like boiling by the heterogeneous spontaneous nucleation (HSN) from the originally flooded cavities on the surface, and that the hypothetical nucleate boiling curve would be the one governed by the HSN from originally flooded cavities. The hypothetical nucleate boiling curve at a fixed pressure can be determined as an envelope of the HSN limits of the heater surface superheats for the transient boiling curves for the increasing heat inputs for convenience. Figure 6-2 shows as a typical the method to determine the hypothetical nucleate boiling curve for the system pressure of 493 kPa. The curve AB in the figure, which exists at the higher superheat side of the steady-state nucleate boiling curve, is the hypothetical nucleate boiling curve.

The mechanism of the transient heat transfer during the pressure reduction will be considered by comparing the results of transient heat transfer with the hypothetical nucleate boiling curve based on the HSN at each pressure.

6.4 RESULTS AND DISCUSSION

The transient heat transfer caused by rapid depressurization depends on many parameters such as the initial pressure, the pressure-reduction rate, the initial heat flux and the cylinder diameter. The effect of each of these parameters on transient heat transfer was investigated by fixing the other parameters. Based on these results, a mechanism of the transition from initial natural convection to film boiling is proposed.

6.4.1 Typical Data of Transition from Initial Non-boiling State to Film Boiling

Typical time traces of the system pressure P, the heater surface temperature T_w and the heat flux q during the transient caused by a rapid depressurization from initial natural convection, are shown in Fig. 6-3. The test heater of 1.2 mm-diameter was initially in single-phase natural convection, at a constant heat flux of 0.38 MW/m^2, in a water pool at 373 K and 1.08 MPa. The pressure-reduction period in this case is 2.2 ms. The surface temperature and heat flux remain at their initial values until the initiation of boiling at point B, 3 ms after the beginning of pressure reduction at point A. The heat flux increases rapidly after the boiling inception to a maximum value at point C, that is about 3 times larger than the initial value. Then, it rapidly decreases down to a minimum value at point D, which is about one tenth of the initial value, remains

at the minimum value for about 24 ms, and gradually increases toward the final steady-state value $(q = q_{in})$ of film boiling. The surface temperature first decreases slightly and then continues to increase, toward a stable film boiling point corresponding to the initial heat flux. In the case that the stable point corresponding to $q = q_{in}$ in film boiling is near the melting point for platinum, the heating current was shut off when the surface temperature reached a preset critical value.

The relation between the transient heat flux, q, and the instantaneous surface superheat, ΔT_{sat}, for the same run, is shown in Fig. 6-4. The naked number and number in parenthesis beside each point on the curve are the pressure and subcooling at that point in MPa and K, respectively. Point A is the starting point of the pressure transient. The natural convection heat transfer can be described by the general correlation of natural convection heat transfer for different cylinders in various liquids given by Takeuchi et al. (1995). The heater surface superheat increases from point A along the natural convection heat transfer curve for a constant heat flux at each pressure and subcooling, to the incipient boiling point B. The heater surface temperature is constant before the inception of boiling and the increase in the surface superheat is due to the decrease in saturation temperature. Though the heater surface temperature slightly decreases after the initiation of boiling as shown in Fig. 6-3, the heater surface superheat continues to increase with an increase in heat flux, up to a

transient critical heat flux, q_{cr}, at point C. At a given heat flux, the surface superheat in nucleate boiling at the instantaneous pressure is higher than that for the steady-state nucleate boiling curve at the same pressure. The transient critical heat flux is one third of the steady-state critical heat flux, q_{st}, at the corresponding pressure. After point C, the heat flux decreases with an increase in surface superheat down to point D, and again increases along the steady-state film boiling curve. The region CD with a negative slope is the transition region dividing nucleate from film boiling. The transient film boiling heat transfer after point D is well described by the general correlation of steady-state film boiling heat transfer given by Sakurai et al. (1990).

6.4.2 Effect of Initial Heat Flux

Figures 6-5 and 6-6 show q versus ΔT_{sat} plots of the transient heat transfer processes on a 1.2 mm-diameter test heater for pressure-reduction periods around 2.0 ms and 2.5 ms and initial pressures of 1.57 MPa and 1.08 MPa, respectively. The initial steady states for heat fluxes from 0.3 to 0.5 MW/m^2 at 1.57 MPa shown in Fig. 6-5(a), and those for the heat fluxes from 0.34 to 0.42 MW/m^2 at 1.08 MPa shown in Fig. 6-6(a), are in the single-phase natural convection regime. For higher initial heat fluxes, as shown in Figs.

6-5(b) and 6-6(b), the initial steady states are in partial nucleate boiling. The upper limit of the heat flux which is in the initial natural convection regime, is higher for higher initial pressure. As shown in Figs. 6-5 and 6-6, the transient heat transfer process is characterized by a constant heat flux value before the start of explosive nucleate boiling, even for an initial heat flux in the partial nucleate boiling regime. The pressure at the start of the explosive-like HSN boiling (where the heat flux begins to increase steeply) increases with an increase in the initial heat flux. The superheat for the pressure-reduction period around 2 ms is about 40 K for initial heat fluxes in the natural convection regime and appears to decrease with an increase of the initial heat flux in the partial nucleate boiling regime.

The pressure at the critical heat flux point becomes higher as the initial heat flux increases. The surface superheat at the critical heat flux point for a pressure-reduction period around 2 ms is about 60 K for initial natural convection conditions and appears to decrease with an increase in initial heat flux in the partial nucleate boiling regime.

The ratio of transient critical heat fluxes to the steady-state critical heat fluxes at their corresponding pressures, q_{cr}/q_{st}, for the values of q_{cr} shown in Figs. 6-5 and 6-6 are shown versus the initial heat flux in Fig. 6-7. It can be seen from Fig. 6-7 that the ratios appear to decrease with an increase in initial heat flux, have a minimum value at the initial heat flux near the upper limit of that

for natural convection regime, and then increase with an increase in initial heat flux. All the transient processes shown in Figs. 6-5 and 6-6 in each of these figures made a transition to film boiling after the transient critical heat fluxes except for that with the lowest initial heat flux. For the lowest initial heat flux, the transient process moves to the transition boiling after the critical heat flux but return to stable nucleate boiling finally, because pressure reduction and resultant increase in surface superheat stops after reaching the atmospheric pressure. It seems that there is a sharp minimum initial heat flux value below which the transient heat transfer process caused by the depressurization does not make a transition to film boiling but returns to nucleate boiling.

Figures 6-8(a), 6-8(b) and 6-9(a), 6-9(b) show the $\alpha/q^{0.7}$ versus P plots, for the transient heat transfer processes shown in Figs. 6-5(a), 6-5(b) and 6-6(a), 6-6(b), respectively. The number beside each point on the curve is the subcooling at that point in K.

The values of $\alpha/q^{0.7}$ derived from the steady-state FDNB curve and those from the hypothetical nucleate boiling curve for each fixed pressure are also shown with their existing range in these figures for comparison. If the steady-state FDNB curve and hypothetical nucleate boiling curve such as shown in Fig. 6-2 have the gradient of 3.3 on the $\log q$ vs. $\log \Delta T_{sat}$ graph, these curves can be expressed as two single values of $\alpha/q^{0.7}$. The fact that the value

of $\alpha/q^{0.7}$ has some existing range for a fixed pressure means that the gradient is somewhat different from 3.3. It can be seen from Figs. 6-8(a) and 6-9(a) that the transient heat transfer process from the initial single-phase natural convection caused by the pressure release with the period of around 2 ms is such that the value of $\alpha/q^{0.7}$ decreases with increases in surface superheat along the natural convection heat transfer curve down to the hypothetical nucleate boiling curve. The transient process departs from the natural convection heat transfer curve at the inception of explosive-like HSN boiling. After that, the heat transfer process follows the hypothetical nucleate boiling curve very closely, until it departs from the curve, at the transient critical heat-flux point. It then moves downwards to film boiling, for the initial heat fluxes higher than a certain value, or it moves upwards to a final steady-state FDNB regime, for initial heat fluxes lower than the value.

As shown in Figs. 6-8(b) and 6-9(b), the transient heat transfer processes from the initial partial nucleate boiling regime are such that the values of $\alpha/q^{0.7}$ from the start of boiling to q_{cr} are higher for the higher initial heat fluxes. As shown in Fig. 6-9(b), the transient heat transfer processes, for initial heat fluxes slightly higher than the upper limit value for the single-phase natural convection, are characterized by slightly higher values of $\alpha/q^{0.7}$ before reaching q_{cr}, but they are almost in agreement with those for the processes from

initial natural convection. As shown in Fig. 6-8(b), the transient heat transfer process, for the initial heat flux of 0.6 MW/m^2 approaches the steady FDNB after the start of explosive boiling. However, the transient critical heat flux is reached beforehand, and it begins to move downwards to film boiling. For the initial heat flux of 0.8 MW/m^2 the transient heat transfer process lies slightly beneath, but almost in agreement with the successive steady FDNB curves before reaching the transient critical heat flux.

As mentioned above, the transition from initial single-phase natural convection or partial nucleate boiling on the test heater to film boiling after the rapid depressurizations took place at considerably lower critical heat fluxes than the steady-state critical heat fluxes at the corresponding pressures, for a certain range of initial heat fluxes. It is obvious that the mechanism of the transition to film boiling at the transient critical heat flux is different from that of the usual transition at the critical nucleate boiling heat flux due to the hydrodynamic instability (HI).

In the initial non-boiling regime of the pressure transient, active (originally unflooded) cavities, with mouth radii ranging from the largest one to a certain smaller one on the surface, are flooded by the liquid because of high pressure and high subcooling. It can be assumed that the rapid depressurization initiates the explosive-like boiling by the HSN from originally flooded cavities, on the cylinder surface, at relatively high surface superheats. The reactivation of

originally flooded cavities with larger mouth radii would progress little for high growth rate of the surface superheat. Then, the transient heat transfer processes and critical heat fluxes on the hypothetical nucleate boiling curve would be mainly governed by the HSN and the critical heat flux would be lower than the usual critical heat flux based on hydrodynamic instability (HI). The transient heat transfer curve for an initial heat flux of 0.8 MW/m^2 shown in Fig. 6-7(b) lies slightly beneath the successive steady FDNB curves. In addition, the transient critical heat flux for the process is slightly smaller than the corresponding steady-sate critical heat flux as mentioned above. The transient process, though following closely the lower side of the nucleate boiling curve would be influenced by the HSN.

6.4.3 Effect of Pressure-reduction Rate

This section deals with the effect of pressure-reduction rate on the transient heat transfer from initial single-phase natural convection. Figures 6-10 and 6-11 show the q versus ΔT_{sat} plots of the transient heat transfer processes on 1.2 mm-diameter test heater for the pressure reductions with various periods from the initial pressures of 1.57 MPa and 1.08 MPa, respectively. In Fig. 6-10, the initial heat flux is fixed to be 0.5 MW/m^2 which is slightly lower than the upper limit of that for single-phase natural convection regime and in Fig. 6-11, it

is fixed to be 0.39 MW/m^2 .

As shown in Figs. 6-10 and 6-11, for the shorter pressure-reduction period, boiling starts at a higher surface superheat and a lower system pressure. In case of rapid transients such as those for τ_p less than about 3 ms, the transient critical heat fluxes near the upper limit of the initial natural convection regime reaches only up to about 30% or less of the steady-state critical heat fluxes, at the corresponding pressures, as mentioned above. The transient critical heat flux increases and the surface superheat at the critical heat flux decreases as the pressure-reduction period becomes longer. For pressure-reduction periods shorter than 7 ms, the transient boiling processes on the 1.2 mm-diameter test heater move into film boiling. For longer periods, such as $\tau_p = 12.6$ ms in Fig. 6-10 and $\tau_p = 13.0$ ms in Fig. 6-11, the thermal energy stored in the test heater before the transient is insufficient for the heat flux to reach the minimum heat flux of film boiling, or to reach the critical heat flux of nucleate boiling and the transient process finally returns to nucleate boiling.

The $\alpha/q^{0.7}$ versus P plots for the transient heat transfer processes in Figs. 6-10 and 6-11 are shown in Figs. 6-12 and 6-13, respectively. The transient heat transfer process on this graph for a pressure-reduction period of 2 ms follows very closely the hypothetical nucleate boiling curve, after the inception of explosive boiling. It departs from the curve at the transient critical heat flux

and moves downwards to film boiling as explained in the previous section. For longer pressure-reduction periods, reactivation of originally flooded cavities occurs in the middle of the pressure transient after the start of boiling. It can be seen from Figs. 6-12 and 6-13 that, as the pressure-reduction period becomes longer, the transient boiling process moves beyond the hypothetical nucleate boiling curve and approaches the steady FDNB curve, after departing from the natural convection curve at the inception of explosive boiling. For $\tau_p = 4.6$ ms in Fig. 6-12, the critical heat flux corresponds to a slightly higher value of $\alpha/q^{0.7}$ than that for the hypothetical nucleate boiling curve. The transient process moves downwards to film boiling. The transient critical heat flux in this case is about 60% of the steady-state critical heat flux at the corresponding pressure as seen from Fig. 6-10. It is assumed that the critical heat fluxes of the heat transfer processes lying between the hypothetical nucleate boiling curve and steady FDNB curve would occur due to the HSN in originally flooded cavities on the solid surface in the insufficiently developed nucleate boiling at the surface superheat of around the lower limit HSN temperature. The critical heat fluxes of the heat transfer processes in this region become lower with an increase in surface superheat increasing rate (i.e. with a decrease in the pressure-reduction period), just similar to those of the third group in the power transient mentioned in Chapter 4. For $\tau_p = 12.6$ ms in Fig. 6-12, the transient heat transfer process moves beyond the hypothetical nucleate boiling curve and then

approaches the final nucleate boiling under atmospheric pressure without reaching the transient critical heat flux. For $\tau_p = 13.0$ ms in Fig. 6-13, the transient heat transfer process reaches the hypothetical nucleate boiling curve at a pressure above the atmospheric and then moves to final steady-state nucleate boiling.

6.4.4 Effect of Cylinder Diameter

Transient heat transfer processes caused by depressurization plotted on $\alpha/q^{0.7}$ versus P graph shown above after the start of explosive boiling can be roughly classified into the following cases.

Case 1: Transient process departs from the natural convection heat transfer curve and moves along the hypothetical nucleate boiling curve until it reaches the transient critical heat flux point. Then, it moves down to film boiling. The transient critical heat flux value in this case is far lower than the steady-state critical heat flux at the corresponding pressure.

Case 2: The process approaches and reaches the steady FDNB curve after the start of explosive boiling. Then, it follows the curve as pressure decreases and makes a transition to film boiling at the critical heat flux, almost agreeing with the steady-state critical heat flux. A transition region connecting Case 1 to Case 2 also exists. This transition exists if the transient heat transfer at

the critical heat flux occurs during the process approaching the steady FDNB curve and the critical heat flux value is lower than the steady-state critical heat flux. This is called the Case 2'.

Case 3: Transient heat transfer process does not make a transition to film boiling at all but returns to the steady-state nucleate boiling or natural convection after the pressure reduction.

Figures 6-14 and 6-15 show the mapping of these cases for the data obtained on 1.2 and 3.0 mm-diameter cylinders, respectively, on the q_{in} versus τ_p plane. It can be seen from these figures that a transition to film boiling occurs for the initial heat fluxes higher than a certain minimum value and for the pressure reduction periods shorter than a certain maximum value. The lower limit for the initial heat flux is lower for a 3.0 mm-diameter cylinder; it is about 0.3 MW/m^2 for the 3.0 mm-diameter cylinder and about 0.36 MW/m^2 for the 1.2 mm-diameter one. This is because the natural convection heat transfer is small and as a result the necessary heat flux for the same surface temperature is correspondingly lower for the larger diameter cylinder. The maximum pressure-reduction period appears to be longer for 3.0 mm-diameter cylinders; it is about 14 ms for 3.0 mm-diameter cylinder and 8 ms for 1.2 mm-diameter one.

Figure 6-16 shows the q versus ΔT_{sat} plots of the transient heat transfer processes on a 3.0 mm-diameter cylinder for various pressure-reduction

periods, from an initial pressure of 1.08 MPa and at a fixed initial heat flux of 0.3 MW/m^2. Fig. 6-17 shows the $\alpha/q^{0.7}$ versus P plots for the transients. By comparing the transient heat transfer process for the period of 14.1 ms on 3 mm-diameter cylinder in Fig. 6-16 with that for the period of 13 ms on 1.2 mm-diameter cylinder in Fig. 6-11, it can be seen that the transient heat transfer for relatively long period is very much affected by the heat capacity of the cylinder after the inception of boiling. The transient process for the thicker cylinder successively follows the hypothetical nucleate boiling curve for each pressure and reaches the transient critical heat flux, which is seen from Fig. 6-16 to be about 23% of the steady-state critical heat flux. On the contrary, the transient process for the thinner cylinder approaches the steady FDNB curve and cannot reach the transient critical heat flux which is expected to be almost in agreement with the steady-state critical heat flux that is much larger than that for the transient process following the hypothetical nucleate boiling curve.

It can be assumed that the reactivation of originally flooded cavities after boiling inception will have less effect on the growth rate of the surface superheat on a larger diameter cylinder. As a result, the growth rate will be higher for thicker cylinders for the same pressure-reduction period. Therefore, the transient process on a large diameter cylinder corresponds to a more rapid pressure transient on a thin one. That is why the former one follows the hypothetical nucleate boiling curve and has a lower critical heat flux.

It should be noted that it is easier for a heated rod with larger heat capacity to make a transition to film boiling upon depressurization from an initial non-boiling state.

6.5 CONCLUSIONS

Transient boiling phenomena on single horizontal cylinders of 1.2 and 3.0 mm-diameter initially steady state natural convection or partial nucleate boiling in a pool of water, were investigated. The transient boiling was caused by rapid depressurization from initial pressures of 1.08 and 1.57 MPa. The initial heat fluxes ranged from 0.2 to 0.8 MW/m^2. The pressure-reduction periods ranged from 0.8 to 25 ms, and the water temperature was 373 K. The experimental results lead to the following conclusions:

(1) The surface superheat for the start of explosive boiling is as high as 42 K for rapid depressurization from initial natural convection with the period of 2.2 ms, and it becomes smaller with an increase in pressure-reduction period and with an increase in initial heat flux in partial nucleate boiling regime.

(2) The transition from natural convection or partial nucleate boiling to film boiling through nucleate boiling is due to the rapidly increasing surface

superheat caused by the rapid depressurization. The observed q_{cr} is very much lower than the steady-state q_{cr} at the corresponding pressures.

(3) Transient boiling heat transfer processes caused by depressurization can be roughly classified into the following cases on the $\alpha/q^{0.7}$ vs. P graphs.

Case 1:

Transient process departs from the natural convection heat transfer curve and moves along the hypothetical nucleate boiling curve until it reaches the transient critical heat flux point, where it departs from the curve to film boiling.

Case 2:

The process approaches the steady FDNB boiling curve after the start of explosive boiling and follows the curve with the decrease in the pressure and departs from the curve to film boiling at the critical heat flux.

Case 2':

Transition region from Case 1 to Case 2.

Case 3:

Transient heat transfer process does not finally make a transition to film boiling. It returns to the steady-state nucleate boiling or natural convection after the pressure reduction.

Case 1 is observed for initial heat fluxes ranging from a certain lower limit to an upper limit in the natural convection regime, and for pressure-

reduction periods shorter than a certain maximum value. In the partial nucleate boiling regime when the initial heat flux increases, or when pressure-reduction period increases, the transient boiling process changes to Case 2 through Case 2'. Case 3 occurs for initial heat flux values less than the lower limit mentioned above and for pressure-reduction period longer than a certain maximum value. Mapping of the experimental data shows these cases.

(4) It was found that a heated rod with larger heat capacity (down to lower initial heat flux and longer pressure-reduction period) will make a transition to film boiling more easily upon depressurization.

(5) The ratio of the transient critical heat flux to the steady-state critical heat flux at the corresponding pressure in Case 1 and Case 2 (2') transients, for a fixed pressure-reduction period around 3 ms, decreases as initial heat fluxes increase, goes through a minimum value of about 30 % at the initial heat flux value near the upper heat flux value for natural convection and then increases with an increase of initial heat flux. The ratio for a fixed initial heat flux increases with increasing pressure-reduction period.

(6) Transient film boiling heat transfer due to depressurization, after the minimum heat flux, agrees well with the steady-state film boiling curve, for a

cylinder of the same diameter described by the correlation of Sakurai et al. (1990).

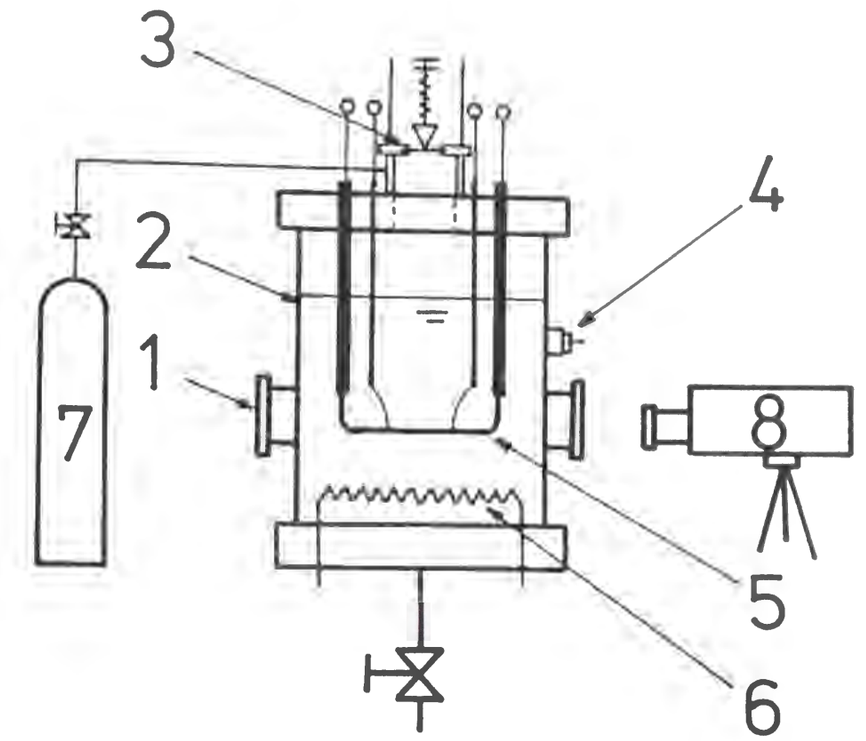

1.GLASS WINDOW 2.BOILING VESSEL
3.RUPTURE DISC 4.PRESSURE TRANSDUCER
5.TEST HEATER 6.SHEATHED HEATER
7.HE GAS CYLINDER 8.HIGH-SPEED VIDEO CAMERA

Fig. 6-1 Schematic of experimental apparatus.

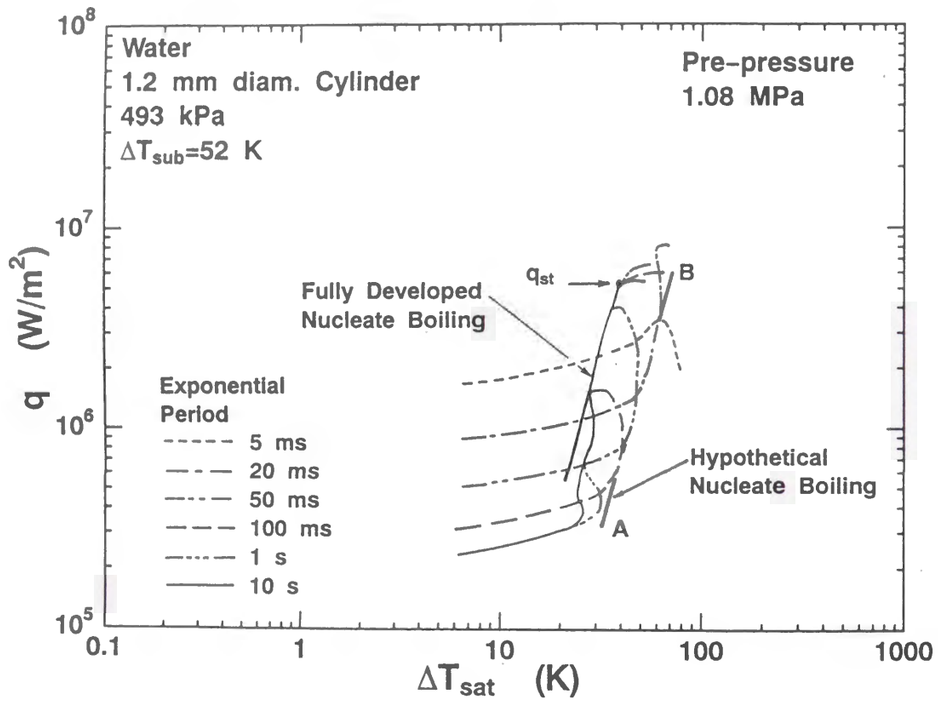

Fig. 6-2 Transient boiling curves for various exponential periods of heat inputs and hypothetical nucleate boiling curve, at 493 kPa.

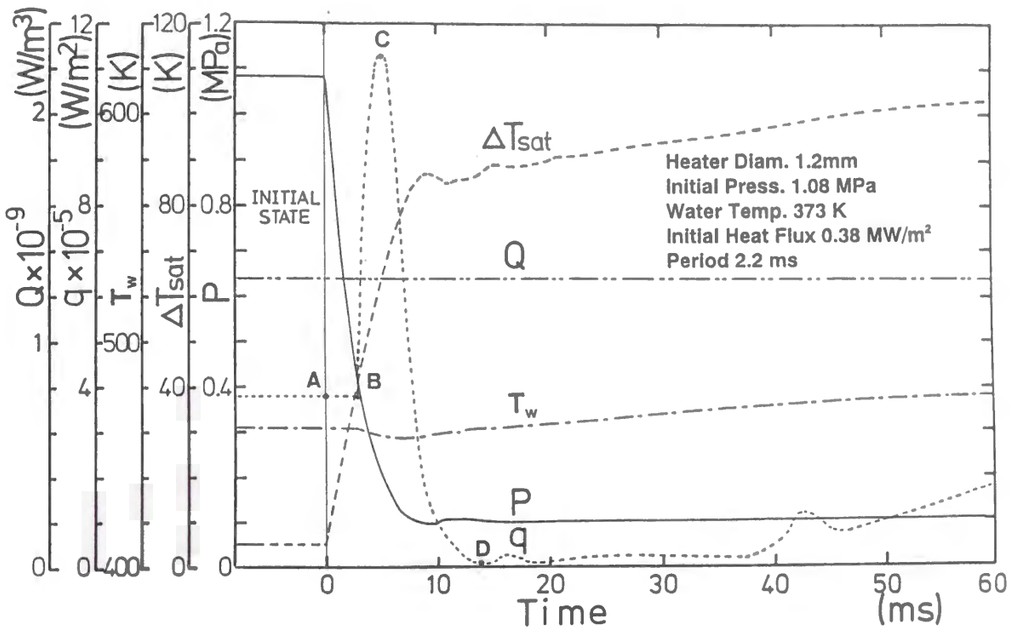

Fig. 6-3 Typical time traces of system pressure P, heater surface temperature T_w, heater surface superheat ΔT_{sat}, heat flux q and heat generation rate Q for 1.2mm-diameter cylinder caused by pressure reduction.

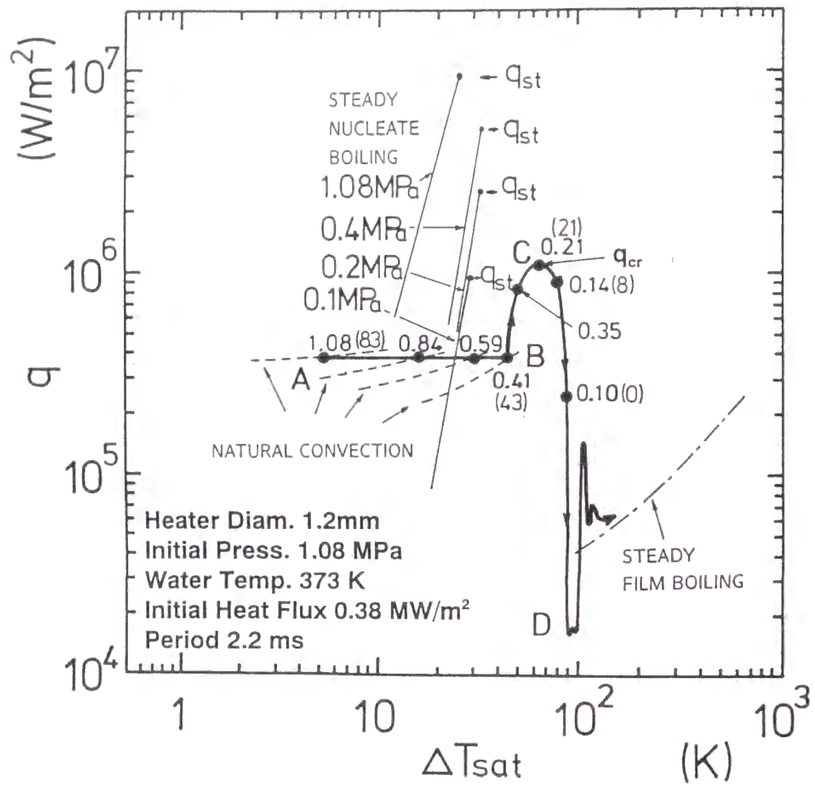

Fig. 6-4 Relation between instantaneous heater surface superheat and heat flux for the run shown in Fig. 6-3.

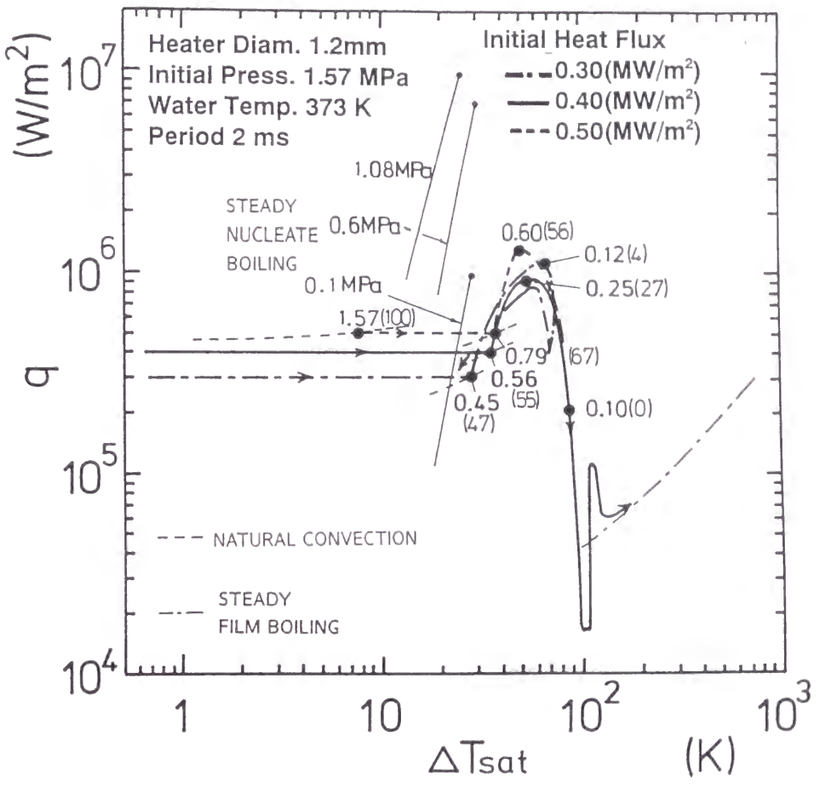

Fig. 6-5(a) Effect of initial heat flux in natural convection regime on transient boiling processes for the pressure reduction from the initial pressure of 1.57MPa.

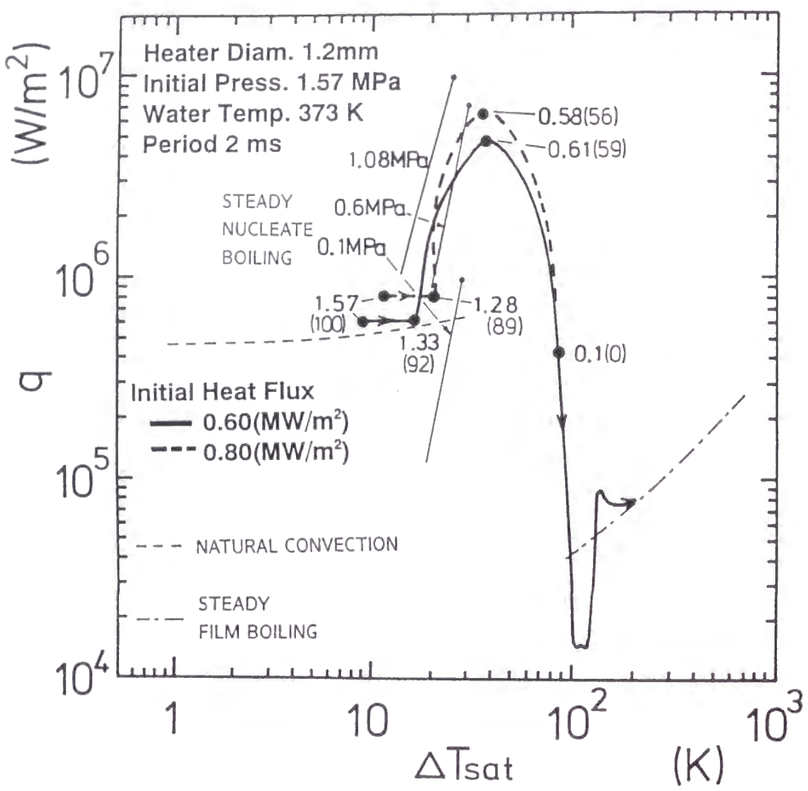

Fig. 6-5(b) Effect of initial heat flux in nucleate boiling regime on transient boiling processes for the pressure reduction from the initial pressure of 1.57MPa.

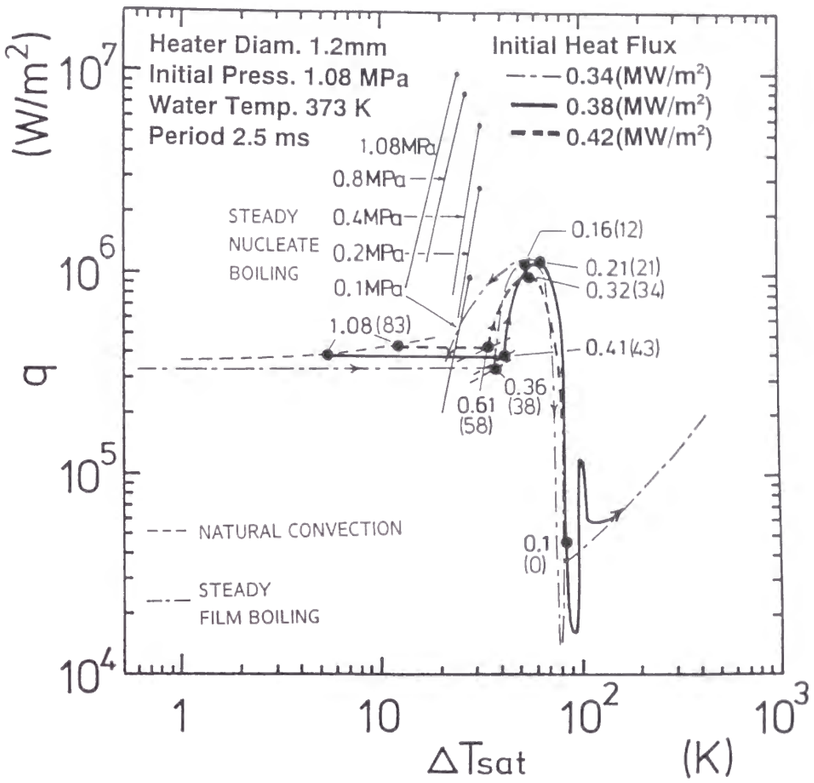

Fig. 6-6(a) Effect of initial heat flux in natural convection regime on transient boiling processes for the pressure reduction from the initial pressure of 1.08MPa.

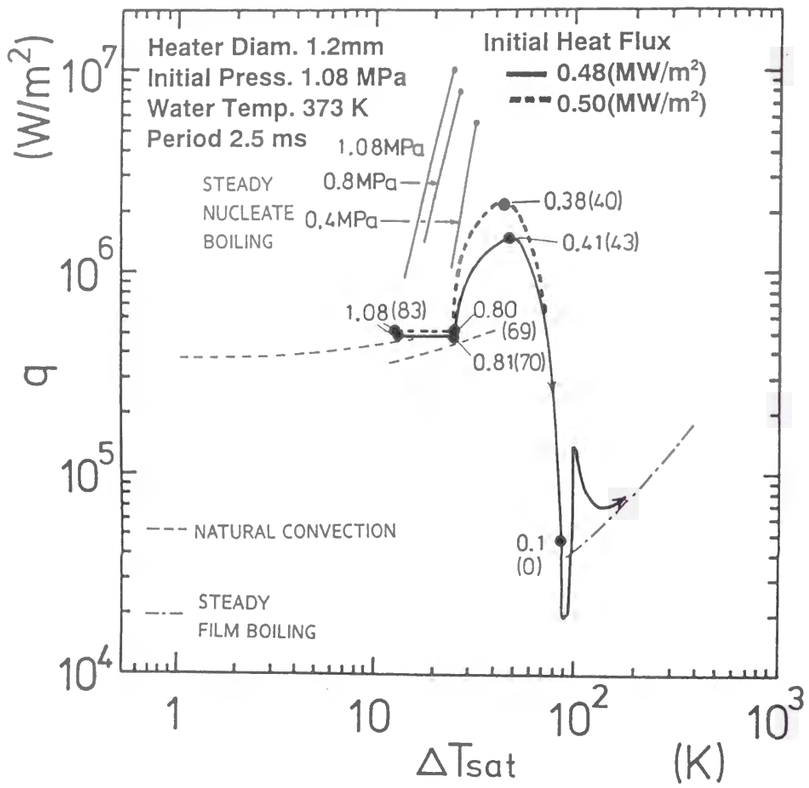

Fig. 6-6(b) Effect of initial heat flux in nucleate boiling regime on transient boiling processes for the pressure reduction from the initial pressure of 1.08MPa.

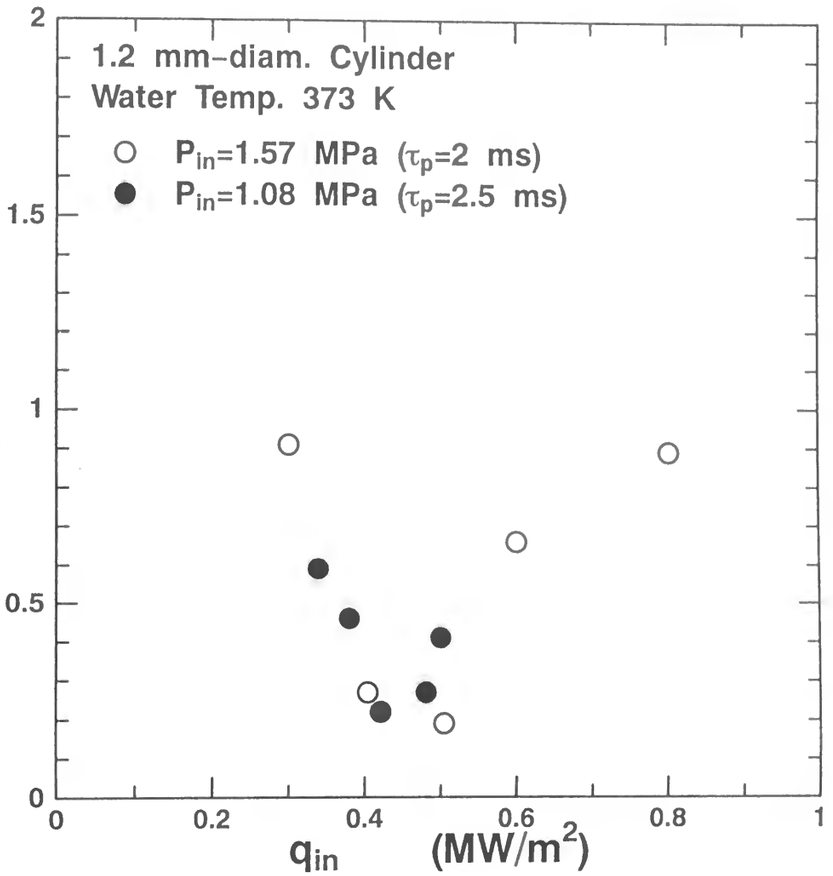

Fig. 6-7 Ratio of the transient critical heat flux to the corresponding steady-state critical heat flux.

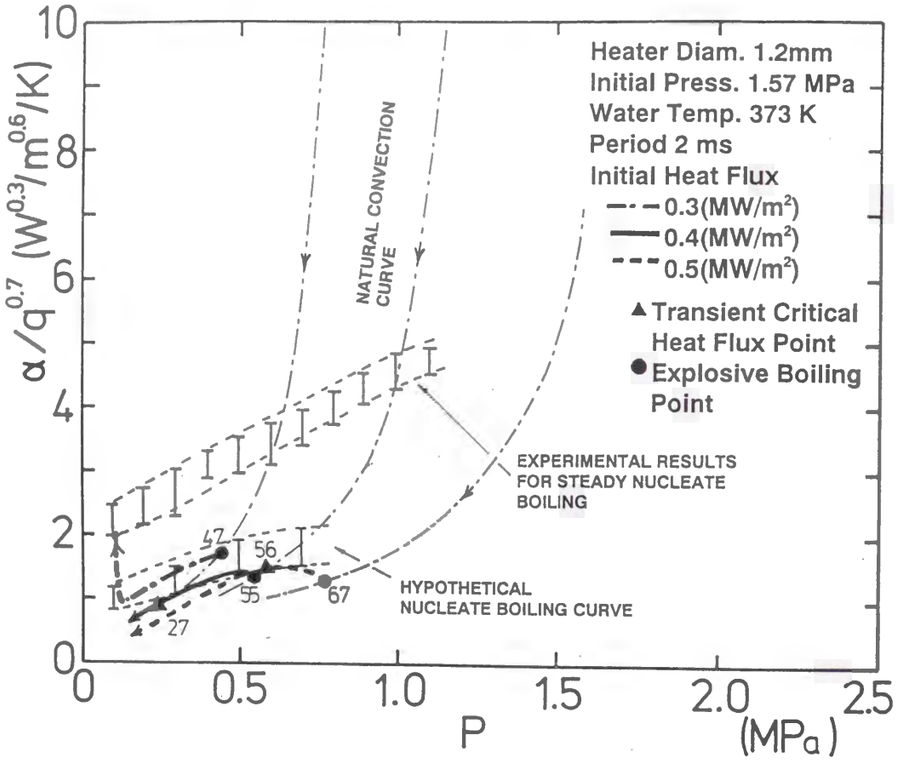

Fig. 6-8(a) Effect of initial heat flux in natural convection regime on transient boiling heat transfer for pressure reduction from the initial pressure of 1.57MPa.

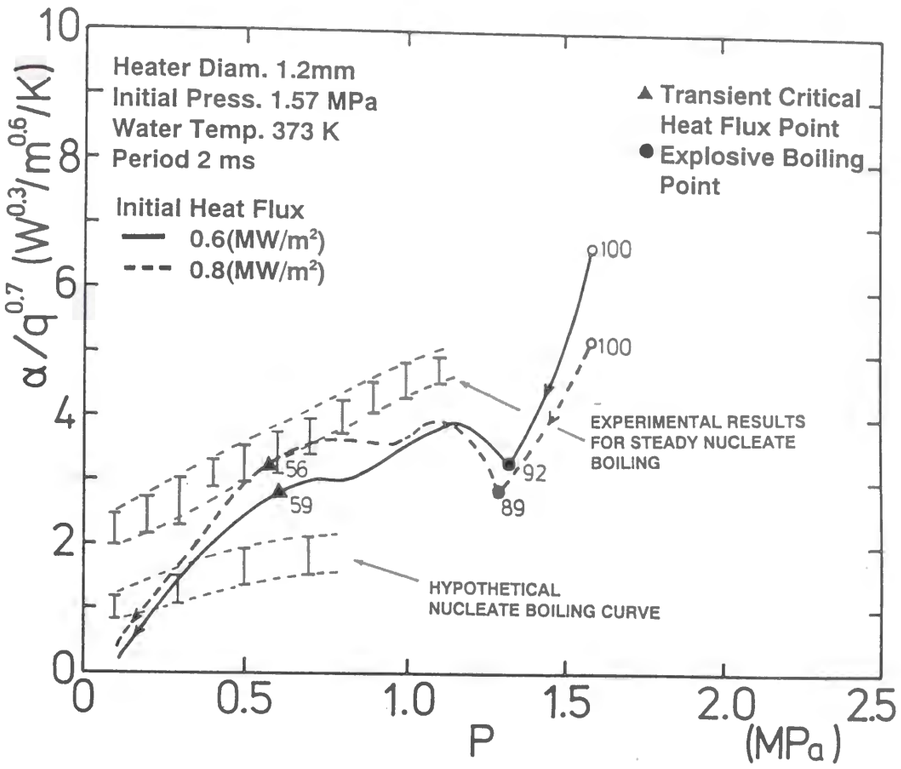

Fig. 6-8(b) Effect of initial heat flux in nucleate boiling regime on transient boiling heat transfer for pressure reduction from the initial pressure of 1.57MPa.

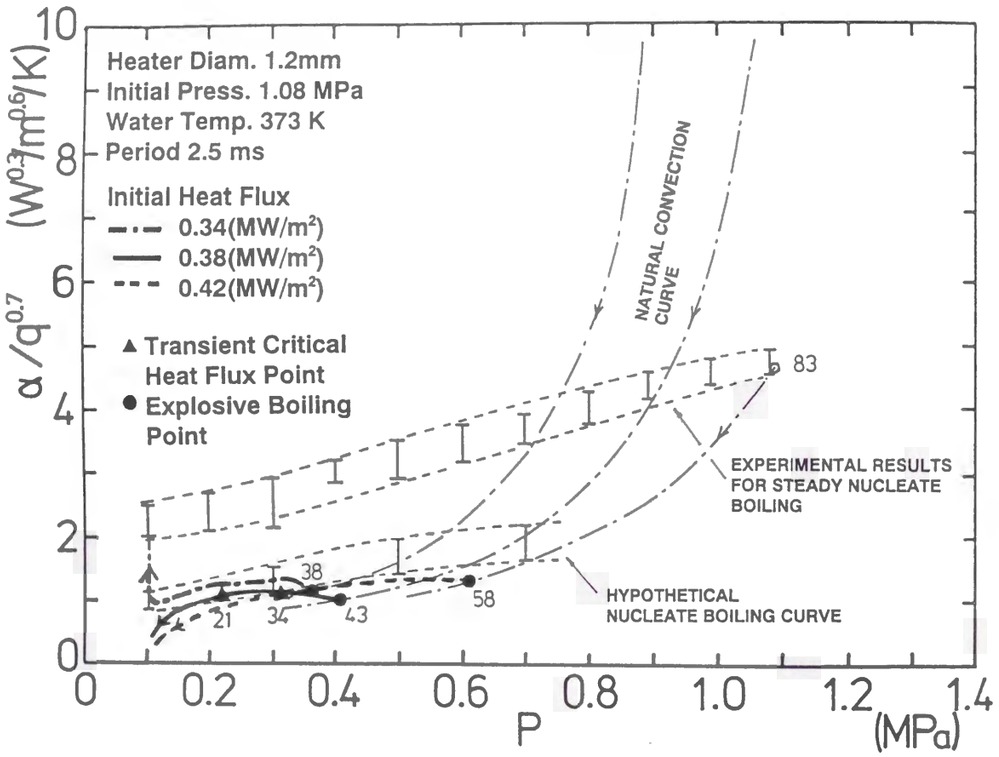

Fig. 6-9(a) Effect of initial heat flux in natural convection regime on transient boiling heat transfer for pressure reduction from the initial pressure of 1.08MPa.

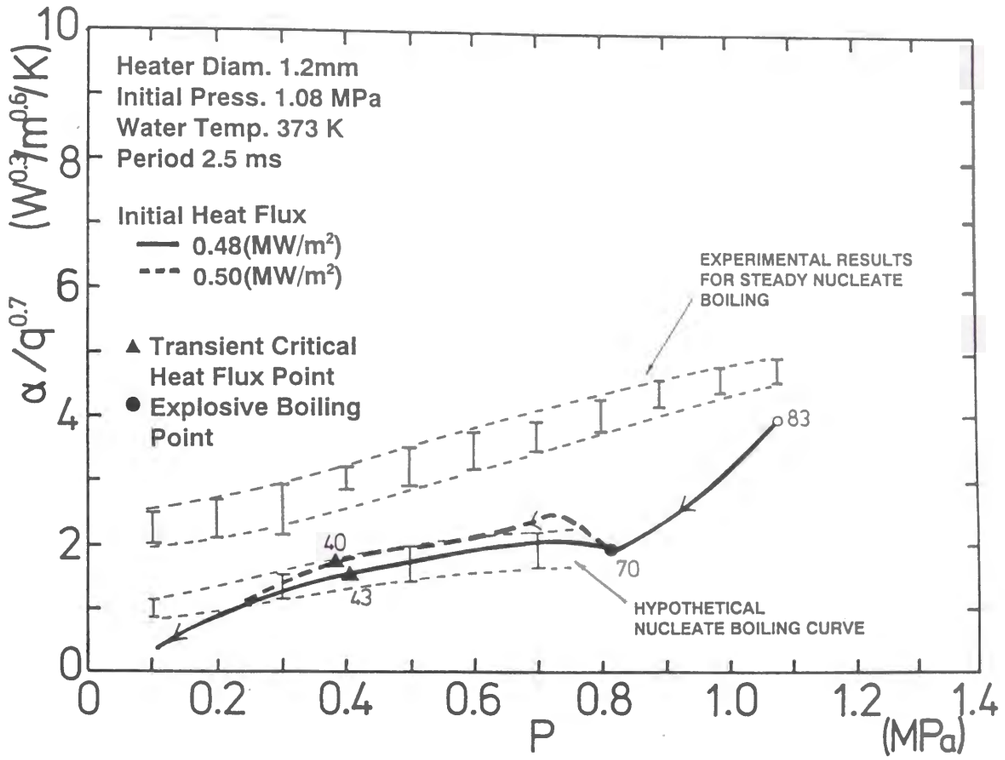

Fig. 6-9(b) Effect of initial heat flux in nucleate boiling regime on transient boiling heat transfer for pressure reduction from the initial pressure of 1.08MPa.

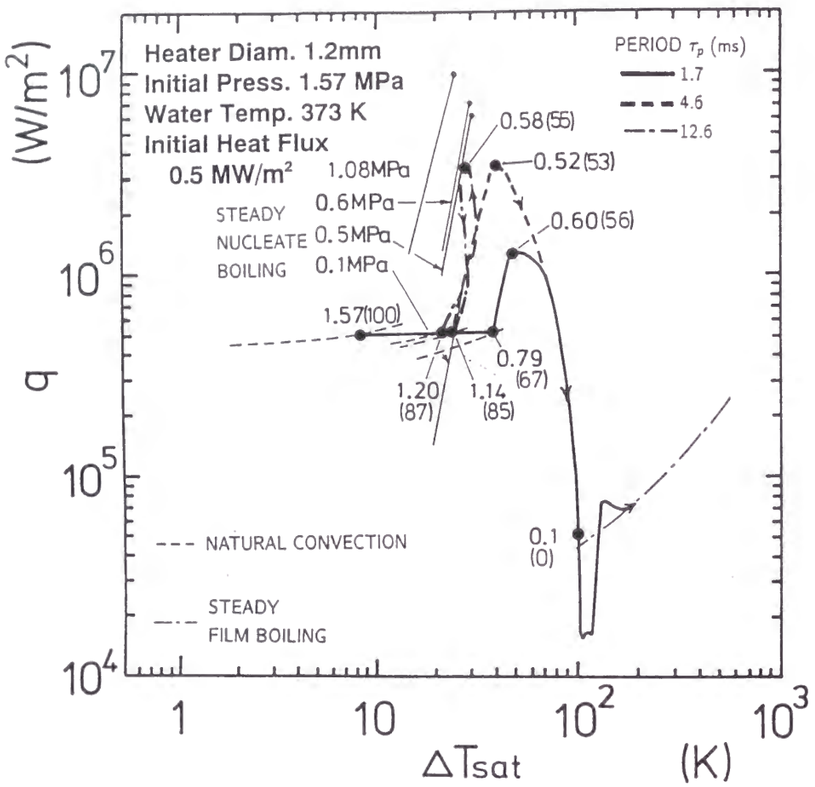

Fig. 6-10 Effect of pressure reduction period on transient boiling processes from initial natural convection for the initial pressure of 1.57MPa.

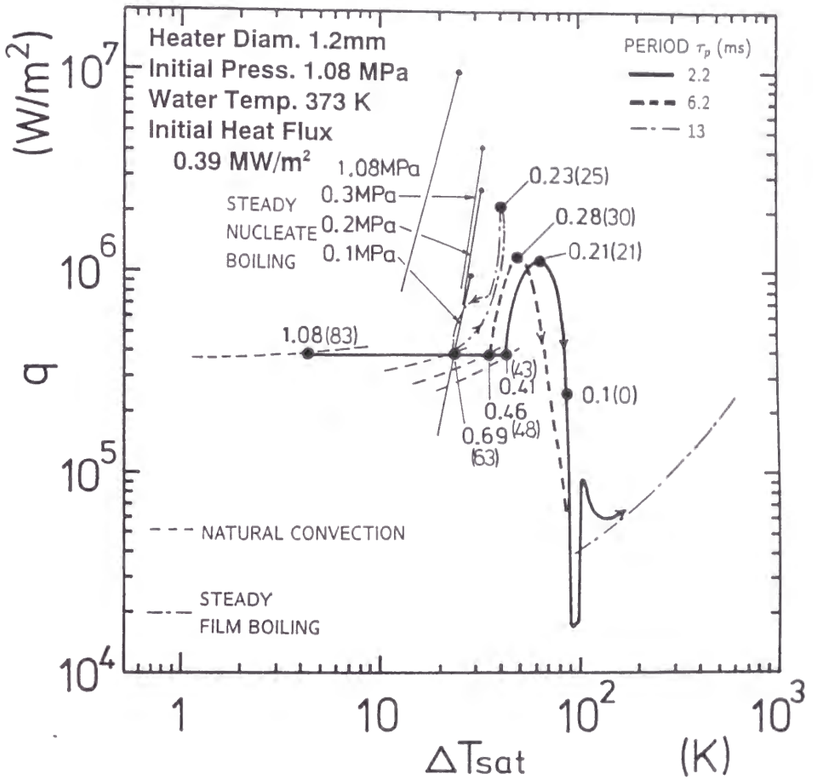

Fig. 6-11 Effect of pressure reduction period on transient boiling processes from initial natural convection for the initial pressure of 1.08MPa.

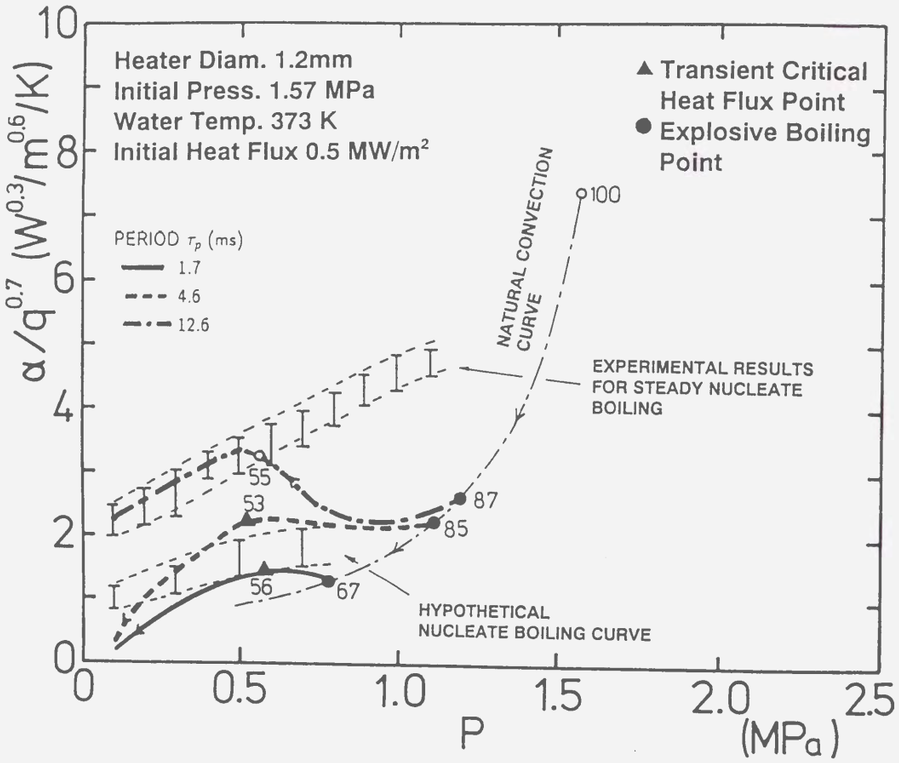

Fig. 6-12 Effect of pressure reduction period on transient boiling heat transfer from initial natural convection for the initial pressure of 1.57MPa.

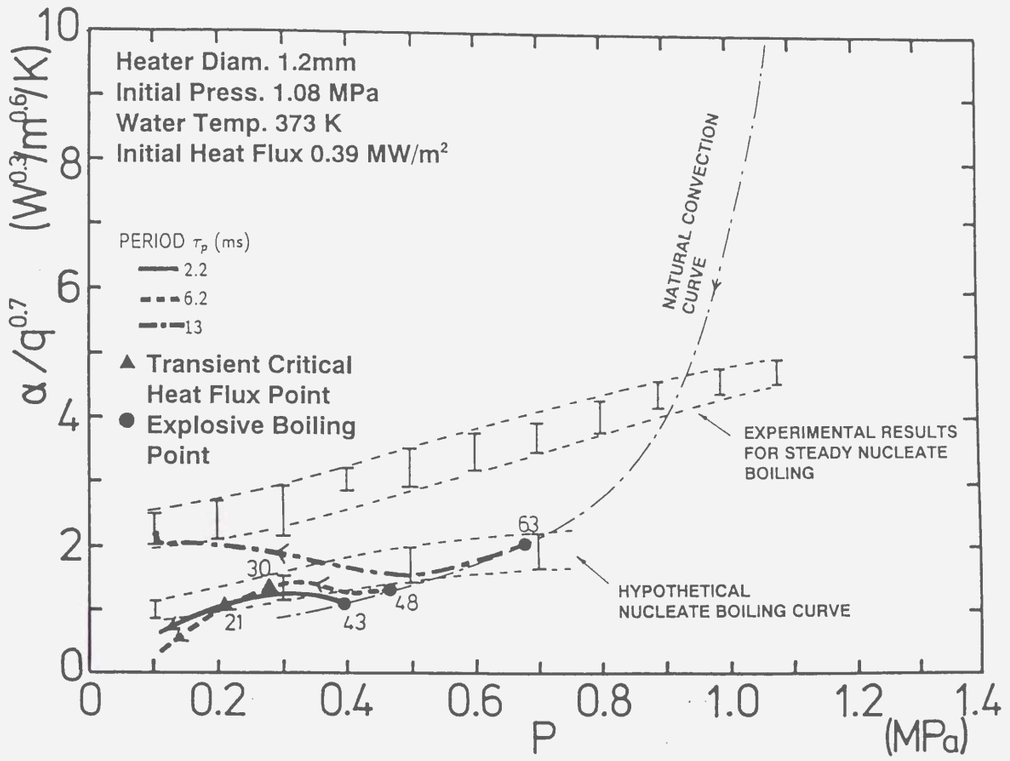

Fig. 6-13 Effect of pressure reduction period on transient boiling heat transfer from initial natural convection for the initial pressure of 1.08MPa.

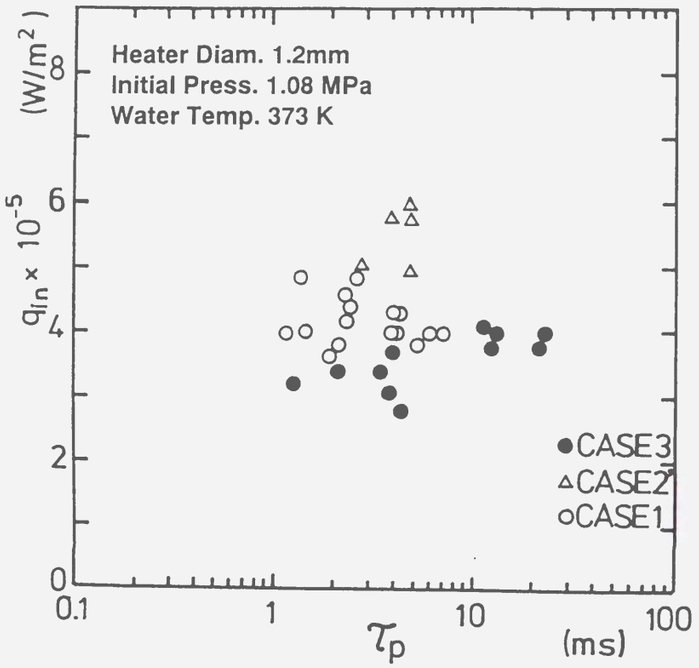

Fig. 6-14 Mapping of data classified into three cases for 1.2mm-diameter test heater.

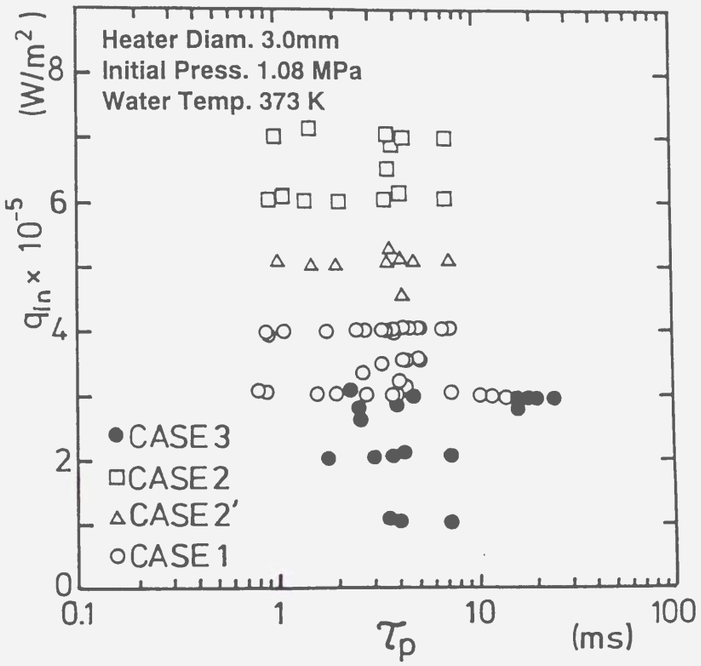

Fig. 6-15 Mapping of data classified into three cases for 3.0mm-diameter test heater.

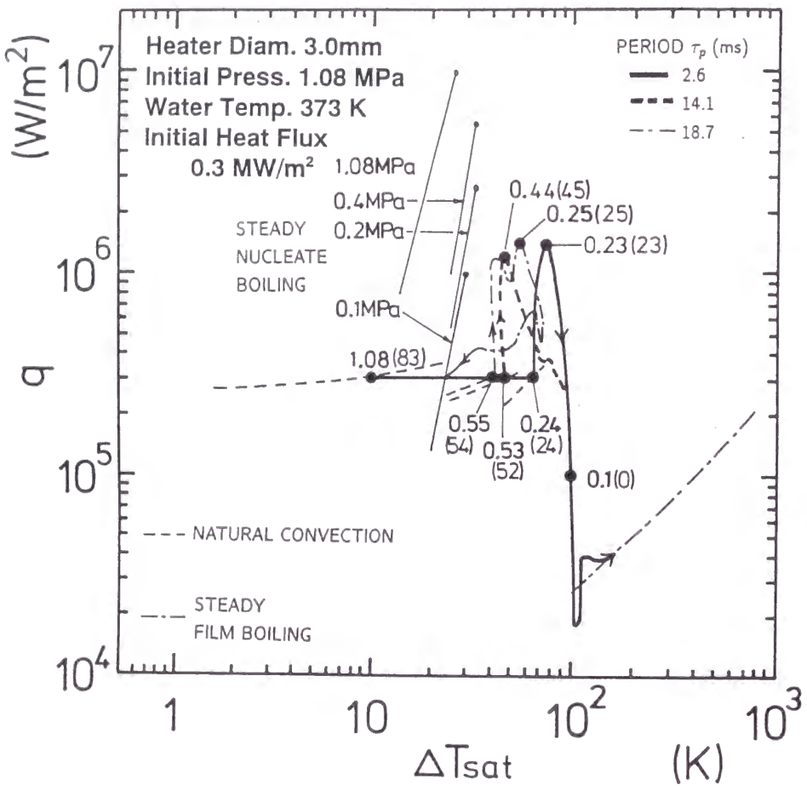

Fig. 6-16 Transient boiling processes on q versus ΔT_{sat} with various pressure reduction periods from the initial pressure of 1.08MPa for 3.0mm-diameter test heater.

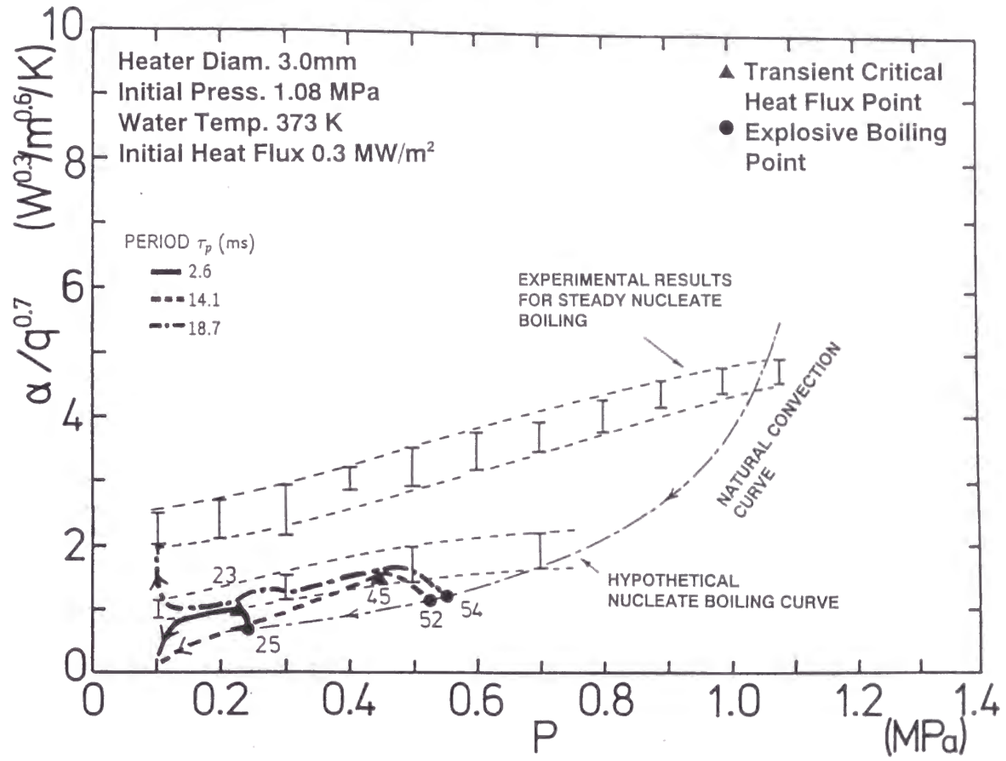

Fig. 6-17 Transient boiling heat transfer processes for the run shown in Fig. 6-16.

CHAPTER 7

CONCLUSIONS

A series of studies in this thesis have been performed to obtain systematically the database for the critical heat fluxes in transient boiling caused by exponentially increasing heat inputs and by a rapid reduction of system pressure, and to clarify the mechanisms of the critical heat flux under these conditions.

In Chapter 3, the steady-state CHF values were measured for wide ranges of subcoolings and pressures on various shaped test heaters such as horizontal cylinders with various diameters, a vertical ribbon, a vertically oriented horizontal ribbon and a lower-side insulated horizontal flat ribbon in water.

(1) The CHF data on 1.2 mm diameter horizontal cylinder in water for subcoolings from zero to 40 K at all the pressures, and those for the subcoolings from zero to 80 K at the pressures of atmospheric and 199 kPa are dependent on the pressure. On the contrary, the CHF data for the subcoolings from 60 K to 180 K at pressures from around 0.4 MPa to 2 MPa are almost independent of the pressure and gradually increase with an increase in subcooling. The CHF data in the former region of lower subcooling are in good agreement with the corresponding values predicted

by a presented CHF correlation based on the hydrodynamic instability. The CHF data in the latter region are well expressed by the empirical equation given for the range of subcooling and pressure. The constants of correlations based on the hydrodynamic instability and the heterogeneous spontaneous nucleation (HSN) for low and high subcoolings were determined by the corresponding experimental data for the test heaters with various shapes.

In Chapter 4, transient CHF values due to exponentially increasing heat inputs were obtained in water for various exponential periods and subcoolings over the ranges of 2 ms to 20 s and zero to 80 K at pressures ranging from 101.3 to 2063 kPa in cases with and without pre-pressurization.

(2) The CHFs for short periods for the cases without and with the prepressure of 5Mpa, which increase with a decrease in period from the minimum CHF, become almost in agreement with each other. The mechanism of the transition to film boiling regime was considered to be a consequence of the HSN in originally flooded cavities on the cylinder surface not only for the pre-pressurized case but also for the non-pre-pressurized case. Typical trend of CHF with respect to the period for the high subcoolings at pressures higher than 400 kPa is independent of the pressure and almost same each other for both cases. The CHF values for short periods that are significantly lower than the steady-state values were confirmed even for

non-pre-pressurized case.

In Chapter 5, the transient CHFs caused by exponentially increasing heat inputs on the horizontal cylinders with mirror surface and rough surface were measured in water for the cases without and with the pre-pressure of 5MPa. The effect of surface conditions on the transient CHFs was clarified in comparison with those obtained for the horizontal cylinder with commercial surface under the same condition.

(3) The CHFs versus periods were separated into the first, second and third groups on CHF for longer, shorter and intermediate periods. The trend of CHFs with respect to periods belonging to the first group on the cylinders with rough surface (RS) agreed with those obtained for the cylinder with commercial surface (CS) at lower and higher subcoolings. On the contrary, the trends of CHFs versus the periods belonging to the first group on the cylinder with mirror surface (MS) at saturated pressures higher than around 400 kPa are different from CS and RS because the CHFs are determined by the HSN for the cylinder with MS at the pressures. The mirror surface condition gives the significant effect on CHFs under saturated and subcooled conditions. More study on the effect of cylinder surface conditions on the CHFs is necessary not only for the academic interests but also for the safety assessment of nuclear reactor for abnormal conditions such as power burst in the reactor.

In Chapter 6, the effects of initial pressure, pressure-reduction rate, initial heat transfer regimes such as natural convection or nucleate boiling, and cylinder diameter, on the transition mechanism to film boiling caused by a rapid depressurization were made clear experimentally.

(4) The transition from natural convection or partial nucleate boiling to film boiling through nucleate boiling is due to the rapidly increasing surface superheat caused by the rapid depressurization. The observed CHF is very much lower than the steady-state CHF at the corresponding pressures. It was found that a heated rod with larger heat capacity will make a transition to film boiling more easily upon depressurization. Transient film boiling heat transfer due to depressurization, after the minimum heat flux, agrees well with the steady-state film boiling curve by the correlation of Sakurai et al. (1990). A mechanism based on heterogeneous spontaneous nucleation (HSN) from the originally flooded cavities on the solid surface was suggested for the transition from steady-state heat transfer at low initial heat fluxes to film boiling after rapid depressurization.

REFERENCES

[1] Chen, J.C., 1968, Incipient Boiling Superheat in Liquid Metals, ASME Journal of Heat Transfer, Vol.90, pp.303-312.

[2] Churchill, S.W., and Chu, H.H.S., 1975, Correlating Equations for Laminar and turbulent Free Convection from a Horizontal Cylinder, Int. J. Heat Mass Transfer, Vol.18, pp.1049-1053.

[3] Crapo H. S., Jensen M. F. and Sackett K. E., 1975, Experimental Data Report for Semiscale Mod-1 Test S-02-1 (Blowdown Heat Transfer Test).

[4] Dwyer, O.E., 1969, On Incipient Boiling Wall Superheats in Liquid Metals, Int. J. Heat Mass Transfer, Vol.12, pp.1403-1419.

[5] Elkassabgi, Y., and Lienhard, J. H., 1988, Influence of Subcooling on Burnout of Horizontal Cylindrical Heaters, ASME Journal of Heat Transfer, Vol.110, pp.479-486.

[6] Fabic, S., 1964, Vapor Nucleation on Surfaces Subjected to Transient Heating, Ph.D. Thesis, University of California (Reactor Heat Transient Res. Tech. Rep. SAN-1008) Berkeley, CA.

[7] Griffith, P., and Wallis, J.D., 1960, The Role of Surface Conditions in Nucleate Boiling, Chem. Eng. Prog. Symp. Ser., ¥rm Vol.56, pp.49-63.

[8] Hall, W. B., and Harrison, W. C., 1966, Transient Boiling of Water at Atmospheric Pressure, International Heat Transfer Conference, Institute of Mechanical Engineering, pp.186-192.

[9] Haramura, Y., and Katto, Y., 1983, A New Hydrodynamic Model of Critical Heat Flux Applicable Widely to Both Pool and Forced Convection of Submerged Bodies in Saturated Liquids, Int. J. Heat Mass Transfer, Vol.26, pp.389-399.

[10] Henry R. E. and Leung J. C., 1977, A Mechanism for Transient Critical Heat Flux, ANS Special Topic Meeting, Sun Valley, Idaho(August).

[11] Holtz, R.E., 1966, The Effect of the Pressure-Temperature History upon Incipient Boiling Superheat in Liquid Metals, USAEC Report ANL-7184, Argonne, Illinois.

[12] Ivey, H. J. and Morris, D. J., 1962, On the Relevance of the Vapor-Liquid Exchange Mechanism for Subcooled Boiling Heat Transfer at High Pressures, UKAEA, AEEW-R 137.

[13] Johnson, H.A., Schrock, V.E., Selph, F.B., Lienhard, J.H., Rosztoczy, Z.R.,1962, Transient Pool Boiling of water at Atmospheric Pressure, International Development in Heat Transfer, ASME, pp.244-254.

[14] Johnson, H.A. et al, 1966, Reactor Heat Transients Project, USAEC Report SAN 1001 to SAN 1013.

[15] Kutateladze, S. S., and Schneiderman, L. L., 1953, Experimental Study of the Influence of the Temperature of a Liquid on a Change in the Rate of Boiling, AEC-tr-3405, USAEC.

[16] Kutateladze S. S., 1959, Heat Transfer in Condensation and Boiling, AEC-tr-3770, USAEC.

[17] Lienhard, J.H., and Dhir, V.K., 1973, Hydrodynamic Prediction of Peak Pool-boiling Heat Fluxes from Finite bodies, ASME Journal of Heat Transfer, Vol.95, pp.152-158.

[18] Marcus, B. D. and Dropkin, D., 1965, Measured Temperature Profiles Within the Superheated Boundary Layer Above a Horizontal Surface in Saturated Nucleate Boiling of Water, J. of Heat Transfer, Trans. ASME, Series C, Vol.87, pp.333-341.

[19] Ponter, A. B. and Haigh, C. P.,1969, The Boiling Crisis in Saturated and Subcooled Pool Boiling at Reduced Pressures, Int. Heat and Mass Transfer, Vol.12, No.4, pp.429-437.

[20] Raithby, G.D., and Hollands, K.G.T., 1985, Natural Convection, Handbook of Heat Transfer Fundamentals, W.M. Rohsenow et al. ed., McGraw-Hill, New York, pp.6-1 - 6-94.

[21] Rosenthal, M.W., 1957, An Experimental Study of Transient Boiling, Nuclear Science and Engineering, Vol.2, pp.640-656.

[22] Sakurai, A., and Shiotsu, M., 1974, Transient Pool-Boiling Heat Transfer, ASME Paper, 74-WA/HT-41, pp.1-16.

[23] Sakurai, A. and Shiotsu, M., 1977a, Transient Pool Boiling Heat Transfer, Part 1:Incipient Boiling Superheat, ASME J. Heat Transfer, pp.547-553.

[24] Sakurai, A. and Shiotsu, M., 1977b, Transient Pool Boiling Heat Transfer, Part 2: Boiling Heat Transfer and Burnout, ASME J. Heat Transfer, pp.554-560.

[25] Sakurai A., Shiotsu M. and Hata K., 1980, Transient Boiling Caused by Rapid Depressurization from Initial Non-boiling State, Multiphase Transport, Fundamentals, Reactor Safety, Applications, Vol. II, ed. T. N. Veziroglu (Hemisphere Pub. Corp., Washington D.C.) pp. 727-747.

[26] Sakurai A., Shiotsu M. and Hata K., 1990, A general Correlation for Pool Film Boiling Heat Transfer From a Horizontal Cylinder to Subcooled Liquid: Part 2, Journal of Heat Transfer, Trans. ASME, Series C, Vol. 112, pp.441-450.

[27] Sakurai A., Shiotsu M. and Hata K., 1992, Heat Transfer from a Horizontal Wire in Liquid Nitrogen, Heat Transfer and Superconducting Magnetic Energy Storage, ASME HTD-Vol.211, pp.7-18.

[28] Sakurai, A., Shiotsu, M. and Hata, K., 1993, New Transition Phenomena to Film Boiling due to Increasing Heat Inputs on a Solid Surface in Pressurized Liquids, ASME HTD-Vol.260, pp.27-39.

[29] Sakurai A., Shiotsu M. and Hata K., 1994, Mechanism of Nucleate Boiling on a Solid Surface in Liquid Helium, Advances in Cryogenic Engineering, Vol.39A, Plenum Pub. Corp., pp.1759-1768.

[30] Sakurai, A., Shiotsu, M., and Hata, K., 1995, Transition Phenomena from Non-Boiling Regime to Film Boiling on a Cylinder Surface in Highly Subcooled and Pressurized Water due to Increasing Heat Inputs, ASME Paper 95-WA/HT-

[31] Sakurai, A., Shiotsu, M. and Fukuda, K., 1996, Pool Boiling Critical Heat Flux on a Horizontal Cylinder in Subcooled Water for Wide Ranges of Subcooling and Pressure and Its Mechanism, National Heat Transfer Conference, Houston, Texas, ASME HTD-Vol.326, Vol.4, pp.93-104.

[32] Sakurai A., 1997, Mechanism of transitions to Film Boiling in Subcooled and Pressurized Liquids due to Steady and Increasing heat Inputs, Proc. of 8th International Topical Meeting on Nuclear Reactor Thermal Hydraulics (NURETH-8), Kyoto, Japan, pp.989-1018.

[33] Serizawa A., 1983, Theoretical Prediction of Maximum Heat Flux in Power Transients, Int. J. Heat and Mass Transfer, Vol.26, No.6, pp.921-932.

[34] Takeuchi, Y., Hata, K., Shiotsu, M., and Sakurai, A., 1995, A General Correlation for Laminar Natural Convection Heat Transfer from Single Horizontal Cylinders in Liquids and Gases with All Possible Prandtl Numbers, 1995 International Mechanical Engineering Congress and Exposition, ASME HTD-Vol. 317-1, pp.259-270.

[35] Zuber N., Hydrodynamic Aspects of Boiling Heat Transfer, 1959, AECU-4439, USAEC.

LIST OF PAPERS CONCERNING WITH THIS STUDY

(1) Fukuda, K., Shiotsu, M., and Sakurai A., 1990, Transient Boiling Heat Transfer caused by Rapid Depressurization, Annual Meeting of the Atomic Energy Society of Japan, University of Tokyo, pp.265, (In Japanese).

(2) Fukuda, K., and Shiotsu, M., 1991, Transient Boiling Heat Transfer caused by Depressurization, 28th National Heat Transfer Symposium of Japan, Fukuoka, pp.736-738, (In Japanese).

(3) Fukuda, K., Shiotsu, M., and Hata, K., 1992, Transient Boiling Heat Transfer caused by Rapid Depressurization, 1992 Annual Meeting of the Atomic Energy Society of Japan, Tokai University, pp.600, (In Japanese).

(4) Sakurai, A., Shiotsu, M., Hata, K., and Fukuda, K., 1993a, Transient Pool Boiling Heat Transfer from a Horizontal Cylinder in Water at Pressures, Proc. of 6th International Topical Meeting on Nuclear Reactor Thermal Hydraulics (NURETH-6), Grenoble, ed. by Courtaud and Delhaye J.M., pp.231-239.

(5) Fukuda, K., Shiotsu, M., Hata, K., and Sakurai, A., 1993b, Transient Pool Boiling Heat Transfer from Initial Steady-State caused by Rapid

Depressurization, Proc. of 6th International Topical Meeting on Nuclear Reactor Thermal Hydraulics (NURETH-6), Grenoble, ed. by Courtaud and Delhaye J.M., pp.444-455.

(6) Fukuda, K., Shiotsu, M., Hata, K., and Sakurai, A., 1994a, Transient Boiling Heat Transfer caused by Rapid Depressurization (1), Annual Meeting of the Atomic Energy Society of Japan, Tukuba University, pp.431, (In Japanese).

(7) Fukuda, K., Shiotsu, M., Hata, K., and Sakurai, A., 1994b, Transient Boiling Heat Transfer caused by Rapid Depressurization (2), 1994 Annual Meeting of the Atomic Energy Society of Japan, Tukuba University, pp.432, (In Japanese).

(8) Fukuda, K., Shiotsu, M., Hata, K., and Sakurai, A., 1994c, Transient Boiling Heat Transfer caused by Rapid Depressurization (3), Annual Meeting of the Atomic Energy Society of Japan, Tukuba University, pp.433, (In Japanese).

(9) Sakurai, A., Shiotsu, M., Hata, K., and Fukuda, K., 1994d, Mechanism of Transition from Non-boiling to Film Boiling in Various Liquids, 31st National Heat Transfer Symposium of Japan, Sapporo, pp.31-33, (In Japanese).

(10) Fukuda, K., Shiotsu, M., Hata, K., and Sakurai, A., 1994e, Transient

Boiling Heat Transfer caused by Rapid Depressurization, 1st National Heat Transfer Symposium of Japan, Sapporo, pp.451-453, (In Japanese).

(11) Fukuda, K., Shiotsu, M., Hata, K., and Sakurai, A., 1994f, Transient Pool Boiling Heat Transfer from Initial Steady-State caused by Rapid Depressurization, Nuclear Engineering and Design, Vol. 149, pp.97-110.

(12) Sakurai, A., Shiotsu, M., Hata, K., and Fukuda, K., 1995a, Transition Mechanism from Non-boiling to Film Boiling due to Increasing Heat Inputs in Typical Liquids, 32nd National Heat Transfer Symposium of Japan, Yamaguchi, pp.271-272, (In Japanese).

(13) Fukuda, K., Shiotsu, M. and Sakurai, A., 1995b, Transient Pool Boiling Heat Transfer due to Increasing Heat Inputs in Subcooled Water at High Pressures, Proc. of 7th International Topical Meeting on Nuclear Reactor Thermal Hydraulics (NURETH-7), Saratoga Springs, NY, NUREG/CP-0142, pp.554-573.

(14) Sakurai, A., Shiotsu, M., Hata, K., and Fukuda, K., 1995c, Transition Phenomena from Non-Boiling Regime to Film Boiling on a Cylinder Surface in Highly Subcooled and Pressurized Water due to Increasing Heat Inputs, 1995

ASME International Mechanical Engineering Congress and Exposition, San Francisco, CA, 95-WA/HT-17, pp.1-11.

(15) Fukuda, K., Shiotsu, M. and Sakurai, A., 1996a, Steady and Unsteady Critical Heat flux in a Pool of Water under Wide Ranges of Subcooling and Pressure (1)(Critical Heat Fluxes due to Exponential Heat Inputs), 33rd National Heat Transfer Symposium of Japan, Niigata, pp.273-274, (In Japanese).

(16) Sakurai, A., Shiotsu, M. and Fukuda, K., 1996b, Steady and Unsteady Critical Heat flux in a Pool of Water under Wide Ranges of Subcooling and Pressure (2)(Mechanism of Critical Heat Flux), 33rd National Heat Transfer Symposium of Japan, Niigata, pp.279-280, (In Japanese).

(17) Sakurai, A., Shiotsu, M. and Fukuda, K., 1996c, Pool Boiling Critical Heat Flux on a Horizontal Cylinder in Subcooled Water for Wide Ranges of Subcooling and Pressure and Its Mechanism, National Heat Transfer Conference, Houston, Texas, ASME HTD-Vol.326, Vol.4, pp.93-104.

(18) Fukuda, K., Hata K., Shiotsu, M. and Sakurai, A., 1997a, Pool Boiling Critical Heat Fluxes on Test Heaters with Various Configurations in Subcooled Liquids for Wide Ranges of Subcooling and Pressure (Part 1: Experimental

Results), 34th National Heat Transfer Symposium of Japan, Sendai, pp.777-778, (In Japanese).

(19) Sakurai, A., Shiotsu, M., Hata K. and Fukuda, K., 1997b, Pool Boiling Critical Heat Fluxes on Test Heaters with Various Configurations in Subcooled Liquids for Wide Ranges of Subcooling and Pressure (Part 2: Its Mechanism), 34th National Heat Transfer Symposium of Japan, Sendai, pp.779-780, (In Japanese).

(20) Fukuda, K., Shiotsu, M. and Sakurai, A., 1997c, Effect of Surface Conditions on Transient Critical Heat Fluxes for a Horizontal Cylinder in a Pool of Water at Pressures due to Exponentially Increasing Heat Inputs, Proc. of 8th International Topical Meeting on Nuclear Reactor Thermal Hydraulics (NURETH-8), Kyoto, Japan, pp.1050-1058.

(21) Sakurai A., Shiotsu M., Hata K. and Fukuda, K., 1997d, Photographic Study on Transitions from Non-boiling and Nucleate Boiling Regimes to Film Boiling due to Increasing Heat Inputs in Liquid Nitrogen and Water, Proc. of 8th International Topical Meeting on Nuclear Reactor Thermal Hydraulics (NURETH-8), Kyoto, Japan, pp.1038-1049

ACKNOWLEDGMENT

The author would like to acknowledge the guidance and support of Professor emeritus Akira Sakurai and Professor Masahiro Shiotsu of Kyoto University for this work. The author also would like to express his grateful acknowledgement to Professor Akimi Serizawa of Kyoto University for his fruitful discussion and reviewing this work. The author would like to thank Professor emeritus Toshiki Morita of Kobe University of Mercantile Marine for providing the opportunities of the investigation. The author would like to express his sincere gratitude to Dr. K. Hata, of Kyoto University, who had taught the author lots of techniques in doing experiments. The author wishes to thank my wife, Taeko, and my daughter, Yuko for their years of encouragement and patience during this endeavor.